Strong Dynamics in Theories Beyond the Standard Model

by

Witold Skiba

Submitted to the Department of Physics
in partial fulfillment of the requirements for the degree of

Doctor of Philosophy

at the

MASSACHUSETTS INSTITUTE OF TECHNOLOGY

May 1997

Author .....
Department of Physics
May 2, 1997

Certified by .....
Lisa Randall
Associate Professor of Physics
Thesis Supervisor

Accepted by .....
George Koster
Chairman, Physics Graduate Committee

Strong Dynamics in Theories Beyond the Standard Model

by

Witold Skiba

Submitted to the Department of Physics
on May 2, 1997, in partial fulfillment of the
requirements for the degree of
Doctor of Philosophy

Abstract

We present several applications of non-perturbative methods to physics beyond the Standard Model. First, we investigate the Strongly-Coupled Standard Model (the Abbott-Farhi model) and examine the model in the light of precision electroweak measurements. We construct an effective Lagrangian describing the interaction of the lowest energy states and an isotriplet of excited vector particles. The couplings of the exited vector bosons are restricted to be unnaturally small. We then investigate signatures of pseudo-Goldstone bosons in technicolor theories with the Glashow-Iliopoulous-Maiani mechanism. We use chiral Lagrangian techniques to describe the spectrum and the interactions of the pseudo-Goldstone particles in these theories. Free parameters of such models can be constrained by experimental data. We also outline the most promising signatures at the next generation of particle colliders. Next, we address issues of confinement in supersymmetric theories. We give necessary criteria for $N = 1$ supersymmetric theories to be in a smoothly confining phase without chiral symmetry breaking and with a dynamically generated superpotential. Using our general arguments we find all such confining theories with a single gauge group and no tree-level superpotential. For models with vector-like fields we obtain descriptions for theories with smaller matter content by integrating out fields. Finally, we show how to apply exact results in supersymmetric theories to construct models of dynamical supersymmetry breaking. We introduce a new class of theories which dynamically break supersymmetry based on the gauge group $SU(n) \times SU(m) \times U(1)$ with $m = 3, 4, 5$. We present a renormalizable superpotential which lifts all flat directions and argue that these theories break supersymmetry dynamically.

Thesis Supervisor: Lisa Randall
Title: Associate Professor of Physics

Acknowledgments

I am indebted to my research advisor, Lisa Randall, for her guidance and support. I am grateful to have had four years of innumerable hours of discussions, help and advice. Hopefully, these exciting sessions of discussions may continue in the years to come.

I am grateful to Bolek Wysłouch for convincing me to come to MIT. His advice during my first year here was invaluable.

It was not only fun, but also very productive to collaborate with Csaba Csáki and Martin Schmaltz on supersymmetry related issues. I also thank Daniel Freedman, Joshua Erlich, Eric Sather and John Terning for present and past collaborations.

I thank the members of my thesis committee Lisa Randall, Edward Farhi and Nihat Berker for reading my thesis. Finally, I would like to thank the members of the Center for Theoretical Physics for all the interactions we had.

This research has been supported in part by the DOE under cooperative agreement #DE-FC02-94ER40818.

Contents

List of Tables

List of Figures

Chapter 1

Introduction

One of the most difficult problems in quantum field theory is understanding strongly interacting theories. The standard approach to solving the theory in terms of perturbation expansion in powers of the gauge coupling fails when the value of the coupling is large. There are several alternatives to perturbation theory which are useful in the strong coupling regime. While it is usually hopeless to attempt solving the full theory, there are certain regimes of the theory which are more easily accessible to analytical methods. In particular, the low-energy limit is frequently easier to analyze than the full theory.

There are two important issues in analyzing strongly interacting theories: these are identifying the symmetries of the problem and the relevant degrees of freedom. Then one tries to construct an effective description of the interactions between these degrees of freedom. Usually, in the low-energy limit there are sufficiently few degrees of freedom, such that their interactions are constrained by the symmetries. Depending on the symmetry of the problem, it may or may not be possible to solve the theory. The more symmetries there are, the more constrained the effective interactions are. Even when symmetries are not exact, they still can be useful for finding the effective description. One can solve the problem in the limit of exact symmetry and then construct an expansion in powers of symmetry breaking operators.

We will show several examples of theories beyond the Standard Model, in which strong dynamics plays a crucial role. For phenomenological purposes, it is frequently sufficient to describe the low-energy limit. Any unknown new interactions must be characterized by high energy scales, and only the low-energy dynamics is relevant for processes accessible experimentally. It is plausible that apart from QCD there are other strongly interacting theories. One can speculate on various possibilities for such theories, and how they may explain parameters of the Standard Model. We will discuss several examples of models created with the use of strongly interacting theories and non-perturbative dynamics.

In the next chapter we review the Strongly-Coupled Standard Model (Abbott-Farhi model). Our goal is then checking if this theory passes stringent experimental tests of the precision electroweak measurements. The Strongly-Coupled Standard Model (SCSM) is a model of compositeness, in which the electroweak gauge group, $SU(2)_L$, is strongly interacting. All fields carrying $SU(2)_L$ quantum numbers are confined at low energies. It turns out that the SCSM mimics the perturbative Standard Model under some dynamical assumptions. We will describe the SCSM including not only the lightest particles but also some excited states, which are not present in the Standard Model. In particular, we will include a triplet of vector gauge bosons W'. Such vector bosons affect the parameters of

the low-energy theory. Their effect on the low-energy theory can be effectively summarized in terms of the parameters S, T and U. By using high-precision electroweak measurements we constrain the couplings and the masses of the W' triplet. Their couplings are restricted to be unnaturally small, which indicates that the SCSM is no longer a compelling theory of weak interactions.

In Chapter 3, we investigate pseudo-Goldstone bosons in technicolor theories with the GIM mechanism (TC-GIM). We briefly describe the basic idea of technicolor and then examine the phenomenology of a specific model. TC-GIM theories contain exotic fermion families that do not interact under the weak $SU(2)_L$. These fermions form pseudo-Goldstone bosons, which are the lightest exotic particles in such theories. We outline the spectrum of the pseudo-Goldstone bosons and their interactions. The tool for describing these particles is the non-linear sigma model, known to describe pions in the low-energy QCD. This happens because the technicolor theories we analyze are based on a scaled-up version of QCD. The non-perturbative dynamics in such theories spontaneously breaks chiral symmetries. The pseudo-Goldstone bosons are associated with the breaking of chiral symmetries. In the TC-GIM models, relevant symmetries are not exact, but explicitly violated by mass terms and gauge interactions. Therefore, the pseudo-Goldstone particles are not massless. Pseudo-Goldstone bosons are important for phenomenology since they are the particles most likely to be observed in experiments. We explain what kind of signatures are expected in future experiments and how the current data constrain the free parameters of these models.

We turn into investigations of supersymmetric theories in the following two chapters. Supersymmetry imposes additional constraints on the form of the low-energy interactions. In $N = 1$ supersymmetry, the superpotential must be a holomorphic function of the chiral superfields. This restriction is so powerful that in many theories one can find exact low-energy superpotentials. We review the basic facts about infrared limit of supersymmetric gauge theories in Chapter 4. Also in Chapter 4 we present general arguments for identifying "s-confining" theories. We also find all s-confining theories with a single gauge group. For all confining theories we identify the massless degrees of freedom and explain consistency checks supporting the picture of confinement in our examples.

In Chapter 5, we use the results on low-energy behavior of supersymmetric theories to construct models which break supersymmetry dynamically. If supersymmetry is relevant to nature it has to be broken. Dynamical supersymmetry breaking is an appealing possibility for supersymmetry breaking at scales smaller than the Planck scale. We first outline general observations about dynamical supersymmetry breaking. We then investigate supersymmetry breaking in product group theories. The product group theories we consider are particularly interesting because depending on the sizes of non-abelian gauge groups, the low-energy theories can exhibit various kinds of non-perturbative phenomena. We show that models which are naively in the confining, conformal or even infrared-free phase can break supersymmetry. In the analyzed theories, it is important that the dynamics of one gauge group can affect the dynamics of the other group. We also explain the dynamical role of the tree-level superpotential. The tree-level superpotential can be a relevant perturbation and change the phase of the theory. We will see explicitly that the number of massless fields can be changed when the tree-level Yukawa couplings become mass terms in the effective theory. This chapter contains many models which dynamically break supersymmetry.

Chapter 2

Strongly-Coupled Standard Model[1]

In this chapter we consider the Strongly-Coupled Standard Model (Abbott-Farhi model) including an isotriplet of W' vector bosons [2]. First we calculate the corrections to the low-energy theory, which can be effectively summarized in terms of the parameters S, T and U. Then we use high-precision electroweak measurements to constrain the mass and couplings of the W'. The W' couplings are restricted to be unnaturally small, and we conclude that this model is no longer compelling as a theory of the electroweak interactions.

The Strongly-Coupled Standard Model (SCSM) is based on an underlying Lagrangian identical in form to the Standard-Model Lagrangian. However, the parameters of the gauge-Higgs sector are adjusted so that the Higgs field does not spontaneously break the $SU(2)_L$ gauge symmetry. Instead the $SU(2)_L$ interactions become confining, and the observed particle spectrum consists of $SU(2)_L$ singlets. Nevertheless, given dynamical assumptions such as unbroken chiral symmetry, the low-energy theory of the SCSM looks very much like the spontaneously-broken Standard Model. The striking similarity of the confining and spontaneously broken phases of the theory exemplifies the concept of "complementarity." The exciting possibility that nature might in fact be described by a confining version of the Standard Model, which predicts the discovery of new particles and strong interactions at future colliders, motivates the study of the SCSM.

Of course, if the SCSM really is the theory of the weak interactions, evidence for particle compositeness must eventually emerge. The effective theory of the SCSM must deviate from the renormalizable Standard-Model Lagrangian: resonances and higher-dimensional interactions should appear. In this work we ask: Are the deviations expected in the SCSM allowed by current experimental constraints? We will attempt to answer this question by studying a test case in which we introduce an isotriplet of W' vector bosons into the effective theory. We calculate the corrections to Standard-Model predictions which result from including the W' bosons. Then we use high-precision electroweak data to constrain these corrections, and thereby bound the allowed region of the W' mass and couplings.

In an earlier analysis of experimental constraints on the SCSM, Korpa and Ryzak [3] added both an W' isotriplet and an isoscalar vector boson to the usual Standard-Model particle content. They concluded that experiment could accommodate these new particles without severely restricting their masses and couplings. Since then many new electroweak

[1]This chapter is based on the research done in collaboration with Eric Sather reported in Ref. [1].

observables have been measured, and the accuracy of earlier measurements has greatly increased. Here we exploit this new data to find much stronger constraints on the model. In particular, the precise measurement of the Z mass permits a new approach to parameterizing the corrections to Standard-Model predictions in the SCSM.

In the original formulation of the model [2], the W and Z were not expected to have the masses predicted by the Standard Model; however, it was known that the Standard-Model values could be recovered by invoking vector dominance [4]. Specifically, they follow from the assumption that the W-pole graph saturates the isovector electromagnetic form factor of the composite fermions. When the W and Z were later discovered with masses near the Standard-Model values, it became necessary to add to the SCSM the assumption that vector dominance holds at least approximately [5]. In our analysis we find that the W must saturate this form factor to within a few percent. We consider this unnatural and conclude that, in its present form, the SCSM is no longer a candidate for a theory of the electroweak interactions.

In the next section we review the effective theory for the SCSM in a limit where non-Standard particle content and higher-dimensional interactions are absent, and show that it reduces to the Standard Model in this limit. In Section 2.2, we introduce a W' isotriplet and discuss the resulting modification of vector-dominance relations. In Section 2.3, we calculate the W'-induced corrections to electroweak observables, which we summarize in terms of contributions to S, T and U in Section 2.4. We then use high-precision electroweak measurements in Section 2.5 to determine the allowed region of the W' mass and couplings, and present our conclusions in the last section.

2.1 Review of the SCSM

The fundamental insight which underlies the SCSM is that the particle spectrum and interactions in the strong-coupling version of the Standard Model could closely resemble those of the familiar spontaneously-broken Standard Model. This is an example of complementarity: there is no phase transition between confinement and spontaneous symmetry breaking in a gauge-Higgs theory with a Higgs in the fundamental representation [6]. In this Section we review how the effective theory of the SCSM approximates the ordinary Standard Model (given certain dynamical assumptions). We closely follow the presentation and notation of Claudson, Farhi and Jaffe [5]. In the next Section we will begin our discussion of the deviations from Standard-Model predictions which appear when a W' isotriplet is added.

The SCSM is based on an underlying Lagrangian which has the same form as the Standard-Model Lagrangian. However, the parameters of the theory are adjusted so that the $SU(2)_L$ interactions are not spontaneously broken, and instead become confining at low energies. All the observed particles are then $\mathrm{SU}(2)_L$ singlets.

Consider the potential for the fundamental scalar field,

$$V(\Omega) = \frac{\lambda}{2}(\mathrm{tr}\ \Omega^\dagger\Omega - 2v^2)^2\ , \tag{2.1}$$

where

$$\Omega = (\ \phi\quad \tilde{\phi}\ ) = \begin{pmatrix} \phi_1 & -\phi_2^* \\ \phi_2 & \phi_1^* \end{pmatrix}\ . \tag{2.2}$$

Note that $\Omega^\dagger\Omega = |\phi|^2 1$. By expressing the potential in terms of Ω, we make explicit the invariance of the potential under the custodial $SU(2)_W$ symmetry, defined by $\Omega \to \Omega h$ for

$h \in SU(2)_W$. This symmetry is an invariance of the full Lagrangian when the hypercharge and Yukawa couplings of the fermions are turned off.

The scale dependence of the $SU(2)_L$ gauge coupling is characterized by a scale parameter Λ_2, analogous to $\Lambda_{\rm QCD}$. This scale parameter and the constant v^2, which appears in the scalar-field potential in Eq. (2.1), together control whether the $SU(2)_L$ interactions are confining or spontaneously broken. The $SU(2)_L$ gauge symmetry will not be spontaneously broken if $v^2 < 0$ or if $v^2 \ll \Lambda_2^2$, in which case the gauge interactions get strong at energies well above v^2 and prevent spontaneous symmetry breaking. The fundamental fields which carry $SU(2)_L$ charge will then be confined into $SU(2)_L$ singlets. These can be classified using the custodial symmetry, $SU(2)_W$.

For example, the elementary left-handed fermions ψ_L^a (where $a = 1, \ldots, 12$ labels the $SU(2)_L$ doublet) bind with the scalar particles ϕ to form composite left-handed fermions,

$$F_L^a = \Omega^\dagger \psi_L^a = \begin{pmatrix} \phi^{*\alpha} \psi_{L\alpha}^a \\ \phi_\alpha \epsilon^{\alpha\beta} \psi_{L\beta}^a \end{pmatrix}, \tag{2.3}$$

which transform as $SU(2)_W$ doublets. Here α and β are $SU(2)_L$ indices, which are contracted so that the F_L^a are $SU(2)_L$ singlets. The hypercharge of a composite fermion is the sum of the elementary fermion and scalar hypercharges, $y^a + \tau^3/2$. This is simply the electric charge Q^a of the fermion, which implies that the hypercharge $U(1)$ in the SCSM is actually electromagnetism.

From the scalar fields alone we can form a composite Higgs field, $H = \frac{1}{2}$ tr $(\Omega^\dagger \Omega)$, which is an $SU(2)_W$ singlet. We can also form an $SU(2)_W$ triplet of vector bosons, with interpolating field $\mathbf{W}_\mu =$tr $(\Omega^\dagger D_\mu \Omega \boldsymbol{\tau})$. In these examples we can see the crucial role played by the custodial symmetry in organizing the composite particles into multiplets analogous to the familiar $SU(2)_L$ multiplets of the Standard Model. (We will later see how this symmetry also ensures that the interactions of the composite particles have the standard form.)

Of course, in addition to the particles that are contained in the Standard Model, experience with the Strong Interactions leads us to expect in the SCSM a rich spectrum of bound states, including excited W' bosons, leptoquarks and so on. Since these particles have yet to be observed, we must assume that these exotic states are considerably more massive than the left-handed fermions and the W bosons.

Claudson, Farhi, and Jaffe enumerated three dynamical assumptions concerning the confining $SU(2)_L$ sector of the theory, which must hold if the SCSM is to describe the observed electroweak phenomena [5]:

(i) The approximate $SU(12)$ chiral symmetry which relates the 12 $SU(2)_L$ fermion doublets is not spontaneously broken by a condensation of left-handed fermions (i.e., $\langle \psi_L^a \psi_L^b \rangle = 0$). This chiral symmetry then protects the composite left-handed fermions F_L^a from acquiring large masses. (If this chiral symmetry were broken, there would be light Goldstone bosons consisting of two left-handed fermions, and the composite fermions would be heavy, as their analogs are in QCD.)

(ii) The W vector bosons are much lighter than the typical mass scale in the theory (e.g., Λ_2), and in particular, the W and Z are much lighter than their recurrences, the W' and Z'.

(iii) The effective coupling of the W bosons to left-handed fermions is small ($\bar{g} \approx 0.66$) even while the underlying theory is strongly-coupled.

With these assumptions we can write down the low-energy effective Lagrangian for the SCSM. Interactions with dimension greater than four should be suppressed by the characteristic mass scale, Λ_2, which by assumption (ii) is much larger than M_W. As long as we work at energies no higher than the Z mass, we should be able to omit these higher-dimensional operators from the effective theory. Then the most general $SU(2)_W$-symmetric effective Lagrangian involving the composite fermion and vector-boson fields is

$$\mathcal{L}^0_{\rm eff} = i\bar{F}_{La}\partial\!\!\!/ F^a_L - \frac{1}{4}\mathbf{W}^{\mu\nu}\cdot\mathbf{W}_{\mu\nu} + \frac{1}{2}M_W^2\mathbf{W}^\mu\cdot\mathbf{W}_\mu + \bar{g}\mathbf{W}_\mu\cdot\mathbf{j}^\mu_L + \ldots, \tag{2.4}$$

where the W self-couplings have not been listed. Here $\mathbf{j}^\mu_L = \frac{1}{2}\bar{F}_{La}\boldsymbol{\tau}\gamma^\mu F^a_L$, and $\mathbf{W}_{\mu\nu} = \partial_\mu\mathbf{W}_\nu - \partial_\nu\mathbf{W}_\mu$ Electromagnetism, which breaks the custodial symmetry, can then be added by minimal substitution of the vector potential, a_μ, and insertion of the field-strength, $\mathcal{F}_{\mu\nu} = \partial_\mu a_\nu - \partial_\nu a_\mu$:

$$\mathcal{L}_{\rm eff} = \mathcal{L}^0_{\rm eff} + i\bar{\psi}_{Rb}\partial\!\!\!/\psi^b_R + ea_\mu j^\mu_{\rm em} - \frac{1}{4}\mathcal{F}^{\mu\nu}\mathcal{F}_{\mu\nu} - \frac{k}{2}\mathcal{F}^{\mu\nu}W^3_{\mu\nu} + \cdots. \tag{2.5}$$

Again cubic and quartic vector-boson interactions have not been listed. Here $j^\mu_{\rm em}$ is the contribution of the fermions to the electromagnetic current. If we now assume vector dominance, so that the isovector electromagnetic form factor of the F^a_L is saturated by the W boson, then as will be discussed in the next Section, we find that the strength k of the photon-W^3 mixing[2] is given in terms of the $U(1)$ coupling and the $W\bar{F}_L F_L$ coupling as $k = e/\bar{g}$. Diagonalizing the quadratic terms in the Lagrangian (2.5) which involve the neutral vector bosons, we find the propagating fields

$$\begin{aligned} A_\mu &= a_\mu + kW^3_\mu\,, \\ Z_\mu &= (1-k^2)^{1/2}W^3_\mu\,, \end{aligned} \tag{2.6}$$

which couple to the neutral currents as

$$\mathcal{L}_{\rm NC} = eA\cdot j_{\rm em} + Z\cdot\frac{\bar{g}}{\sqrt{1-k^2}}\left(j^3_L - \frac{ek}{\bar{g}}j_{\rm em}\right). \tag{2.7}$$

Hence the value of $\sin^2\theta$ that would be measured in low-energy neutrino scattering is $\sin^2\theta = ek/\bar{g} = k^2$, where we have used the vector-dominance result $k = e/\bar{g}$. This implies that $\bar{g} = e/\sin\theta$, which leads to the standard prediction for the mass of the W: $M_W^2 = \pi\alpha/(\sqrt{2}G_F\sin^2\theta)$. In the above diagonalization process one additionally finds a Z mass of $M_Z = M_W/\sqrt{1-k^2}$. Applying the vector-dominance result again, we recover the Standard-Model relation

$$\frac{M_W^2}{{M_Z}^2\cos^2\theta} = 1\,. \tag{2.8}$$

We see therefore how the additional assumption of vector dominance leads to the Standard-Model predictions for the masses of both the W and the Z. A vector-dominance analysis of the electromagnetic form factors of the W shows that the cubic and quartic self-couplings of the W are those of an $SU(2)$ gauge theory with coupling $\bar{g}$, and that the corresponding couplings of the propagating fields, A and Z, are just those of the Standard Model [5].

[2]This mixing is analogous to the familiar case of photon-ρ mixing.

2.2 Including a W' Isotriplet

We have just seen that with certain dynamical assumptions, and invoking vector dominance, the effective theory of the SCSM approximates the Standard Model. We now begin our analysis of the corrections to the effective theory that result when we introduce an isotriplet of W' vector bosons. A W' should arise in this model as a radial excitation of the W, analogous to the ρ' in QCD. Because there is no evidence yet for deviations from the Standard Model, the W' must be considerably more massive than the W and/or less strongly coupled. We will therefore treat the inclusion of the W' as a perturbation of the Standard Model.

Of course, we could include other non-Standard particles in the theory. Alternatively, we could include in the Lagrangian all operators up to some dimension which are consistent with the symmetries of the theory. However, as we will soon show, the W' is the degree of freedom which corresponds to relaxing the assumption that the W saturates the isovector electromagnetic form factor. Adding a W' thus allows us to consider corrections to the effective theory due to new particle content, and also to study deviations from exact vector dominance. At the same time, including a W' isotriplet adds only three new parameters to the low-energy effective theory, and therefore it is possible to significantly constrain the theory. The Lagrangian terms for the W' are similar in form to those for the W, Eqs. (2.4) and (2.5):

$$\begin{aligned}\mathcal{L}_{\text{eff}}^{W'} &= -\frac{1}{4}\mathbf{W}'^{\mu\nu}\cdot\mathbf{W}'_{\mu\nu} + \frac{1}{2}{M'_W}^2\,\mathbf{W}'^{\mu}\cdot\mathbf{W}'_{\mu} + \bar{g}'\mathbf{W}'_{\mu}\cdot\mathbf{j}_L^{\mu} \\ &\quad -\frac{k'}{2}\mathcal{F}^{\mu\nu}{W'^3}_{\mu\nu} + \cdots . \end{aligned} \tag{2.9}$$

In constructing $\mathcal{L}_{\text{eff}}^{W'}$ we have proceeded much as before in arriving at Eqs. (2.4) and (2.5). We have first constructed the most general $SU(2)_W$-symmetric Lagrangian. Next we have diagonalized the Lagrangian to eliminate terms which mix the W and W' bosons. Finally we have included electromagnetism, which leads to mixing of the photon with W^3 and W'^3. For later purposes, we note that by substituting $\mathbf{W}' \to -\mathbf{W}'$ we can reverse the signs of both $\bar{g}'$ and k', showing that only the relative sign of these two couplings is meaningful.

2.2.1 Vector Dominance

We now show how the W' parameterizes the deviation from vector-meson dominance: Consider the isovector electromagnetic form factor of the composite fermions, $F_V(q^2)$, defined through

$$e\langle \bar{F}_{La},\, F_L^a | J_{\text{em}}^{\mu} | 0\rangle = e\bar{U}_L\gamma^{\mu}y^a V_L + e\,F_V(q^2)\,\bar{U}_L\gamma^{\mu}\frac{\tau^3}{2}V_L\,. \tag{2.10}$$

Here J_{em}^{μ} is the total electromagnetic current, which includes terms linear in W^3 and W'^3. The sum of the contributions to the form factor (see Fig. 2-1) from direct coupling of the current to the left-handed fermions and from the W^3- and W'^3-pole diagrams is

$$eF_V(q^2) = e - k\bar{g}\frac{q^2}{q^2 - M_W^2} - k'\bar{g}'\frac{q^2}{q^2 - M_W'^2}\,. \tag{2.11}$$

Because the F_L are composite and the confining $SU(2)_L$ interactions are asymptotically free, $F_V(q^2) \to 0$ as $|q^2| \to \infty$. Then, assuming that $F_V(q^2)$ is saturated by the W^3 and

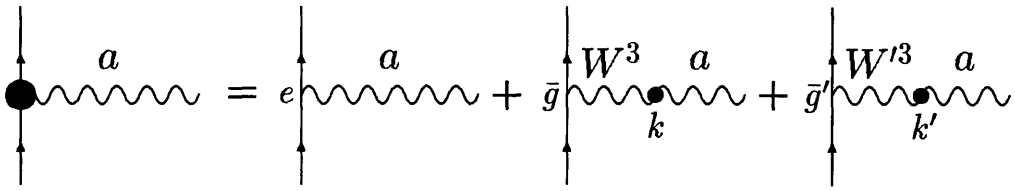

Figure 2-1: Diagrammatic expansion of the isovector electromagnetic form factor including the direct-coupling graph and the W- and W'-pole graphs.

W'^3 poles (i.e., there are no other contributions to the form factor, such as from a W''), we conclude that

$$e = k\bar{g} + k'\bar{g}' = k\bar{g}(1 + \kappa\gamma)\,, \tag{2.12}$$

where we have introduced the ratios of W and W' couplings

$$\kappa \equiv k'/k\,, \quad \gamma \equiv \bar{g}'/\bar{g}\,. \tag{2.13}$$

Had we assumed strict vector dominance so that only the W-pole diagram contributed, we would have found the result $e = k\bar{g}$, which leads to the Standard-Model Lagrangian as was shown in Section 2.1. By including the W', however, we depart from exact vector dominance. The W' contributes a fraction $k'\bar{g}'/e \approx \kappa\gamma$ to the saturation of $F_V(q^2)$, so that $\kappa\gamma$ measures the degree of the departure.

For the model to approximately reproduce the Standard Model, the W must nearly saturate this form factor. Here we have further assumed that the W' contribution to the saturation, though of necessity much smaller than that of the W, is nevertheless more important than contributions from higher-lying resonances, which have been ignored. In essence, we are claiming that the W' can be viewed as a stand-in for all the resonances beyond the W which contribute to $F_V(q^2)$. The quantity $\kappa\gamma$ accordingly represents the combined contribution of these resonances to the saturation of this form factor.

2.2.2 The Physical Neutral Vector Bosons

The mixing of the photon with the neutral W^3 and W'^3 bosons introduces off-diagonal terms into the free (quadratic) part of the Lagrangian. We need to diagonalize the free Lagrangian to find the physical photon, Z and Z' fields. In the previous section we gave expressions for the physical photon and Z fields that diagonalize the free part of Lagrangian in the absence of the W' bosons. These expressions, and also the result for the Z mass, are modified by the mixing of the photon with W'^3. For the masses of the Z and Z' we find

$$\begin{aligned} M_Z^2 &\approx \frac{M_W^2}{c^2}\left[1 - \frac{s^4}{c^2(c^2-\mu)}\mu\kappa^2\right]\,, \\ M_{Z'}{}^2 &\approx M_{W'}{}^2\left[\frac{1+\frac{s^4}{c^4}\mu\kappa^2}{1-\frac{s^2}{c^2}\kappa^2} + \frac{s^4}{c^2(c^2-\mu)}\mu\kappa^2\right]\,. \end{aligned} \tag{2.14}$$

Here $s \equiv \sin\theta \equiv k$, $c \equiv \cos\theta$, and μ is the ratio of the W and W' squared masses:

$$\mu \equiv M_W^2 / {M_{W'}}^2 \ . \tag{2.15}$$

Terms containing extra factors of $\mu\kappa^2$ have been omitted. Note that we must restrict κ to the interval $|\kappa| < \cot\theta$, since otherwise the Z' would have a negative squared mass and be a tachyon. The neutral vector-boson fields a, W^3 and W'^3 are given in terms of the physical fields A, Z and Z' as

$$\begin{aligned} a &= A - s(W^3 + \kappa W'^3) \ , \\ W^3 &\approx \left[1 - \left(1 - \frac{\mu}{2c^2}\right)\left(\frac{s^2}{c^2-\mu}\right)^2 \mu\kappa^2\right]\frac{Z}{c} + \frac{s^2}{c^2-\mu}\mu\kappa\frac{Z'}{\sqrt{1-\frac{s^2}{c^2}\kappa^2}} \ , \\ W'^3 &\approx -\frac{s^2}{c^2-\mu}\mu\kappa\frac{Z}{c} + \frac{Z'}{\sqrt{1-\frac{s^2}{c^2}\kappa^2}} \ . \end{aligned} \tag{2.16}$$

Corrections to the coefficients of Z and Z' are suppressed by additional factors of $\mu\kappa^2$. If we substitute these expressions into the interaction terms that couple a, W, and W' to the fermions, we find the couplings of the Z and Z' to left-handed and electromagnetic currents.

These results for the Z and Z' masses (2.14) and the expressions for W^3 and W'^3 in terms of Z and Z' (2.16) were calculated by expanding in powers $s^2\mu\kappa/(c^2-\mu) \ll 1$, which is assumed to be small. This assumption reflects our intuition that the W' should be heavier than the W ($\mu \ll 1$) and should also mix more weakly with the photon ($\kappa \ll 1$).

Note that all of the above corrections to Standard-Model relations — the vector dominance result for the electromagnetic coupling (2.12) and the mass and couplings of the W and Z, (2.14) and (2.16) — contain factors of at least two of the W' parameters κ, γ and μ. The same is true of corrections to four-fermi interactions mediated by W' exchange, which are of order $\mu\gamma^2$. Hence if any two of the W' parameters vanish, the effective low-energy theory reduces to that of the Standard Model, leaving the remaining W' parameter completely unconstrained. This means that we will be unable to obtain constraints on any individual parameter independent of the other parameters. We will either have to fix one of the parameters and then constrain the other two, or else constrain products of the parameters, e.g., the product $\kappa\gamma$.

As mentioned above, Korpa and Ryzak in their earlier analysis of SCSM constraints considered the SCSM with not only an isotriplet of W' vector bosons but also with isoscalar vector bosons which are bound states of a left-handed fermion and a left-handed antifermion: $(V_\mu)^b_a \sim \bar{\psi}_{La}\gamma_\mu\psi^b_L$. Assuming that those V bosons which are color octets, and thus mix with gluons, saturate the (isoscalar) color form factor of the composite, left-handed quarks, they were able to place a very stringent bound on the mass of the isoscalar bosons ($m_V >$ 700 GeV), so that the V bosons would be just as massive as the rest of the non-Standard resonances. This called into question the assumption of vector dominance of the isoscalar form factors. Of course, vector dominance of the *isoscalar* channel is not a necessary ingredient in the SCSM. By contrast, vector dominance of the *isovector* channel must at least approximately hold in order to account for the W and Z masses. By including a W' we can determine to what accuracy vector dominance must be maintained in the isovector channel in order to retain agreement with electroweak data.

2.3 Corrections to Standard-Model Predictions

We have seen that the SCSM as formulated here reduces to the Standard Model if the W' is absent or if it has infinite mass and vanishing couplings. And, of course, the Standard Model is in impressive agreement with experiment. It is therefore logical to treat the SCSM with a W' as a perturbation of the Standard Model and calculate the corrections to SM predictions due to the W'.

2.3.1 Corrections to the Mass and Couplings of the W

The corrections induced by the W' are not simply given by the sum of the new graphs that include W's. The three quantities α, G_F and M_Z are known to very high accuracy, and their values cannot change when the W' bosons are added to the theory. In the Standard Model, their values determine the masses and couplings of the vector bosons. However, as the W' parameters are turned on, the W parameters must deviate from their Standard-Model values if α, G_F and M_Z are to remain fixed. There are then two ways in which the W' modifies the effective theory: (1) W' exchange induces new effective (four-fermi) interactions, *and* (2) the W mass and couplings depart from their Standard-Model values in order to preserve the values of α, G_F, and M_Z.

Let us first compute the deviations of the W mass and couplings from their Standard-Model values by working at tree level. We define M_{W0}, $\bar{g}_0$ and k_0 as the mass and couplings of the W when the W' is absent, and we define M_W, $\bar{g}$ and k as the mass and couplings when the W' is included. We compute e, G_F and M_Z (at tree level) in the Standard Model when the W' is absent, and then in the SCSM, with a W' in the theory. Combining these results we have

$$\begin{aligned} e &= k_0\bar{g}_0 = k\bar{g}(1+\kappa\gamma)\,, \\ 4\sqrt{2}G_F &= \frac{\bar{g}_0^2}{{M_{W0}}^2} = \frac{\bar{g}^2}{{M_W}^2} + \frac{\bar{g}'^2}{{M_{W'}}^2} = \frac{\bar{g}^2}{{M_W}^2}(1+\mu\gamma^2)\,, \\ M_Z^2 &= \frac{{M_{W0}}^2}{c_0^2} \approx \frac{M_W^2}{c^2}\left[1 - \frac{s^4}{c^2(c^2-\mu)}\mu\kappa^2\right]\,. \end{aligned} \tag{2.17}$$

Here $c_0 \equiv \cos\theta_0 = \sqrt{1-k_0^2}$, and as before, $s = k$ and $c = \sqrt{1-k^2}$. The expressions for $e = \sqrt{4\pi\alpha}$ and M_Z come from the previous section, Eqs. (2.12) and (2.14). The result for G_F is simply the sum of W and W' exchange. These formulas can be used to express the deviations of the W mass and couplings from their Standard-Model values in terms of $M_{W'}$, $\bar{g}'$ and k' (or, equivalently, in terms of μ, κ and γ). Let $\delta M_W = M_W - M_{W0}$, $\delta\bar{g} = \bar{g} - \bar{g}_0$ and $\delta k = k - k_0$. Then

$$\begin{aligned} \frac{\delta M_W}{M_W} &\approx \frac{1}{2}\frac{1}{c^2-s^2}\left[2s^2\kappa\gamma - s^2\mu\gamma^2 + \frac{s^4}{c^2-\mu}\mu\kappa^2\right]\,, \\ \frac{\delta\bar{g}}{\bar{g}} &\approx \frac{1}{2}\frac{1}{c^2-s^2}\left[2s^2\kappa\gamma - c^2\mu\gamma^2 + \frac{s^4}{c^2-\mu}\mu\kappa^2\right]\,, \\ \frac{\delta k}{k} &\approx -\frac{1}{2}\frac{1}{c^2-s^2}\left[2c^2\kappa\gamma - c^2\mu\gamma^2 + \frac{s^4}{c^2-\mu}\mu\kappa^2\right]\,. \end{aligned} \tag{2.18}$$

Terms containing more powers of $\kappa\gamma$, $\mu\gamma^2$ or $\mu\kappa^2$ have been omitted. The corrections to

Standard-Model predictions we will find, such as all those found above, will in general be linear in these quantities, and so they will be forced to be small by our constraint analysis. In Eq. (2.18) where s and c multiply small quantities like $\kappa\gamma$, we could just as well use s_0 and c_0, since the expressions would be unchanged within the accuracy to which we are working. Here and in the following, wherever the choice of $\sin\theta_W$ is immaterial, we will use $\sin\theta = k$ and write simply s (and c) for brevity. It should be understood however, that another convention would do just as well.

These results have been obtained at tree level. Of course, in addition to the W'-induced corrections to the effective theory, there are also radiative corrections. Radiative corrections to the small W'-induced corrections are negligible, comparable to two-loop corrections in the Standard Model. Hence the effective theory is well approximated by adding the W'-induced corrections calculated here at tree level to the Standard-Model effective theory calculated to one-loop accuracy. In particular, the mass and couplings of the W in the SCSM are obtained from their renormalized Standard-Model values by simply adding the deviations δM_W, $\delta\bar{g}$ and δk calculated above.

2.3.2 Neutral-Current Interactions at the Z Pole

Having calculated the correction to M_W, we need to compute the corrections to the neutral-current interactions in order to obtain the remaining constraints on the W' parameters. (Charged-current interactions are precisely constrained only at low energy, and there they are completely fixed by the value of G_F.) Above we presented expressions for the fields a, W and W' in terms of the physical neutral vector bosons A, Z and Z' (2.16). Using those results we can write down the coupling of the physical bosons to the fermion currents j_L^3 and $j_{\rm em}$ (again, we only need to calculate the W'-induced corrections at tree-level):

$$\begin{aligned}
\mathcal{L}_{\rm NC} &= ea\cdot j_{\rm em} + \bar{g}W^3\cdot j_L^3 + \bar{g}'W'^3\cdot j_L^3 \\
&\approx eA\cdot j_{\rm em} \\
&\quad +\bar{g}\left[1-\frac{1}{2}\frac{s^4}{c^2}\frac{2c^2-\mu}{(c^2-\mu)^2}\mu\kappa^2 - \frac{s^2}{c^2-\mu}\mu\kappa\gamma\right] \\
&\quad \times\frac{Z}{c}\cdot\left[j_L^3 - \frac{ek}{\bar{g}}\left(1+\frac{s^2}{c^2-\mu}\mu\kappa(\gamma-\kappa)\right)j_{\rm em}\right] \\
&\quad +\bar{g}Z'\cdot\left[\left(\gamma+\frac{s^2}{c^2-\mu}\kappa\right)j_L^3 - \frac{ek}{\bar{g}}\left(1+\frac{s^2}{c^2-\mu}\right)\kappa j_{\rm em}\right] \qquad (2.19) \\
&\approx eA\cdot j_{\rm em} \\
&\quad +\bar{g}_0(1+\zeta)\frac{Z}{c_0}\cdot\left[j_L^3 - s_0^2(1+\delta_Z)j_{\rm em}\right] \\
&\quad +\bar{g}Z'\cdot\left[\sqrt{\frac{-\zeta}{\mu}}(j_L^3 - s^2 j_{\rm em}) - s^2(\kappa-\gamma)j_{\rm em}\right]. \qquad (2.20)
\end{aligned}$$

From the coupling of the Z in (2.20), we see that corrections to observables measured at the Z pole are summarized by the quantities δ_Z and ζ, which are given by

$$\delta_Z = \left.\frac{\delta\sin^2\theta}{\sin^2\theta}\right|_{Z\text{ pole}} = -\frac{c^2}{c^2-s^2}\left[\frac{s^2}{c^2-\mu}\mu\kappa^2 + \frac{1-(1+2s^2)\mu}{c^2-\mu}\kappa\gamma - \mu\gamma^2\right], \qquad (2.21)$$

$$\zeta \;=\; -\mu\left(\gamma+\frac{s^2}{c^2-\mu}\kappa\right)^2 \;. \tag{2.22}$$

δ_Z is the fractional deviation of $\sin^2\theta$ that is measured by the Z-pole asymmetries, and ζ (≤ 0) is the fractional deviation of the coupling of the Z to j_L^3. In deriving Eqs. (2.20)–(2.22) we have used the results for δM_W, $\delta\bar{g}$ and δk given in Eq. (2.18).

2.3.3 Neutral-Current Interactions at Low Energy

Experimental constraints on the effective value of $\sin^2\theta$ measured at low energy, via neutrino scattering and atomic parity violation, no longer match the precision of measurements at high energy which constrain δ_Z, ζ and M_W, and thus will not be part of our constraint analysis, which will be the subject of the next section. Nevertheless, such a low-energy measurement of $\sin^2\theta$ can in principle have different sensitivity to Z' bosons, and so we conclude this section by presenting the correction to the low-energy value of $\sin^2\theta$ that would be measured in this model. We can use the results for $\mathcal{L}_{\rm NC}$ to calculate the the neutral-current matrix element, $\mathcal{M}_{\rm NC}$, at zero momentum transfer. To establish notation, we first mention that in the Standard Model, $\mathcal{M}_{\rm NC}$ is given (at tree level) by

$$\mathcal{M}^0_{\rm NC}(q^2\approx 0)=\frac{e^2}{q^2}Q\cdot Q'-4\sqrt{2}G_F(I_3-s_0^2Q)\cdot(I_3'-s_0^2Q')\;, \tag{2.23}$$

where (I_3,Q) and (I_3',Q') stand for the matrix elements of the neutral $\mathrm{SU}(2)_W$ and electromagnetic currents in the external fermionic states. The matrix element including corrections resulting from the W' isotriplet, $\mathcal{M}_{\rm NC}$, is then given at zero momentum transfer by

$$\begin{aligned}\mathcal{M}_{\rm NC}(q^2\approx 0) \;\approx\; & \frac{e^2}{q^2}Q\cdot Q' \\ & -4\sqrt{2}G_F\Big[(I_3-s_0^2(1+\delta_0)Q)\cdot(I_3'-s_0^2(1+\delta_0)Q') \\ & +\left(2\delta_0+\mu(\kappa-\gamma)^2\right)s^2Q\cdot s^2Q'\Big]\;.\end{aligned} \tag{2.24}$$

Here δ_0 is the $q^2=0$ analog of δ_Z:

$$\delta_0=\left.\frac{\delta\sin^2\theta}{\sin^2\theta}\right|_{q^2\approx 0}=\delta_Z+\mu(\kappa-\gamma)\left(\gamma+\frac{s^2}{c^2-\mu}\kappa\right)\;. \tag{2.25}$$

The correction to the coefficient of $Q\cdot Q'$ is unobservable in practice. Note the absence of a correction to the term proportional to $I_3\cdot I_3'$ in $\mathcal{M}_{\rm NC}$, i.e., $\rho(q^2=0)$ is exactly 1 (apart from the usual Standard-Model radiative corrections), which is due to the custodial symmetry and the constraint on G_F measured in low-energy charged-current interactions. This removes some of the possible sensitivity to Z' bosons.

We see that corrections to the low-energy theory due to the W' enter through 4 independent functions of the W' parameters: $\delta M_W/M_W$, ζ, δ_Z, and δ_0. Again it should be noted that all corrections to Standard-Model predictions vanish if any two of the W' parameters κ, γ and μ vanish. As mentioned, the first three of these functions, $\delta M_W/M_W$, ζ and δ_Z, are measured with much greater accuracy than the last, δ_0. We therefore ignore δ_0 in our constraint analysis, which we now present.

2.4 Summary of Corrections in Terms of S, T and U

The above corrections to Standard-Model predictions which result from adding an isotriplet of W' bosons can be conveniently summarized by the S, T and U parameters introduced by Peskin and Takeuchi [7, 8]. At a fundamental level, S, T and U are defined to measure oblique corrections to Standard-Model predictions, i.e., corrections due to non-Standard particles appearing in vacuum polarization graphs for the photon, W and Z. However, at a practical level, S, T and U simply parameterize corrections to the three Standard-Model quantities that are measured with high precision (putting aside α, G_F and M_Z, which are fixed): M_W, the coupling of the Z to j_L^3, and $\sin^2\theta$ measured at the Z pole. Therefore, although corrections due to the W' are in general nonoblique, by comparing the corrections to these three quantities due to the W' with their expressions in terms of S, T and U, we can find the effective contributions of the W' to S, T and U.

Contributions to $\delta M_W/M_W$, δ_Z and ζ are given in terms of S, T and U as [7],

$$\begin{aligned}
\frac{\delta M_W}{M_W} &= \frac{1}{2}\frac{\alpha}{c^2-s^2}\left[-\frac{1}{2}S + c^2 T + \frac{c^2-s^2}{4s^2}U\right] , \\
\delta_Z &= \frac{\alpha}{c^2-s^2}\left[\frac{1}{4s^2}S - c^2 T\right] , \\
\zeta &= \alpha T . \qquad (2.26)
\end{aligned}$$

Equating these expressions with the corresponding expressions for these quantities in terms of the W' parameters, Eqs. (2.18) and (2.22), we obtain the contributions of the W' to S, T and U:

$$\begin{aligned}
\frac{\alpha}{4c^2}S &= -(1-\mu)\tilde{\kappa}(\mu\tilde{\kappa}+\gamma) , \\
\alpha T' &= -\mu(\tilde{\kappa}+\gamma)^2 , \\
\frac{\alpha}{4s^2}U &= \mu(\mu\tilde{\kappa}^2 + 2\tilde{\kappa}\gamma + \gamma^2) . \qquad (2.27)
\end{aligned}$$

Here we have introduced $\tilde{\kappa} \equiv s^2\kappa/(c^2-\mu)$, in terms of which the contributions of the W' to S, T and U can be expressed very concisely. We denote the contribution of the W' to T as T' because there is another important contribution to T, $T_{\rm top}$, due to the top quark. Using these expressions, limits on S, T and U can be converted into limits on the mass and couplings of the W'. However, the contribution to T from the top quark must first be removed, as we now describe.

2.4.1 The Likelihood Function

The electroweak constraints on S, T and U are combined [7] by first constructing χ_0^2:

$$\chi_0^2(S,T,U) = \sum_i \left[\frac{x_i(S,T,U) - x_i^{\rm exp}}{\sigma_i}\right]^2 . \qquad (2.28)$$

Observable	Theoretical Value	Measured Value	Experiment
M_W	80.23 GeV	80.23 ± 0.18 GeV	CDF and D0 [9]; UA2 [10]
$\Gamma(Z \to \text{leptons})$	83.68 MeV	83.96 ± 0.18 MeV	LEP [11]
$\sin^2\theta(M_Z)$	0.2331	0.2317 ± 0.0004	LEP [12]; SLD [13]

Table 2.1: Theoretical and measured values of the electroweak observables used to constrain the W' couplings. The theoretical values correspond to vanishing W' couplings, a top mass of 174 GeV, and a Higgs of mass 1000 GeV (with Standard-Model couplings).

Here the x_i are electroweak observables, namely M_W, the Z width,[3] and $\sin^2\theta(M_Z)$, as shown in Table 2.1. The $x_i(S,T,U)$ are the theoretical predictions for these observables obtained by adding the oblique corrections linear in S, T and U to Standard-Model predictions; x_i^{exp} are the experimental values; and σ_i are the experimental errors. All these are shown in Table 2.1. The theoretical values are given for a 1000 GeV Higgs with Standard-Model couplings. Of course we do not know the mass of the Higgs in the SCSM, though it should be of order the weak scale. Further, unlike the Standard-Model Higgs, the couplings of the SCSM Higgs to the W bosons are unspecified. However, this represent a small uncertainty in the predictions of the SCSM which does not alter our basic conclusions.

As mentioned above, there is a contribution from the top quark to T, which is quadratic in m_t and can be sizable if the top is heavy. (There are also small contributions from the top which are only logarithmic in m_t, which can safely be neglected.) In the absence of information about the top mass, an arbitrarily negative value of T' could be canceled by an opposite, positive value of T_{top} due to a heavy top. In this case, bounds on T would tell us nothing about T', and only the bounds on S and U would constrain the W' parameters.

Of course, we now have information about the top mass from CDF, and we use the result of their fit: $m_t = 174 \pm 16$ GeV [14]. However, the error in this measurement is not negligible, which can be seen by noting that an S-T-U analysis of the Standard Model predicts the top mass with comparable uncertainty. To incorporate the CDF result for m_t, including the error, we convert it to a measurement of T_{top}: $T_{\text{top}} = T^0_{\text{top}} \pm \delta T_{\text{top}}$. We then add a term to χ^2_0,

$$\chi^2_t(S,T',U;T_{\text{top}}) = \chi^2_0(S,T'+T_{\text{top}},U) + \left(\frac{T_{\text{top}} - T^0_{\text{top}}}{\delta T_{\text{top}}}\right)^2 . \tag{2.29}$$

This leads to a likelihood function $L_t(S,T',U;T_{\text{top}}) \equiv N_t \exp[-\chi^2_t/2]$. Since we are here interested in the W' parameters, and not m_t, we integrate over T_{top} to find a likelihood function of S, T' and U alone:

$$L(S,T',U) = \int dT_{\text{top}}\, L_t(S,T',U;T_{\text{top}}) \equiv N \exp[-\chi^2(S,T',U)/2] . \tag{2.30}$$

In $L(S,T',U)$ the only unknowns are μ, κ, and γ, i.e., the W' mass and couplings. We will now exploit this likelihood function to constrain these parameters.

[3] In particular, we use the measurement of the leptonic width of the Z, which is free of the theoretical uncertainties from α_s and $\Gamma_b(Z)$ that plague the hadronic component of the Z width.

2.5 Constraints on a W' in the SCSM

2.5.1 Bounds on $\kappa\gamma$

From the expressions in Eq. (2.27) for S, T' and U in terms of κ, γ and μ, we can derive bounds on the product $\kappa\gamma$. We first express the product $\tilde{\kappa}\gamma$ as

$$\tilde{\kappa}\gamma = -\frac{1}{1-\mu}\frac{\alpha}{4c^2}S - \mu\tilde{\kappa}^2 \ . \tag{2.31}$$

Using $\alpha(T' + U/4s^2) = -\mu(1-\mu)\tilde{\kappa}^2$, we find

$$\kappa\gamma = \frac{c^2-\mu}{1-\mu}\frac{\alpha}{s^2}\left(-\frac{S}{4c^2} + T' + \frac{U}{4s^2}\right) \ . \tag{2.32}$$

Then because $(c^2-\mu)/(1-\mu)$ is at most c^2, $\kappa\gamma$ is bounded as

$$\frac{\alpha c^2}{s^2}\left(-\frac{S}{4c^2} + T' + \frac{U}{4s^2}\right)_{\rm min} < \kappa\gamma < -\frac{\alpha c^2}{s^2}S_{\rm min} \ , \tag{2.33}$$

where in deriving the upper bound we used $\alpha(T' + U/4s^2) = -\mu(1-\mu)\tilde{\kappa}^2 < 0$. Here $S_{\rm min}$ refers to the smallest (nonpositive) allowed value of S. From the 95% Confidence Level (CL) bounds on S and on $(-S/4c^2 + T' + U/4s^2)$, obtained from the likelihood function in Eq. (2.30), we find that

$$-0.049 < \kappa\gamma < 0.0055 \qquad (95\%\ \text{CL}) \ . \tag{2.34}$$

2.5.2 Allowed Region of W' Mass and Couplings

Our remaining results are obtained by exploring the volume of κ-γ-μ space allowed by the likelihood function (2.30). Specifically, we consider points (κ, γ, μ) for which (S, T', U) falls inside an S-T'-U ellipsoid defined by the value of χ^2 corresponding to 95% CL. This maximum allowed value, $\chi^2_{\rm max}$, depends on the number of degrees of freedom being constrained: for just one degree of freedom, $\chi^2_{\rm max} = 4$, which corresponds to two standard deviations, while for two degrees of freedom, $\chi^2_{\rm max} \simeq 6.18$.

A numerical search of the boundary of the allowed region of (κ, γ, μ), defined by $\chi^2 \leq 4$, shows that $\kappa\gamma$ is bounded as

$$-0.028 < \kappa\gamma < 0.0052 \qquad (95\%\ \text{CL}) \ . \tag{2.35}$$

Hence we can state, with a confidence level of 95%, that the W boson must saturate the isovector electromagnetic form factor to within 3%.

Figures 2-2 and 2-3 correspond to slices of the allowed region of (κ, γ, μ) at fixed μ and γ respectively. In Fig. 2-2 we show the allowed regions ($\chi^2_{\rm max} \leq 6.18$) of (κ, γ) for $M_{W'} = 150$ and 400 GeV. These regions necessarily lie inside the hyperbolic bounds (solid lines) which correspond to the extreme values of $\kappa\gamma$ allowed for this value of $\chi^2_{\rm max}$. Note that most of each allowed region corresponds to both κ and γ much smaller than one. However, when either κ or γ is extremely small, the other can become large, particularly when the W' is heavy. This is expected since, as was pointed out in Section 2.2.2, if any two of κ, γ and μ vanish, the remaining quantity is unconstrained.

In Figure 2-3 we show the allowed range of κ ($\chi^2 \leq 4$) as a function of $M_W/M_{W'}$ for

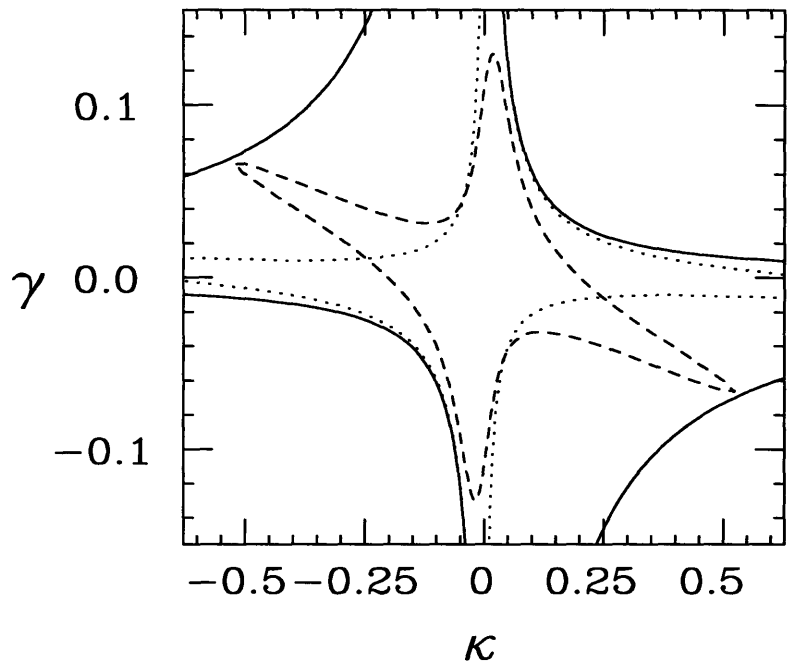

Figure 2-2: Contours bounding the regions of the κ-γ plane allowed at 95% CL for $M_{W'} =$ 150 GeV (dashes) and 400 GeV (dots). The solid lines are hyperbolas defined by the bound on $\kappa\gamma$ at the same value of χ^2.

$\gamma = 1$, 1/2, 1/3 and 1/4. Here we exploit the symmetry noted after Eq. (2.9) — namely invariance under simultaneous change of sign of γ and κ — in order to restrict attention to positive γ. From this Figure we conclude that for reasonable values of γ, κ must be extremely small; in other words the W' must mix much more weakly with the photon than the W. In particular, for $\bar{g}'/\bar{g} > 1/4$, $\kappa < 0.025$.

In Figure 2-4 we show the maximum value of $\bar{g}'$ allowed by our constraints ($\chi^2 \leq 4$) as a function of $M_{W'}$, and we compare our constraints with those obtained in the direct W' search at CDF [15]. Note that our bounds are more restrictive than the CDF bounds. Further, the CDF analysis assumes that the W' decays entirely into left-handed fermions, whereas in the SCSM a W' will primarily decay into WZ for $M_{W'}$ above the decay threshold, $M_W + M_Z$. Hence the CDF bounds do not help us bound γ in the SCSM. Our constraint analysis indicates that at a moderate value of $M_{W'}$ such as 300 GeV, the W' coupling to fermions must be less than a quarter of the W coupling.

2.6 Comparison with an earlier work

Comparing our results with the earlier analysis by Korpa and Ryzak [3], we can see how the continually improving electroweak measurements have drastically pared away the allowed parameter space in this model. In their Figure 4 they found $\kappa\gamma$ allowed to be as large as 0.2, compared to our upper bound of 0.0052. Similarly, for $\gamma = 1$ they found that the W' could be as light as 170 GeV and κ could be as large as 0.13, while for $\gamma = 1$ we now find

that the W' must be heavier than 1075 GeV and κ can be at most 0.006. Moreover, our much more restrictive bounds hold at 95% CL, while the earlier bounds held only at 68% CL.

Korpa and Ryzak concluded from their analysis that there was plenty of room for the non-Standard particle content predicted by the SCSM. From our analysis of the SCSM exploiting recent electroweak data, we conclude that the currently allowed parameter space is so small as to strongly argue against the model. There is no reason to expect vector dominance to hold at a level of 3%. Nor can we understand how the W' could mix with the photon only 1/40 as much as the W mixes; yet we have found that this would have to be the case even if the coupling of the W' to the left-handed fermions is allowed to be as small as 1/4 the W coupling (itself already small for a strongly-coupled theory).

It is possible that by including more resonances in our analysis we could find regions in the enlarged parameter space where the various corrections to Standard-Model predictions cancel, without forcing the masses and couplings of the resonances to be unnaturally small. But from our analysis it is clear that these cancellations would have to be rather delicate, and the agreement of the SCSM with experiment would be just as inexplicable.

Of course, we can never completely exclude the SCSM solely on the basis of experimental constraints. The strongly-coupled dynamics underlying the effective theory do not allow us to find predictions for masses and couplings which could be contradicted by experiment. However, the model offers no natural understanding of how it could continue to evaded detection, disguised as the spontaneously-broken Standard Model. For this reason, we conclude that unless there emerges from a study of the strong dynamics an explanation of how it could be so nearly indistinguishable from the Standard Model, the Strongly-Coupled Standard Model can no longer be viewed as a possible theory of the electroweak interactions.

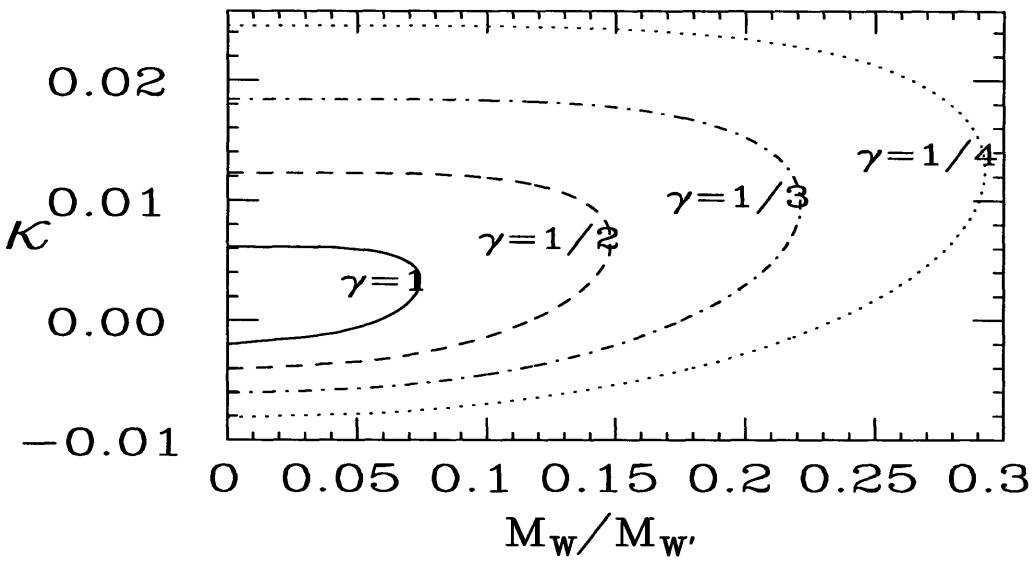

Figure 2-3: Contours bounding the allowed region of the κ-$M_W/M_{W'}$ plane for $\gamma = 1$ (solid), $\gamma = 1/2$ (dashes), $\gamma = 1/3$ (dotdash) and $\gamma = 1/4$ (dots).

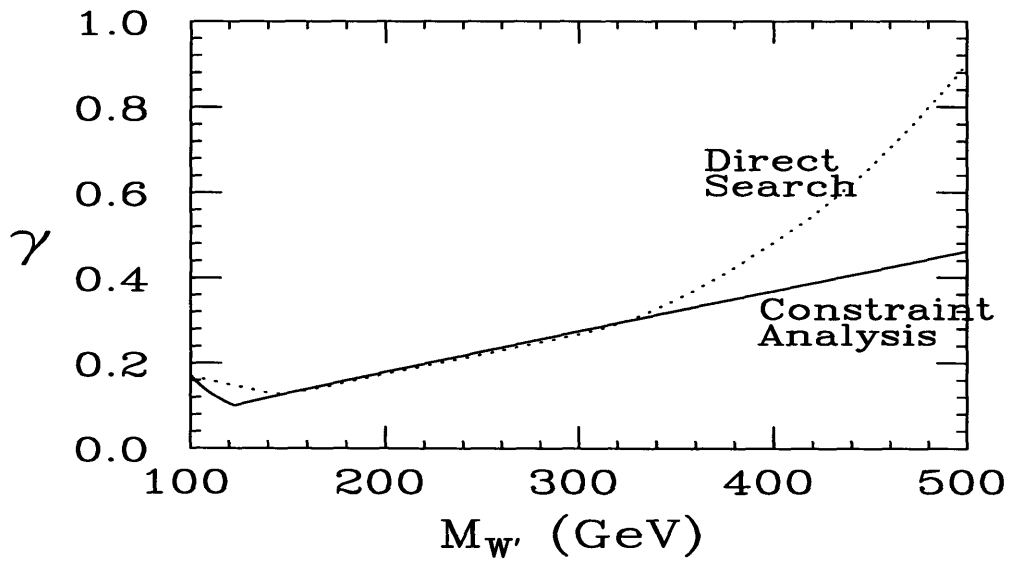

Figure 2-4: Bounds on γ (95% CL) for a range of $M_{W'}$. The dotted curve interpolates through the bounds obtained in the direct W' search at CDF [15] while the solid curve shows the bounds obtained in our analysis of electroweak constraints applied to the SCSM.

Chapter 3

Signatures of Technicolor Models with the GIM Mechanism[1]

In this chapter we investigate the production and the decays of pseudo-Goldstone bosons (PGBs) predicted by technicolor theories with the GIM mechanism (TC-GIM). The TC-GIM models contain exotic fermion families that do not interact under weak $SU(2)$, but they do have color and hypercharge interactions. These fermions form PGBs, which are the lightest exotic particles in the TC-GIM models. The spectrum of PGBs consists of color octets, leptoquarks, and neutral particles. The masses of leptoquarks and color octets depend on a free parameter—the scale of confining interactions. Characteristic for TC-GIM models is a very light ($\approx$1 GeV) neutral particle with anomalous couplings to gauge boson pairs. We show how current experiments constrain the free parameters of the models. The best tests are provided by the $pp \to TT$ and $e^+e^- \to P^0\gamma$ reactions. Experiments at LHC and NLC can find PGBs of TC-GIM models in a wide range of parameter space. However, TC-GIM models can be distinguished from other TC models only if several PGBs are discovered.

Before we explore particular technicolor theories we first summarize the basics of technicolor models [17]. The idea of technicolor is based on spontaneous chiral symmetry breaking similar to the one in QCD. Suppose we consider a two-flavor massless QCD. The Lagrangian for this theory is

$$L = \sum_{f=1,2} \left(i\bar{\psi}^f_L \not{D} \psi^f_L + i\bar{\psi}^f_R \not{D} \psi^f_R \right),$$

where $D_\mu = \partial_\mu - igT^a A^a_\mu$. Classically, this Lagrangian has a $U(2)_L \times U(2)_R$ chiral symmetry of independent rotations of the left- and right-handed fields. Quantum mechanically, only $SU(2)_L \times SU(2)_R \times U(1)_B$ symmetry is preserved, since one of the $U(1)$ symmetries is broken due to anomalies. The QCD interactions break this global symmetry at low energies by forming quark condensates:

$$\langle 0|\bar{\psi}^f_L \psi^g_R|0\rangle = v^3 \delta^{fg}.$$

Therefore, the ground state of the two-flavor QCD preserves only an $SU(2)_V \times U(1)_B$ symmetry instead of the full symmetry of the Lagrangian, where $SU(2)_V$ is the diagonal sum of $SU(2)_L$ and $SU(2)_R$. Consequently, there are three Goldstone bosons associated with the breaking of $SU(2)_L \times SU(2)_R \to SU(2)_V$.

[1] This chapter is based on research reported in Ref. [16].

Suppose that $SU(2)_L$ symmetry is weakly gauged. Below the scale of chiral symmetry breaking the $SU(2)_L$ gauge symmetry is broken. The three Goldstone bosons have non-zero couplings to the currents which couple to the vector bosons of $SU(2)_L$:

$$\langle 0|J^i_{5,\mu}|\Pi^j(q)\rangle = f_\pi \delta^{ij} q_\mu$$

As a result of this coupling the gauge bosons mix with the Goldstone bosons. This mixing modifies the propagators of the gauge bosons to be of the form:

$$\Delta_{\mu\nu} = \frac{g_{\mu\nu} - q_\mu q_\nu/q^2}{q^2(1 - \frac{g^2 f_\pi^2}{4q^2})}.$$

This implies that the pole in the propagator is shifted from $q^2 = 0$ to $q^2 = \frac{f_\pi^2 g^2}{4}$. In this example, all three $SU(2)_L$ vector bosons acquire same masses $M_V = \frac{f_\pi g}{2}$, as a consequence of the remaining global $SU(2)_V$ symmetry.

Let us now gauge an $SU(2)_L \times U(1)_Y$ symmetry, exactly like in the Standard Model. We have two left-handed quark fields forming a doublet of $SU(2)_L$ and two right-handed singlets of $SU(2)_L$, with the following hypercharge assignment: $Y(\psi_L) = 0, Y(\psi^1_R) = \frac{1}{2}$ and $Y(\psi^2_R) = -\frac{1}{2}$. The condensate breaks $SU(2)_L \times U(1)_Y$ gauge symmetry $U(1)_{EM}$, and we get $Q = Y + T_3$ like in the Standard Model with a Higgs doublet. Also, as in the Standard Model the gauge bosons obtain masses: $M_W = \frac{1}{2} g f_\pi$, $M_Z = \frac{1}{2}\sqrt{g^2 + g'^2} f_\pi$ and $M_\gamma = 0$. It is easy to check that, at the lowest order, $M_W^2/(M_Z^2 \cos^2\theta) = 1$, where $\cos\theta = \frac{g}{\sqrt{g^2+g'^2}}$. This relation is the result of the $SU(2)_V$ symmetry, which is an analog of the custodial symmetry of the Higgs sector. If instead of QCD, which has $f_\pi \approx 93$ MeV, we take a theory with $f_\pi \approx 250$ GeV we achieved appropriate pattern of gauge symmetry breaking without introducing the Higgs scalar. This idea is simple and compelling but it does not solve all the problems the Higgs sector does. The fermions in such theory are still massless.

One needs to introduce additional interactions that communicate symmetry breaking to the quarks and leptons. The most popular scenario for generating fermion masses in technicolor theories is the so-called extended technicolor sector. Extended technicolor (ETC) is based on interactions under which both ordinary fermions and technifermions transform [18]. Suppose that those interactions are broken at some high scale Λ_{ETC}. At low energies, one would observe effective four-fermion interactions of the form $\frac{1}{\Lambda^2_{ETC}} \bar\psi_L \gamma^\mu T_L \bar T_R \gamma_\mu \psi_R$, where ψ's denote Standard Model fermions, while T's technifermions. This effective interaction creates mass terms for the Standard Model fields:

$$\bar\psi_L \psi_R \frac{\langle \bar T_R T_L\rangle}{\Lambda^2_{ETC}}.$$

Unfortunately, the same interactions also create four-fermion interactions among quarks, $\frac{1}{\Lambda^2_{ETC}} \bar\psi_L \gamma^\mu \psi_L \, \bar\psi_R \gamma_\mu \psi_R$, which are of the same magnitude as the mass-generating ones. Since the top quark is heavy, Λ_{ETC} cannot be much larger than 1 TeV in this simple scenario. This leads to unacceptably large flavor-changing neutral currents [19].

While introducing fermion masses via extended technicolor interactions we ran into trouble with flavor-changing neutral currents. We also did not explain what breaks the extended technicolor interactions. Realistic models must overcome both difficulties. Yet, there are more limitations on viable technicolor theories, which are imposed by measurements of the electroweak parameters[7, 8].

In the next section we outline the characteristic features of TC-GIM model. In Section 3.2, we begin with a short introduction to the TC-GIM models and explain various possible realizations of the light fermion sectors. In Section 3.3, we present the spectrum of the PGBs and their couplings to ordinary particles. Section 3.4 contains the discussion of the PGB phenomenology. We leave some remarks about the scales of the interactions that confine the light fermions until Section 3.5.

3.1 Motivation for TC-GIM

An interesting solution to the problems of TC models we mentioned are models which incorporate the Glashow-Iliopoulous-Maiani (GIM) mechanism [20]. The first technicolor models that used GIM mechanism to avoid unacceptably large flavor-changing neutral currents were the composite technicolor standard models [21]. These models realize the GIM mechanism by separating the ETC interactions into several ETC groups. There are separate ETC groups for the left-handed fermion fields, the right-handed up quarks, and the right-handed down quarks. Such construction introduces a large global symmetry associated with quark flavor. This flavor symmetry is the essence of the GIM mechanism. Breaking of the global symmetry is responsible for the fermion masses and the quark mixing—the existence of the Kobayashi-Maskawa matrix. However, the composite technicolor models presented in Ref. [21] were toy models of weak interactions, since the models did not incorporate leptons.

Realistic technicolor models with the GIM mechanism were described in Refs. [22] and [23]. We will refer to these models as technicolor-GIM models (TC-GIM). Not only do the TC-GIM models avoid trouble with the flavor-changing neutral currents, but they also limit the number of technifermion doublets to one, thereby avoiding conflict with precise electroweak measurements [7, 8]. Having only one $SU(2)$ doublet of technifermions is important for maintaining small contributions to the S parameter. TC-GIM models also can accommodate approximate custodial symmetry [24], which guarantees that the ρ parameter is sufficiently close to one [22]. A noticeable feature of these models is the presence of exotic light fermions. From the point of view of a model builder, the most difficult task is to create a model with an appropriate pattern of breaking flavor and gauge symmetries. The symmetry breaking is achieved by introducing numerous heavy fermion fields and gauge bosons. The light fermions that were mentioned before exist in the TC-GIM models only to cancel certain anomalies. In QCD-like models the light fermions seem to be a necessary ingredient. Since the light fermions are a necessary feature of TC-GIM models, their signatures are the best place to test and study this kind of models.

In the following sections we explore the phenomenological consequences of the light fermion sector. The light fermions transform under the ETC groups and also some additional confining interactions. The scale of confining interactions, depending on a particular model, can be from tens to hundreds of GeV. Below the confinement scale, there are pseudo-Goldstone bosons (PGBs) in the particle spectrum whose constituents are the light fermions. The PGBs are the lightest exotic particles in the spectrum of the TC-GIM models. While present experiments put a lower bound on the scale of the confining interactions, future experiments may find signatures of the PGBs. The light fermions, constituents of the PGBs, do not transform under the ordinary $SU(2)_L$ gauge group. Their interactions with the quarks and leptons are mediated by the ETC gauge bosons.

PGBs in TC-GIM have a different origin than PGBs in other types of TC models. Usually, PGBs are associated with chiral symmetry breaking by the technicolor group. In

TC-GIM models, PGBs arise from dynamical breaking of symmetry by some new gauge interactions. Of course, the TC group also breaks chiral symmetries of technifermions. However, in TC-GIM, there is only one doublet of technifermions and the Goldstone bosons become longitudinal degrees of freedom of the $W^{\pm}$ and the Z. TC-GIM models, like any other TC models, have techni-ρ mesons, but these are heavier than the technicolor scale and more difficult to observe than PGBs. Therefore, the PGBs are the best test of TC-GIM models. If PGBs are discovered and some of their properties are known, it will be possible to distinguish between different TC scenarios.

We investigate the phenomenology of PGBs in the TC-GIM models described in Refs. [22] and [23]. In those models, PGBs arise from breaking of $SU(12)$ global symmetry groups. Such symmetries are not essential for implementing the GIM mechanism [21]. These large global symmetry groups were chosen in order to have only one doublet of technifermions, and consequently small contributions to the S parameter [7, 8]. Current electroweak data no longer favors negative values of S. Therefore, a larger number of technifermion doublets may be allowed. It might be possible to construct TC-GIM models that posses a smaller set of global symmetries. However, we are not aware of any successful attempt in constructing such models.

3.2 TC-GIM models

The basic building blocks of the TC-GIM models are $SU(N)$ gauge groups and chiral fermions. Because many gauge groups are necessary, a special notation "moose notation" is helpful in describing these models [25]. An $SU(N)$ gauge group is represented by a circle. Fermions in the (anti-)fundamental representation are depicted by an (in-)out-going line. A fermion line connecting two circles represents fermions transforming under both gauge groups depicted by the circles. A line whose one end is not connected to any circle indicates that the fermions transform under a gauge group and a global symmetry group. A graphic illustration of these ideas is presented in Fig. 3-1, where a simple moose diagram represents three fermion fields transforming under two global groups and two gauge groups. When referring to fermion fields, we will label the fermions $[NM]$, where N and M stand for $SU(N)$ and $SU(M)$ groups under which the fermions transform.

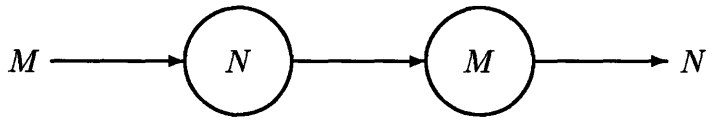

Figure 3-1: An example of moose diagram. The circles represent $SU(N)$ and $SU(M)$ gauge groups, the lines represent fermion fields. Line endings without circles represent global symmetry groups — SU(M) and SU(N).

All gauge groups are guaranteed to be anomaly-free by having the same number of in-going and outgoing fermion lines. This way, all fermions transforming under a given gauge group form a vector representation, which is anomaly-free. The requirement of anomaly cancellation is how the light fermions find their way into TC-GIM models. The ETC gauge groups would not be anomaly-free without these additional fermions.

The structure of a TC-GIM model described in Ref. [22] is illustrated in Fig. 3-2. The gauge groups are ordered by their scale, with the lowest scale groups at the bottom of the

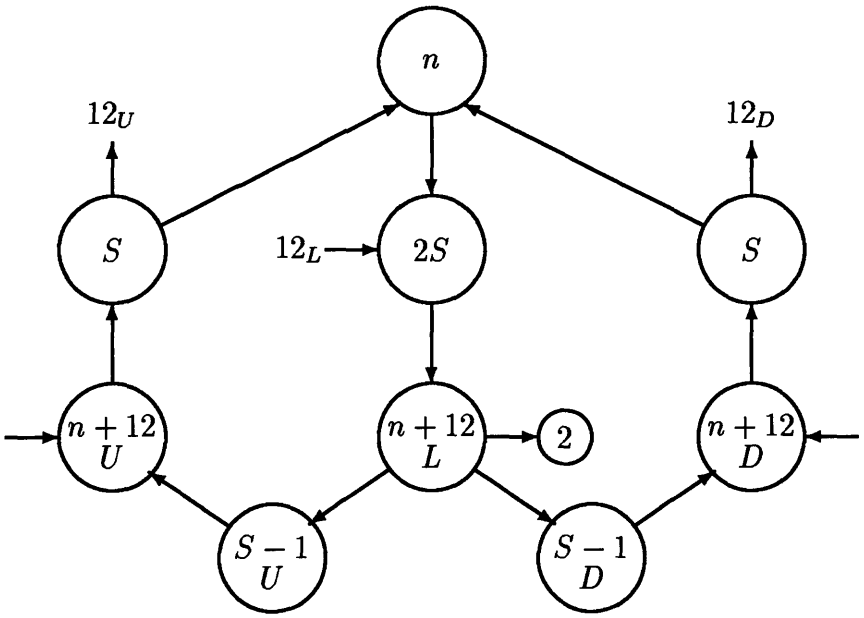

Figure 3-2: The full TC-GIM model with a low-scale PGB sector.

moose. There are two $SU(S-1)$ groups labeled U and D. The fermions transforming under these groups are the light fermions forming PGBs. The single $SU(2)$ group is the familiar group of weak interactions. The model contains three separate ETC groups: one for the left-handed quarks and leptons, one for the right-handed down quarks and charged leptons, and one for the right-handed up quarks and neutrinos. These are the three $SU(N+12)$ groups. N is the number of techni-colors, while 12 is the number of left-handed doublets of quarks and leptons. The fact that there are right-handed neutrinos in the model does not present any problem. There exist several plausible mechanisms to ensure small masses of the neutrinos [22]. The two $SU(S)$'s together with the $SU(2S)$ and $SU(N)$ groups at the top of the moose are the highest scale groups. They break the ETC groups and merge several $SU(N)$ subgroups into one technicolor $SU(N)$. As usual, the technifermion condensates break the weak $SU(2)$. The characteristic scales associated with different ETC groups do not have to be related. Since the value of the ρ parameter is close to 1, only small violations of custodial symmetry [24] are allowed. It is possible not to violate custodial symmetry if the ETC scales of the up and down sectors are degenerate [22]. We will not elaborate on the details of the TC-GIM model building, instead we refer the reader to Refs. [22] and [23]. The $[n+12_L, 2]$ fermions include all left-handed quarks and leptons, and also one technifermion doublet. The right-handed quarks and leptons are contained in the $[n+12_U, 1]$ and $[n+12_D, 1]$ fermion lines.

3.2.1 Light fermions in TC-GIM

We will focus on the PGBs formed from fermions transforming under $SU(S-1)$ groups. The $SU(S-1)$ groups have to become strongly interacting at some scale, otherwise there would be massless or very light fermions (with masses comparable to those of leptons and quarks) present in the particle spectrum. The scale of the $SU(S-1)$ interactions is not related to the technicolor scale. In most technicolor models, the lightest exotic particles

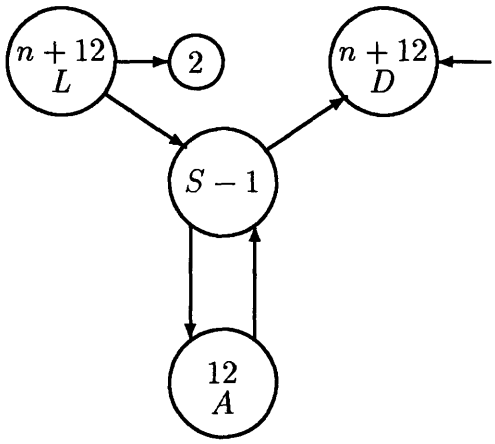

Figure 3-3: High-scale model of the PGB sector.

are PGBs formed by technifermions. Such PGBs form when the TC group dynamically breaks chiral symmetries of the technifermions. The same process gives masses to the electroweak gauge bosons, thus the scale of these PGBs is related to the scale of electroweak symmetry breaking. The situation is different in TC-GIM models. PGBs are created when the $SU(S-1)$ interactions form fermion condensates. Therefore, the scale at which PGBs form in TC-GIM models is a free parameter but there are both upper and lower bounds on its value. It cannot be too low in order to avoid conflict with experiments. On the other hand, too large a scale would give too large contributions to lepton and quark masses, or be so high as to upset the hierarchy of symmetry breaking. We postpone the discussion of these problems to Sec. 3.5, after we discuss the phenomenological constraints.

There are several possibilities for constructing the light-fermion sectors. The one illustrated in Fig. 3-2 is characterized by a relatively low scale of the $SU(S-1)$ interactions. We will later show that this specific model cannot accommodate heavy PGBs. In particular, the lightest leptoquarks have to be lighter than approximately 50 GeV, therefore the low-scale model is ruled out. From now on, we will suppress the structure of the models irrelevant to PGB study, showing only parts of the moose we are interested in: the ETC groups, the ordinary fermions and the light-fermion sector. The up and down sectors of the moose are identical so it is enough to describe any one of the two sectors.

A model similar to the one presented in Fig. 3-2 was also presented in Ref. [22]. We illustrate the relevant part in Fig. 3-3. This model is characterized by a higher scale of the $SU(S-1)$ interactions. The difference between this model and the one introduced before is the addition of $[12_A, S-1]$ and $[S-1, 12_A]$ fermion fields. When the $SU(S-1)$ interactions become strong, we assume that the $[12_A, S-1]$ fermions form condensates with the $[S-1, n+12_D]$ fermions. Likewise $[n+12_L, S-1]$ fermions form condensates with the $[S-1, 12_A]$. This is clearly not the only possibility. If the $[n+12_L, S-1]$ fermions formed a condensate with the $[S-1, n+12_D]$ fermions, this model would not be very different from the model depicted in Fig. 3-2.

It is possible to construct models whose light fermion sectors have unambiguous vacuum state. Such a model was introduced in Ref. [23], whose relevant part we reproduce in Fig. 3-4a. A variation of such a model is illustrated in Fig. 3-4b. There are two separate $SU(S-1)$ groups in these models. For simplicity, we assume that both groups are characterized by the same scale, but it would not present any difficulties to deal with different scales. In these models, the $[12_A, S-1_2]$ fermions form condensates with the $[S-1_2, n+12_D]$ fermions,

and similarly $[n+12_L, S-1_1]$ with $[S-1_1, 12_A]$. We will refer to the model illustrated in Fig. 3-2 as the low-scale model, because the scale of $SU(S-1)$ interactions in this model has a strong upper bound. All other models presented here avoid that upper limit, so we will refer to them as the high-scale models.

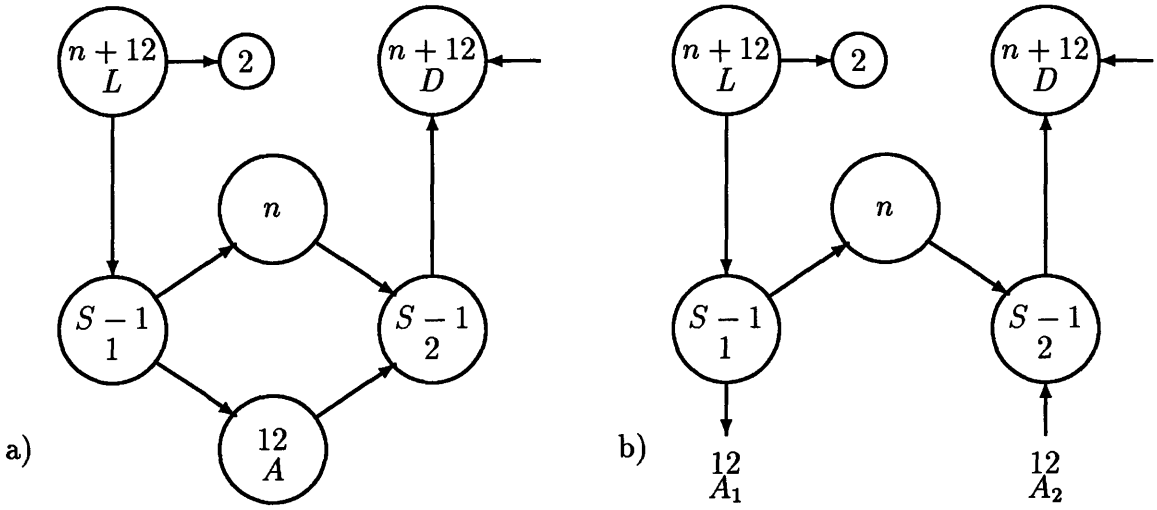

Figure 3-4: High-scale models of PGB sectors without vacuum-alignment ambiguity.

In the limit where there is no lepton mixing and the K-M matrix is diagonal, there are separate conserved lepton and quark numbers for each flavor of quarks and leptons. The exotic fermions transform under the global $U(1)$ symmetries associated with the flavor numbers. Therefore, we can attribute flavor to the exotic fermions and, consequently, refer to them as 'exotic electron' or 'exotic top quark', etc. The exotic and usual fermions carry the same quantum numbers of color and electric charge, however the exotic fermions are always singlets of the weak $SU(2)_L$.

3.3 Spectrum and couplings of Pseudo-Goldstone bosons

We will now describe the PGBs formed below the scale of the $SU(S-1)$ interactions. We first enumerate the PGBs and estimate their masses. We then derive the couplings of the PGBs to ordinary quarks, leptons and gauge bosons. In what follows, we use chiral Lagrangian techniques. Such a description is valid for the momenta of the PGBs smaller than the chiral symmetry breaking scale of the $SU(S-1)$ interactions.

3.3.1 Symmetry breaking patterns

In the low-scale model, the PGBs are associated with the breaking of the $SU(12) \times SU(12)$ flavor symmetry, where the $SU(12)$ groups are subgroups of $SU(n+12)$ ETC groups. The $SU(12)^2$ global symmetry breaks down to $SU(12)$, so there will be $12^2-1 = 143$ PGBs. The symmetry group of the high-scale models is $SU(12)^4$. This group is dynamically broken to $SU(12)^2$, doubling the number of the PGBs. Not all bosons remain in the particle spectrum, some may be eaten by the Higgs mechanism. The $SU(12)^2$ or $SU(12)^4$ are not exact symmetries. Once we take into account symmetry breaking interactions, the PGBs will acquire masses.

We describe here the PGBs formed in the sector associated with the down quarks. Precisely the same analysis applies to the up sector. The $SU(12)$ symmetries contain the ordinary color $SU(3)$ gauge group. The exotic quarks and leptons have the same charge assignment as the quarks and leptons. Therefore, there exist two flavor $SU(3)$ symmetries embedded in the $SU(12)$. These symmetries are associated with independent rotations in the (d,s,b) and (e,μ,τ) spaces, where we use the same letters to describe the ordinary or exotic fermions.

Let Q_c and L denote flavor $SU(3)$ triplets:

$$Q_c = \begin{pmatrix} d_c \\ s_c \\ b_c \end{pmatrix}, \; L = \begin{pmatrix} e \\ \mu \\ \tau \end{pmatrix}$$

and λ^i denote the Gell-Mann matrices, normalized such that $Tr(\lambda^i\lambda^j) = \frac{1}{2}\delta^{ij}$. The upper index refers to flavor space; the lower one to color space.

We classify the PGBs according to the embedding of the $SU(3)_{color} \times SU(3)_Q \times SU(3)_L$ symmetry in the $SU(12)$ group. The spectrum of PGBs is a straightforward generalization of the spectrum in the old one-family technicolor model [26]. The 143 PGBs can be written as the following combinations of fields

$$\begin{array}{ll}
\theta_a^i \sim \sqrt{2}\bar{Q}\gamma_5\lambda_a\lambda^i Q, & \\
\theta_a \sim \frac{1}{\sqrt{3}}\bar{Q}\gamma_5\lambda_a Q, & \\
T_c^i \sim \sqrt{2}\bar{Q}_c\gamma_5\lambda^i L, & \bar{T}_c^i \sim \sqrt{2}\bar{L}\gamma_5\lambda^i Q_c, \\
T_c \sim \frac{1}{\sqrt{3}}\bar{Q}_c\gamma_5 L, & \bar{T}_c \sim \frac{1}{\sqrt{3}}\bar{L}\gamma_5 Q_c, \\
\Pi^i \sim \frac{1}{2}\left(\bar{Q}\gamma_5\lambda^i Q + \bar{L}\gamma_5\lambda^i L\right), & \\
P^i \sim \frac{1}{2\sqrt{3}}\left(\bar{Q}\gamma_5\lambda^i Q - 3\bar{L}\gamma_5\lambda^i L\right), & \\
P^0 \sim \frac{1}{6\sqrt{2}}\left(\bar{Q}\gamma_5 Q - 3\bar{L}\gamma_5 L\right), &
\end{array} \tag{3.1}$$

where $i,a = 1,\ldots,8$ and $c = 1,2,3$. Whenever a flavor or color matrix is omitted, it should be understood that the identity matrix is present in the relevant space.

The 64 θ_a^i bosons and 8 θ_a are color octets. The 48 $T_c^i, \bar{T}_c^i$ and the 6 $T_c, \bar{T}_c$ are color triplets. The T's carry both quark and lepton numbers. We will refer to them as leptoquarks. There are also 17 color singlet states, which are the Π^i, P^i and P^0. Color singlet and octet states do not carry electric charges, the leptoquarks have charge $-\frac{2}{3}e$ ($+\frac{2}{3}e$ for the leptoquarks in the up sector). The spectrum of the high-scale models is a simple replication of the spectrum just described.

3.3.2 Masses

In order to estimate masses of the PGBs, we need to itemize terms that break the $SU(12)$ global symmetries. In the low-scale model there is an explicit mass term for the exotic fermions. The mass term originates from multi-fermion operators [22]. Let

$$\Sigma = \exp\left(2iT_a\pi^a/f_{S-1}\right) \tag{3.2}$$

be the nonlinear representation of the PGBs where T_a are the $SU(12)$ matrices. Let L and D be the $SU(12)$ subgroups of the ETC groups $SU(N+12)_L$ and $SU(N+12)_D$ under

which ordinary fermions transform linearly

$$\psi_L \to L\psi_L \text{ and } d_R \to Dd_R. \tag{3.3}$$

Then Σ transforms in the following manner

$$\Sigma \to L^\dagger \Sigma D. \tag{3.4}$$

The mass matrix for the exotic fermions is related to the mass matrix for the quarks and leptons: $M = m\left(\frac{f_{ETC}}{v_{TC}}\right)^2$, where f_{ETC} is the scale of the ETC interactions, v_{TC} is the value of the technicolor condensate, which is approximately 250 GeV while m is the mass matrix for the down quarks and charged leptons. The lowest-order contribution to the PGBs masses comes from the term

$$v_{S-1}^3 tr(\Sigma^\dagger M) + h.c., \tag{3.5}$$

which gives the following mass-squared matrix:

$$(\Delta m_{ab})^2 = 8\frac{v_{S-1}^3}{f_{S-1}^2} tr\left(T_a T_b M\right). \tag{3.6}$$

Color and electromagnetic interactions also break the $SU(12) \times SU(12)$ symmetry. The standard approach in computing the color and electromagnetic contributions is to rescale the electromagnetic mass splitting in the $\pi^\pm - \pi^0$ system [27]. For the charged pions the leading effect comes from a one-photon exchange. An exchange of one gluon is similar in structure, except for different coupling constant and some $SU(3)$ group factors. Therefore, the contribution to the color octet (triplet) masses can be related to the pion mass difference

$$\frac{(\Delta m_\theta)^2}{m_{\pi^\pm}^2 - m_{\pi^0}^2} = \left(\frac{f_{S-1}}{f_\pi}\right)^2 \frac{\alpha_{QCD}(f_{S-1})}{\alpha_{em}} 3 \quad (\frac{4}{3}), \tag{3.7}$$

where the factor of 3 applies to the octet pseudos and $\frac{4}{3}$ to the triplets. The numerical value of this contribution to the masses of the color octet PGBs is

$$\Delta m_\theta \approx \left(\frac{f_{S-1}}{15\text{GeV}}\right) 45\,\text{GeV}. \tag{3.8}$$

Electromagnetic contributions to the leptoquark masses can be computed in the same manner. Of course, instead of group theory factors there is a factor of $\frac{4}{9}$, which is the charge squared.

The scale f_{S-1} cannot exceed 15 GeV in case of the low-scale model. We will later explain how this bound is obtained. Consequently, the lightest PGB in this model is the color singlet boson associated with symmetry breaking by the electron mass and its mass is about 1 GeV. The lightest leptoquarks in this model have masses approximately 50 GeV. Such a low-scale model is therefore ruled out, as we will show in the next chapter when we discuss leptoquark searches. However, in the high-scale models, the scale of the $SU(S-1)$ interactions can be much larger. Of course, the same formula holds for the contributions to the masses from color and electromagnetic interactions. Therefore, the leptoquarks and the octet particles can be quite heavy with masses of the order of several hundred GeV's.

We now estimate the masses of the PGBs in the high-scale models presented in Figs. 3-3

and 3-4a. We describe contributions arising from breaking of the $SU(12)_L$ and $SU(12)_D$ symmetries by fermion mass terms. These contributions are different from the ones in the low-scale model. The high-scale models do not contain multi-fermion operators that could give explicit mass terms for the light fermions. Instead, the flavor dynamics is generated at a high scale, and its low-energy manifestation is the mixing among the ETC gauge bosons in different ETC groups. Such a mixing generates the same masses for the ordinary fermions and the light ones.

As mentioned before, we assume that in the model of Fig. 3-3 certain fermion condensates form. The $[12_A, S-1]$ fermions form condensates with the $[S-1, n+12_D]$, and $[n+12_L, S-1]$ with $[S-1, 12_A]$. In the model presented in Fig. 3-4a this assumption is fulfilled automatically. As before, we describe the PGBs in terms of their nonlinear representations Σ_1 and Σ_2. Σ_1 refers to the condensate of $[12_A, S-1]$ and $[S-1, n+12_D]$ fermions, Σ_2 to the condensate of $[n+12_L, S-1]$ and $[S-1, 12_A]$.

The Σ_i matrices have the following transformation properties

$$\Sigma_1 \to A_1^\dagger \Sigma_1 D \text{ and } \Sigma_2 \to L^\dagger \Sigma_2 A_2. \tag{3.9}$$

The gauge group A is weakly gauged, so the two sets of fermion fields $[12_A, S-1]$ and $[S-1, 12_A]$ can transform independently. The $SU(12)\times SU(12)$ group of $A_1 \times A_2$ transformations is broken by small terms proportional to the gauge coupling of A. The mass term for the quarks, leptons and the exotic fermions transforms as

$$m \to L^\dagger m D, \tag{3.10}$$

and the generators of the $SU(S-1)_A$ group transform both under the A_1 and A_2 matrices:

$$T_A^a \to A_1^\dagger T_A^a A_1 \text{ and } T_A^a \to A_2^\dagger T_A^a A_2 \tag{3.11}$$

Having written all the symmetry properties, we are ready to estimate the masses of the PGBs. The lowest-order term contributing to the masses has the form

$$\frac{\alpha_{S-1}}{4\pi} f_{S-1}^2 \, tr\left(\Sigma_2 T_A^a \Sigma_2^\dagger m \Sigma_1^\dagger T_A^a \Sigma_1 m^\dagger\right). \tag{3.12}$$

Such a contribution arises from the diagram illustrated in Fig. 3-5a. This term gives masses to the linear combination of PGBs: $\pi_+^a = \frac{1}{\sqrt{2}}(\pi_1^a + \pi_2^a)$, where the mass matrix squared is

$$\Delta m_{ab}^2 = \frac{\alpha_{S-1}}{2\pi} \left[tr(m)\, tr(T_a T_b m) - tr(T_a m)\, tr(T_b m)\right]. \tag{3.13}$$

The above equation reveals an interesting feature of the PGBs spectrum in this model. The contribution to masses of the PGBs from the term in Eq. 3.12 does not depend on the scale of $SU(S-1)$ interactions. Thus, the masses of the neutral PGBs do not depend on the scale f_{S-1} in the lowest order. The estimate for the masses depends on the value of α_{S-1} and an unknown coefficient of order one. For instance, let us evaluate Eq. 3.13 using the flavor matrix corresponding to the P^0 boson from Eq. 3.1, and the masses of the down quarks and charged leptons. This gives the following estimate for the mass of the down-type P^0: $m_{P^0}^2 \approx \alpha_{S-1} \frac{1}{3\pi} m_b m_\tau$, where m_b and m_τ are the masses of the b quark and the τ lepton. Numerically, the mass squared of the P^0 boson is about $1\,\mathrm{GeV}^2$ times α_{S-1}. Of course, there are also higher-order contributions to the PGBs masses. These can arise from the exchange of the ETC gauge bosons. Such terms will be proportional to additional powers

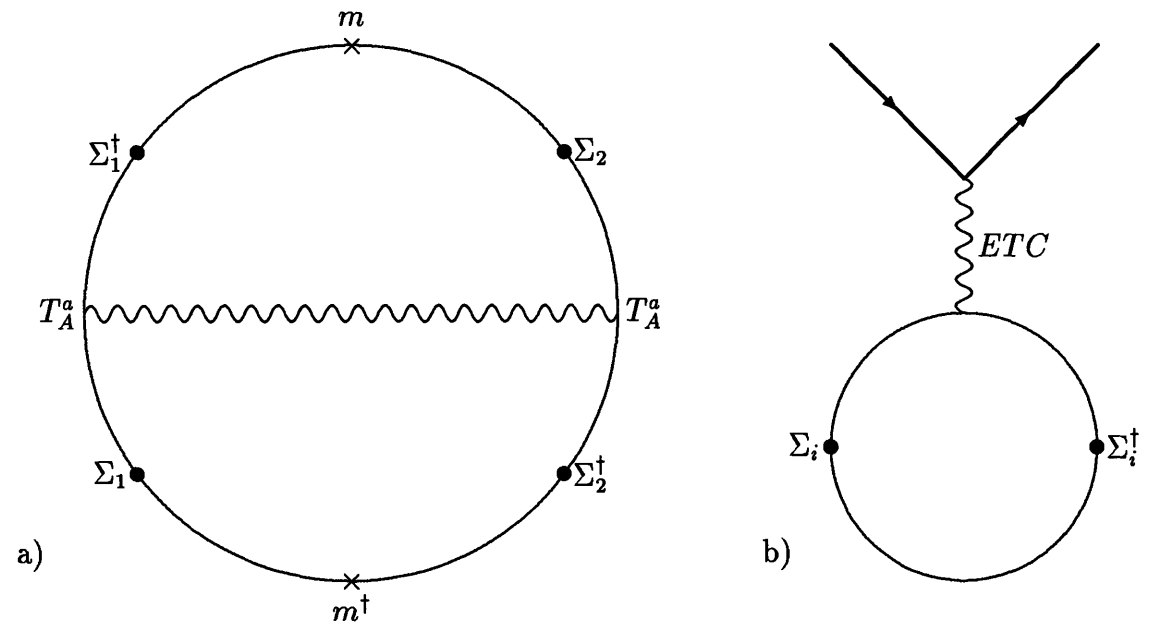

Figure 3-5: a) Diagram contributing to the masses of PGBs in the high-scale models. b) Diagram contributing to the PGB-fermion couplings in the high-scale models.

of $\frac{f_{S-1}^2}{f_{ETC}^2}$ which are significant only for a very large f_{S-1}.

The masses of color octet and triplet states will be much larger due to the gluon exchange contributions described in Eq. 3.7. The orthogonal combination $\pi_-^a = \frac{1}{\sqrt{2}}(\pi_1^a - \pi_2^a)$ remains massless. The π_-^a bosons are the would-be Goldstone bosons which are eaten when the group A gets broken. A is completely broken below the scale of the $SU(S-1)$ interactions. The only unbroken gauge symmetry at low energies are color $SU(3)$ and hypercharge $U(1)$, color group is a linear combination of $SU(3)$ subgroups of the A group and the ETC groups. Thus, the spectrum consists of 143 PGBs, which is the same number as in the low-scale model.

A qualitatively different mass spectrum might be the feature of the high-scale model described in Fig. 3-4b. In this model, the masses of the fermions transforming under $SU(S-1)$ are unrelated to the masses of quarks and leptons. The masses of the neutral PGBs can arise only from explicit mass terms for the $[12_1, S-1_1]$ and $[S-1_1, n+12_D]$ fermions, and mass terms for the $[n+12_L, S-1_2]$ and $[S-1_2, 12_2]$. Such mass terms can result from four-fermion operators created at some very high scale.

Multi-fermion operators are inevitable in the TC-GIM models. Without their presence it is impossible to generate a nontrivial Kobayashi-Maskawa mixing matrix. A non-diagonal form of the mixing matrix implies that independent flavor symmetries for right-handed and left-handed fermions are completely broken. One cannot achieve such breaking by mass terms only, as such terms always leave several $U(1)$ symmetries [21]. The multi-fermion operators are assumed to be generated at some high scale, perhaps as a result of fermion compositeness or some other mechanism. Specific operators needed for generating the Kobayashi-Maskawa matrix are listed in Refs. [22] and [23]. It is plausible that those are not the only multi-fermion operators present in this model. Additional operators may generate masses for the light fermions. For instance, the mass term for the $[12_1, S-1_1]$ and

$[S-1_1, n+12_D]$ fermions can be generated by the operator

$$\frac{1}{f_F^2}[12_1, S-1_1][S-1_1, n+12_D][n+12_D, S_D][S_D, 12_2],$$

where we have used the notation introduced in Fig. 3-2 and f_F is the scale at which such operators arise. When $SU(S_D)$ interactions become strong, this operator gives a mass term with magnitude proportional to $4\pi f_S^3/f_F^2$.

Although we do not know the particular form of the mass matrix, we can estimate an upper bound on the magnitude of its elements. The scale of $SU(S)$ and $SU(2S)$ interactions is the same as the scale at which the ETC groups get broken, since the mechanism that triggers breaking of the ETC groups is the dynamical breaking of $SU(S)$ and $SU(2S)$ symmetries. Therefore, the exotic fermions have masses not larger than

$$0.04\,\mathrm{GeV}\,(\frac{f_{ETC}}{1.5\mathrm{TeV}})^3\,(\frac{1000\mathrm{TeV}}{f_F})^2. \tag{3.14}$$

The form of the term contributing to the masses of the PGBs is identical to the one in Eq. 3.5; the mass matrix should be replaced with the mass matrix for the relevant exotic fermions. As a result, the contributions to the masses cannot exceed approximately $8\,\mathrm{GeV}\sqrt{\frac{f_{S-1}}{15\,\mathrm{GeV}}}$. For the neutral PGBs this is the only contribution, and it can be treated as an upper bound on their masses. Of course, in order to obtain masses of colored PGBs, one should add independent contributions to the square of PGBs masses. In this case, the above contribution from explicit breaking terms has to be added to the gluon exchange contribution described in Eq. 3.7.

3.3.3 Couplings

We now describe the couplings of the PGBs to the quarks and leptons. The symmetry properties of the quarks, leptons and the low-scale PGBs allow very simple invariant couplings:

$$\frac{4\pi f_{S-1}^3 v_{TC}^2}{f_{ETC}^4}\,(\bar{\psi}_L \Sigma d_R + \text{ h.c.})\,, \tag{3.15}$$

where the coefficient $\frac{v_{TC}^2}{f_{ETC}^4}$ reflects the fact that such operator is created by ETC interactions. The lowest-dimension term in the above equation is the contribution of the $S-1$ condensate to the masses of the ordinary fermions. Such a contribution cannot be larger than the electron mass, which limits the scale f_{S-1} to be less than 15 GeV. Given this constraint, the masses of PGBs are small, such that the Tevatron experiments should see signals of leptoquarks. We want to make leptoquarks as heavy as possible, saturating the bound, and then see if such PGBs can evade detection. Therefore, we assume that the factor $\frac{4\pi f_{S-1}^3 v_{TC}^2}{f_{ETC}^4}$ is numerically equal to the electron mass.

The PGBs in the high-scale models exhibit dramatically different couplings to the quarks and leptons. Such couplings are generated by diagrams of the type presented in Fig. 3-5b. The relevant terms are:

$$\left(\frac{f_{S-1}}{f_{ETC}}\right)^2 \bar{\psi}_L \gamma^\mu (\partial_\mu \Sigma_2)\Sigma_2^\dagger \psi_L \text{ and } \left(\frac{f_{S-1}}{f_{ETC}}\right)^2 \bar{d}_R \gamma^\mu (\partial_\mu \Sigma_1)\Sigma_1^\dagger d_R \tag{3.16}$$

Thus, the PGBs couple derivatively to the quarks and leptons. We should mention here that these couplings are quite different from couplings predicted for PGBs in other technicolor models [28, 29]. In generic TC models, the couplings are non-derivative and proportional to the fermion masses. Typically, they are of the form

$$\frac{m_q}{f_\Pi}\,\Pi\,\bar{q}\gamma_5 q.$$

Such terms have a large magnitude for the coupling to the top quark. In TC-GIM models the magnitudes of couplings are much smaller and are also suppressed by the momentum of PGBs. This difference in couplings invalidates bounds on PGBs and leptoquarks obtained by the studies of flavor-changing neutral currents mediated by those particles [30, 31].

The PGBs also couple to gauge bosons. We describe both the minimal couplings of charged or colored particles and couplings arising from the anomalies. The constituents of the PGBs are singlets of the weak $SU(2)$ interactions, thus the PGBs do not couple to the $W^\pm$ bosons. Couplings to the photon and the Z^0 originate from the hypercharge interactions. The lowest-order couplings are contained in the kinetic energy term for the PGBs

$$\begin{aligned} L_{kin} &= \tfrac{f_{S-1}^4}{4} tr\left[(D^\mu\Sigma)^\dagger(D_\mu\Sigma)\right], \\ D_\mu\Sigma &= \partial_\mu\Sigma + ieA_\mu[Q,\Sigma] + ie\tan(\theta_W)Z_\mu[Q,\Sigma] + ig_3G_\mu^a[\lambda_a,\Sigma], \end{aligned} \tag{3.17}$$

where θ_W is the Weinberg angle and Q is the fermion charge matrix. Only the leptoquarks couple to the photon and the Z^0, while other PGBs are neutral.

The anomalous couplings are restricted to particles that are singlets with respect to flavor symmetries. Thus, the P^0 is the only particle that couples to a photon pair. Color octet bosons θ_a couple both to a pair of gluons and to a photon and a gluon. A general coupling of a PGB to a pair of gauge bosons can be written [32] as

$$(S-1)A\frac{g_1g_2}{\pi^2 f_{S-1}}\epsilon_{\mu\nu\rho\sigma}k_1^\mu k_2^\nu\epsilon_1^\rho\epsilon_2^\sigma, \tag{3.18}$$

where k_i and ϵ_i are the momenta and polarizations of the gauge bosons, g_i are the coupling constants. Below, we list all the coefficients of non-vanishing anomalous couplings:

$$\begin{aligned} A_{P^0\gamma\gamma} &= \tfrac{(-2,1)}{3\sqrt{2}} \quad A_{P^0g_ag_b} = \tfrac{1}{16\sqrt{2}}\delta_{ab} \\ A_{\theta_ag_bg_c} &= \tfrac{\sqrt{3}}{8}d_{abc} \quad A_{\theta_ag_b\gamma} = \tfrac{(-1,2)}{4\sqrt{3}}\delta_{ab}\,. \end{aligned} \tag{3.19}$$

The coefficient d_{abc} is the $SU(3)$ symmetric structure constant. The constants $A_{P^0\gamma\gamma}$ and $A_{\theta_ag_b\gamma}$ are different for the up and down sectors because the charge matrices in those sectors are not identical. The first number in parenthesis refers to the down sectors and the second one to the up sector. Obviously, the Z^0 coupling has the same structure as the photon coupling. Therefore, every photon field in the above equations can be replaced by Z^0, while the electric charge is replaced by $e\tan\theta_W$.

3.4 Decays, production rates and signatures

In this section we describe decays of the PGBs and discuss various production mechanisms at both electron and hadron colliders. We present predictions for the operating machines – LEP, HERA and Tevatron, and also for the planned colliders: upgraded Tevatron, LHC

and NLC. The section ends with a comparison of PGBs' features in TC-GIM models with other technicolor scenarios.

The PGBs decay dominantly into fermion-antifermion pairs, but the decay widths are model dependent. In the low-scale model, decays are governed by the couplings described in Eq. 3.15 and the corresponding decay widths are

$$\begin{aligned}\Gamma_{low}(\Pi^a \to f_i\bar{f}_j) &= \frac{2m_e^2|T_{ij}^{\Pi^a}|^2}{\pi M_{\Pi^a}^2 f_{S-1}^2} k\left(\sqrt{k^2+m_i^2}\sqrt{k^2+m_j^2}+k^2+m_i m_j\right) \\ &\approx \begin{cases} \frac{m_e^2|T_{ij}^{\Pi^a}|^2}{2\pi}\frac{M}{f_{S-1}^2}\sqrt{1-\frac{4m^2}{M^2}} & \text{for } m_i \approx m_j = m \\ \frac{m_e^2|T_{ij}^{\Pi^a}|^2}{2\pi}\frac{M}{f_{S-1}^2}(1-\frac{m^2}{M^2})^2 & \text{for } m_i \ll m_j = m \end{cases}\end{aligned} \tag{3.20}$$

where $k^2 = \frac{(M-m_i-m_j)(M-m_i+m_j)(M+m_i-m_j)(M+m_i+m_j)}{4M^2}$, and T^{Π^a} are $SU(12)$ matrices described in Eq. 3.1. These decay widths do not depend, except for the kinematical factors, on fermion masses. For decays into two fermions much lighter than a Π^a, the decay width equals approximately $0.18\,\mathrm{eV}\,|T_{ij}^{\Pi^a}|^2\,(\frac{15\,\mathrm{GeV}}{f_{S-1}})^2\,\frac{M_{\Pi^a}}{1\,\mathrm{GeV}}$. The scale of the $SU(S-1)$ interactions is restricted in low-scale model to be less than 15 GeV, so all PGBs are very short-lived and decay inside a detector.

The high-scale PGBs couple derivatively to the quarks and leptons, as described in Eq. 3.16. The resulting decay widths are

$$\begin{aligned}\Gamma_{high}(\Pi^a \to f_i\bar{f}_j) &= \frac{f_{S-1}^2}{f_{ETC}^4}\frac{|T_{ij}^{\Pi^a}|^2 k}{2\pi M_{\Pi^a}^2}[(m_i^2+m_j^2)(M_{\Pi^a}^2-m_i^2-m_j^2)+4m_i^2m_j^2] \\ &\approx \begin{cases} \frac{f_{S-1}^2}{f_{ETC}^4}\frac{|T_{ij}^{\Pi^a}|^2}{2\pi}m^2M\sqrt{1-\frac{4m^2}{M^2}} & \text{for } m_i \approx m_j = m \\ \frac{f_{S-1}^2}{f_{ETC}^4}\frac{|T_{ij}^{\Pi^a}|^2}{4\pi}m^2M(1-\frac{m^2}{M^2})^2 & \text{for } m_i \ll m_j = m \end{cases}\end{aligned} \tag{3.21}$$

These decay widths are proportional to the masses squared of the fermions in the final state. This is a result of chiral suppression, similar to the familiar $\pi^+ \to \mu^+\nu_\mu$ decay. PGBs decays into fermions are caused by the ETC interactions, which preserve lepton and quark flavor. Therefore, the PGBs decay into quarks and leptons of the same flavor as PGBs constituents. The partial width of the P^0 decay into a $\mu^+\mu^-$ pair equals approximately $1.5\cdot 10^{-5}\,\mathrm{eV}\frac{M}{1\,\mathrm{GeV}}(\frac{f_{S-1}}{15\,\mathrm{GeV}})^2(\frac{1.5\,\mathrm{TeV}}{f_{ETC}})^4$. We frequently use P^0 as an illustration because this particle couples to pairs of photons and gluons, and therefore its properties will be very important later on. It is very interesting that PGBs in the high-scale models are also very narrow resonances, even the heaviest scalars have widths smaller than 1 GeV.

Few PGBs have anomalous couplings to gluons and photons. The couplings are described in Eqs. 3.18 and 3.19. The resulting widths of PGBs decays into a pair of massless vector bosons are

$$\Gamma(\Pi^a \to V_iV_j) = |A_{\Pi^aV_iV_j}|^2\,\frac{g_i^2g_j^2}{32\pi^5}\,(S-1)^2\,\frac{M^3}{f_{S-1}^2}\,\frac{1}{1+\delta_{V_iV_j}}. \tag{3.22}$$

For example, the width of the decay $P^0 \to \gamma\gamma$ equals $0.16\,\mathrm{eV}\,(S-1)^2\,(\frac{M}{1\,\mathrm{GeV}})^3\,(\frac{15\,\mathrm{GeV}}{f_{S-1}})^2$.

We present a summary of the particle spectrum of the high-scale models in Table 1. We list the dimension of $SU(3)_C$ representation the PGBs belong to, their masses and major decay modes. Which decay modes dominate depends on the scale of $SU(S-1)$ interactions and particle masses. The heavier the particle the more important the decays into vector

particle	$SU(3)$	mass [GeV]	decay modes
θ_a^i	8	45 $(f/15)$	$q\bar{q}$
θ_a	8	45 $(f/15)$	$gg, \gamma g, q\bar{q}$
T_c^i, T_c	3	31 $(f/15)$	ql
Π^i, P^i	1	0.1–5	$q\bar{q}, l\bar{l}$
P^0	1	1	$gg, q\bar{q}, l\bar{l}$

Table 3.1: The particle spectrum in the high-scale models.

bosons are, since their widths grow with the mass cubed, while the widths of fermionic decays are linearly proportional to PGBs masses. The scale f_{S-1} suppresses decays into vector bosons, while it enhances fermionic decay modes, compare Eqs. 3.21 and 3.22.

3.4.1 Electron Colliders

Charged PGBs can be pair-produced in e^+e^- collisions. Charged bosons, which are only leptoquarks, couple both to the photon and to the Z^0 with coupling described in Eq. 3.17. Thus, the leptoquarks can be produced at the Z^0 peak and also at energies above the Z^0 mass, where both photon and Z^0 exchanges contribute to the production rate. The decay width of a Z^0 into a pair of leptoquarks is

$$\Gamma(Z^0 \to T\bar{T}) = \alpha \left(\frac{2}{3}\tan\theta_W\right)^2 \frac{M_Z}{4}\left(1 - \frac{4m_T^2}{M_Z^2}\right)^{\frac{3}{2}}. \tag{3.23}$$

Signatures of such events are quite distinct, each leptoquark decays into a hadronic jet and an isolated lepton. The events would have two opposite-sign leptons, two hadronic jets and no missing energy. The main background comes from the $Z^0 \to b\bar{b}$ decays, followed by semileptonic decays of both b quarks. However, the event shape is different and the background can be efficiently rejected. Searches performed at LEP exclude pair-produced leptoquarks up to 45.5 GeV [33], which is almost the kinematic limit. The limit reported in Ref. [33] does apply to leptoquarks in our model, even though both the coupling to the Z^0 and decay modes differ. The couplings of the Z^0 to a pair of leptoquarks in our model and leptoquarks in superstring-inspired models [33] result in cross sections that are numerically very close. Leptoquarks in our model have larger charge, but they do not interact weakly, and the two effects roughly compensate. The decay mode $T \to de^+$ is experimentally indistinguishable from the mode $T \to \bar{u}e^+$, which was searched for at LEP.

There are two production mechanisms of single PGBs at the Z^0 pole. A Z^0 can decay into a fermion pair, and subsequently a PGB is radiated off a fermion line. Such a mechanism is model dependent, since the magnitudes of couplings of PGBs to fermions are not dictated by the gauge invariance. Corresponding decay widths in the low-scale model are

$$\begin{aligned}&\Gamma_{low}(Z^0 \to f_i\bar{f}_j\Pi^a) = \\ &\left(\frac{g\, m_e}{\cos\theta_W f_{S-1}}\right)^2 |T_{ij}^{Pi^a}|^2 \frac{(g_V^2+g_A^2)M_Z}{576\pi^3}(-17 + 9r + 9r^2 - r^3 - 6\log r - 18r\log r),\end{aligned} \tag{3.24}$$

where $r = (\frac{m_{\Pi^a}}{M_Z})^2$. Meanwhile, $g_V = \frac{1}{2}T_3 - Q\sin^2\theta_W$ and $g_A = \frac{1}{2}T_3$ are vector and axial couplings of the Z^0 to an $f_i\bar{f}_i$ pair. We assumed that fermion masses are negligible

compared to the Z^0 mass. The decay rate diverges as the mass of the scalar particle approaches zero, which is a result of divergent fermion propagator when a light scalar is being emitted collinearly with the fermion. However, for reasonable values of PGB masses, even as light as 1 GeV, this decay width is orders of magnitude too small for such a process to be observed.

PGBs couplings to fermions are different in the high-scale models, so the decay width has a different form

$$\Gamma_{high}(Z^0 \to f_i \bar{f}_j \Pi^a) = \left(\frac{g f_{S-1} M_Z}{\cos\theta_W f_{ETC}^2}\right)^2 |T_{ij}^{Pi^a}|^2 \frac{(g_V \mp g_A)^2 M_Z}{1152\pi^3} (1 + 9r - 9r^2 - r^3 + 6r\log r + 6r^2 \log r), \tag{3.25}$$

where $g_V - g_A$ applies to the PGBs that couple to right-handed fermions, and $g_V + g_A$ to left handed ones. PGBs in the model described in Figs. 3-3 and 3-4a are linear combinations of both types of PGBs, they couple to the left and right-handed fermions. This decay width is not divergent for small masses of the scalar, the coupling of the scalar is proportional to its momentum, which annihilates divergence of the fermion propagator. For light PGBs the decay width can be approximated as $\Gamma(Z^0 \to f_i \bar{f}_j \Pi^a) \approx 0.13 \cdot 10^{-7}\text{GeV} \left(\frac{f_{S-1}}{150\,\text{GeV}}\right)^2 \left(\frac{1.5\,\text{TeV}}{f_{ETC}}\right)^4 |T_{ij}^{Pi^a}|^2$, which is too small to be observed at LEP. In principle, this process could provide an upper bound on the scale f_{S-1}. If the scale f_{S-1} is very large, of the order of 1 TeV, and at the same time the scale of the ETC interactions is also around 1 TeV, some events could be observed at LEP. However, such a case is not too interesting, because the hierarchy of symmetry breaking in the model would not work as expected. Such a small decay width of the Z^0 into a PGB and a fermion pair makes this process impossible to observe at LEP. Mass limits on singly-produced leptoquarks presented in Ref. [33] assume a different form of PGBs' couplings to fermions. Therefore, those limits are not valid in the TC-GIM models.

Other sources of PGBs production are anomalous couplings to a Z^0 and a photon. The width of the Z^0 decay into a PGB and a photon has been calculated in Ref. [34]. We use their results together with anomaly factors from Eq. 3.19 and obtain the decay width

$$\begin{aligned} \Gamma(Z^0 \to P^0\gamma) &= \left(\frac{A_{\gamma\gamma}^{P^0}(S-1)}{f_{S-1}}\right)^2 \frac{\alpha^2 \tan^2\theta_W}{6\pi^3} M_Z^3 \left(1 - \frac{m_{P^0}^2}{M_Z^2}\right)^3 \\ &= 1.9\,10^{-5}\text{GeV}\,(S-1)^2 \left(\frac{15\text{GeV}}{f_{S-1}}\right)^2 \left(1 - \frac{m_{P^0}^2}{M_Z^2}\right)^3 \times (4,1), \end{aligned} \tag{3.26}$$

where 4 refers to the down-type P^0 and 1 to the up-type. This decay rate is large enough to constrain the scale of the $SU(S-1)$ interactions. For numerical estimates we will assume that $S = 4$. The signature of such events is quite unique – an isolated monoenergetic photon and P^0 decay products. A one GeV P^0 boson in the high-scale models decays most likely into a small number of pions or a pair of K mesons, therefore the events are characterized by very low hadron multiplicity. Such a signature is similar to the signature of the $Z^0 \to \eta'\gamma$ decays, where the η' decay products contain a $\pi^+\pi^-$ pair. The ALEPH Collaboration reported that the $BR(Z^0 \to \eta'\gamma)$ is less than $4.2 \cdot 10^{-5}$[35]. Assuming that the branching ratio of the decays $P^0 \to \pi^+\pi^- X$ is at least 50%, same bound can be placed on the branching ratio of the $Z^0 \to P^0\gamma$ decays. Using Eq. 3.26 this branching ratio translates to a lower limit of 38 GeV on f_{S-1}. At the time of the analysis the ALEPH collaboration collected only $8.5\,\text{pb}^{-1}$ of integrated luminosity. Currently, the LEP experiments have data

from over $100\,\mathrm{pb}^{-1}$. If all the data were analyzed one could place a limit of 10^{-5} on the $BR(Z^0 \to P^0\gamma)$. Such a limit corresponds to exploring the scale f_{S-1} up to 80 GeV. For the high-scale model depicted in Fig. 3-4b, we obtain a similar number. Even if P^0 is as heavy as it could possibly be, given the estimate in Eq. 3.14, the lower limit on f_{S-1} is 75 GeV. The bound of 80 GeV would surpass the results from the Tevatron, where experiments currently probe f_{S-1} up to 65 GeV.

We now turn our attention to future e^+e^- colliders — LEP2 operating above the W^+W^- threshold and a collider with the CM energy of 500 GeV, which is one of the options for the proposed Next Linear Collider. We assume that LEP2 will collect $500\,\mathrm{pb}^{-1}$ of integrated luminosity per year of running [36] and the NLC will achieve its design luminosity of $50\,\mathrm{fb}^{-1}$ per year [37, 38].

The most obvious process to look for is pair production of leptoquarks. The cross section for this process is

$$\begin{aligned} \sigma(e^+e^- \to T\bar{T}) &= \xi \left(\tfrac{2}{3}\right)^2 \tfrac{\pi\alpha^2}{s} \left(1 - \tfrac{4m^2}{s}\right)^{3/2}, \\ \xi &= \left(1 + \tfrac{g_V}{\cos^2\theta_W(1-y)}\right)^2 + \left(\tfrac{g_A}{\cos^2\theta_W(1-y)}\right)^2, \end{aligned} \tag{3.27}$$

where $\frac{2}{3}$ is the leptoquark charge, $y = \frac{m_Z^2}{s}$, g_V and g_A are the vector and axial couplings of the Z^0 to an e^+e^- pair. The reaction is mediated by both photon and Z^0 exchanges, which are both included in the derivation of Eq. 3.27 and manifest as the factor ξ. Such a simple result for the two diagrams and their interference is caused by the simplicity of the Z^0 couplings to the exotic particles. The Z^0 couples exactly the way photon does with the coupling multiplied by $\tan\theta_W$. The signatures of such events are relatively easy to disentangle from the backgrounds. Therefore, leptoquarks can be discovered if their masses are only few GeV smaller than the kinematic limits. The potential for leptoquark discovery can be translated into limits on the scale f_{S-1} using the leptoquark mass estimate from Eq. 3.7. LEP2 can probe the scale f_{S-1} up to 45 GeV while NLC up to 120 GeV.

Single PGB production via anomaly coupling is a process whose importance grows with energy. The anomaly coupling of a PGB and two vector bosons is proportional to vector boson momentum, so the production cross section does not decrease with $\sqrt{s}$. The cross section for producing a P^0 and a photon equals

$$\begin{aligned} \sigma(e^+e^- \to \gamma P^0) &= \xi \frac{2\alpha^3(S-1)^2}{3\pi^2 f_{S-1}^2} (A_{\gamma\gamma}^{P^0})^2 \left(1 - \frac{m_{P^0}^2}{s}\right)^3 \\ &\approx 3.7\,\mathrm{fb}\,(S-1)^2 \left(\frac{15\,\mathrm{GeV}}{f_{S-1}}\right)^2 \left(1 - \frac{m_{P^0}^2}{s}\right)^3 \times (4,1), \end{aligned} \tag{3.28}$$

where, again, 4 refers to the down-type P^0 and 1 to the up-type one. The study of this process at LEP2 will not provide any new information beyond what we already know from the Z^0 decays, the luminosity will be too small to produce any events. If f_{S-1} is smaller than about 200 GeV dominant decay modes of P^0 are hadronic. For larger values of f_{S-1} the $P^0 \to \mu^+\mu^-$ will dominate. This is a great help in the detection of P^0 as $\mu^+\mu^-$ pairs are measured with large efficiency and good angular resolution. The signature is then a monoenergetic photon and a $\mu^+\mu^-$ pair with the invariant mass about 1 GeV. Such events have very little background, so we assume that as few as 10 produced P^0 bosons are enough to be detected. Consequently, the NLC is likely to probe the scale of $SU(S-1)$ interactions up to 390 GeV. As before, limits on the f_{S-1} scale in the model depicted in Fig. 3-4b are

at most few GeV lower than the limits in other high-scale models. One can also look for P^0 produced together with a Z^0. The corresponding cross section

$$\sigma(e^+e^- \to Z^0P^0) = \tan^2\theta_W \xi \frac{2\alpha^3(S-1)^2}{3\pi^2 f_{S-1}^2}(A_{\gamma\gamma}^{P^0})^2(1-\frac{(m_Z+m_{P^0})^2}{s})^{\frac{3}{2}}(1-\frac{(m_Z-m_{P^0})^2}{s})^{\frac{3}{2}} \tag{3.29}$$

is about 28% of that for $e^+e^- \to \gamma P^0$. This process can be useful only for relatively small scales f_{S-1}, not larger than 100 GeV. A large number of events is needed because the Z^0 can be measured precisely only in leptonic channels, whose branching ratios are small.

3.4.2 Hadron Colliders

There are variety of processes in which the PGBs can be produced in hadron colliders. Gluon-gluon and quark anti-quark annihilations are sources of PGB pair production. Quark-gluon fusion produces single PGBs. The production of single PGBs via anomalous couplings to two gluons is also a possibility. Unfortunately, neutral PGBs, with the exception of P^0, do not have large enough production rates to be observed in hadron collisions. PGBs' couplings to fermions are too small to give significant cross section. For this reason, HERA does not provide any information about PGBs in the TC-GIM models.

The cross section for the pair production of PGBs has been calculated in Ref. [39] for the general case of scalar particles in the D-dimensional representation of color $SU(3)$. The quark anti-quark fusion cross section is

$$\frac{d\sigma}{d\hat{t}}(q\bar{q} \to \Pi\Pi) = \frac{2\pi\alpha_s^2}{9\hat{s}^2} k_D \beta^2(1-z^2) \tag{3.30}$$

and for gluon-gluon annihilation

$$\frac{d\sigma}{d\hat{t}}(gg \to \Pi\Pi) = \frac{2\pi\alpha_s^2}{\hat{s}^2} k_D \left(\frac{k_D}{D} - \frac{3}{32}(1-\beta^2z^2)\right)\left(1-2V+2V^2\right). \tag{3.31}$$

In the above formulas, k_D is the Dynkin index of the D-dimensional representation ($k_3 = \frac{1}{2}$, $k_8 = 3$), z is the cosine of parton scattering angle in the center of mass,

$$V = 1 - \frac{1-\beta^2}{1-\beta^2z^2} \quad \text{and} \quad \beta^2 = 1 - \frac{4m_\Pi^2}{\hat{s}},$$

while $\hat{s}$ and $\hat{t}$ are Mandelstam variables for the annihilating partons. Using these formulas and parton distributions from Ref. [40] (set 1), we obtain production rates for leptoquarks and octet particles. The cross sections are presented in Figs. 3-6 and 3-7, which agree with the results of Refs. [39, 41].

Leptoquarks are a feature of many extensions of the Standard Model [42]. Several conclusions about leptoquark searches do apply to TC-GIM models. For instance, pair production of leptoquarks is almost model independent. Since gluon-gluon annihilation dominates over quark anti-quark annihilation, the production rates do not depend on leptoquarks' couplings to quark pairs. There is a difference, however: in most models leptoquarks decay into a quark and a lepton of the same generation. In the TC-GIM models, the leptoquarks carry lepton and quark numbers of any generation. There are single-generation leptoquarks, but there exist leptoquarks that mix different generations as well.

A leptoquark decaying into an electron and a d quark has the same signature as the

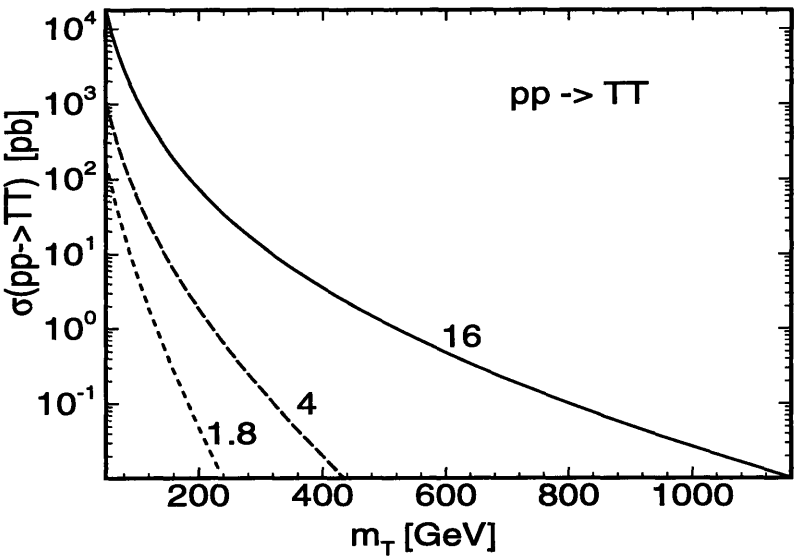

Figure 3-6: The cross section for pair production of leptoquarks in pp collisions. The three curves correspond to $\sqrt{s} = 1.8$, 4 and 16 TeV.

so-called first generation leptoquark. The first generation leptoquarks decay into an electron and a first generation quark with branching ratio β or into a neutrino and a quark with branching ratio $1 - \beta$. The experimental limits depend on the unknown ratio β. The down-type leptoquarks in the TC-GIM models have $\beta = 1$, while the up-type ones have $\beta = 0$. The strongest limit on the leptoquark masses has been obtained by the D0 Collaboration [43]. Their results exclude down-type leptoquarks up to 130 GeV. The second generation leptoquarks are excluded up to 133 GeV [44]. These results limit the scale f_{S-1} to be larger than approximately 65 GeV. That is why, as we previously claimed, the low-scale model is excluded.

The signatures of pair-produced leptoquarks are quite unique. Hundred $T\bar{T}$ pairs should suffice to discover leptoquarks at the $\sqrt{s} = 4$ TeV upgraded Tevatron. Using the cross sections from Fig. 3-6, we estimate that the upgraded Tevatron can push the leptoquark mass limit up to 440 GeV, when $10\,\text{fb}^{-1}$ is collected in one year of running [45]. At the LHC, one expects CM energy of 16 TeV and the integrated luminosity of $100\,\text{fb}^{-1}$ per one year of running [46], so the LHC can discover leptoquarks up to approximately 1160 GeV. Thus, the f_{S-1} scale can be probed up to 215 GeV at the upgraded Tevatron and up to 560 GeV at the LHC.

We now turn our attention to color-octet particles. The production cross sections for octets are about an order of magnitude larger than those for leptoquarks due to color factors. Unfortunately, the detection of octet particles is difficult. Octet PGBs decay into two hadronic jets, so pair-produced octets yield four-jet signals. The QCD four-jet production is the main source of background, the QCD resulting rate has been estimated [47], and it is quite large. The authors of Ref. [48] have studied four-jet processes as a probe of new physics signals. They propose certain kinematic variables designed to study such events. First, out of the three possible groupings of four jets into pairs the one that gives most equal invariant masses is chosen. The average of the two invariant masses, called balanced doublet mass, is an important parameter in the study. Then, a strong cut on the transverse jet momentum is imposed. The value of the transverse momentum cut depends on the mass of the particle one looks for. The QCD background peaks at approximately $3p_T^{min}$,

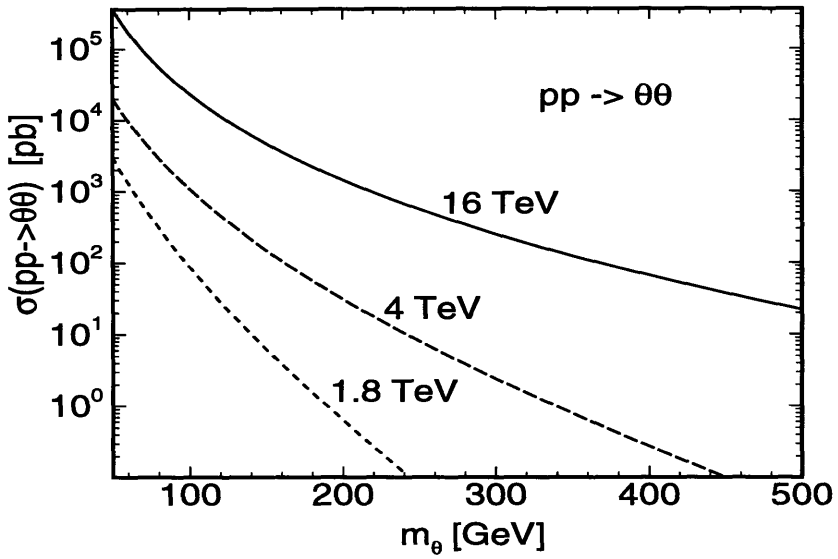

Figure 3-7: The cross section for pair production of color-octet PGBs in pp collisions. Different curves correspond to the CM energy at the Tevatron, upgraded Tevatron and the LHC.

so particles lighter than $3p_T^{min}$ can be observed by using such a cut. An excess of events on the balanced-doublet mass plot would be a signal of pair-produced octet particles. The authors conclude that a 375 GeV octet PGBs can be detected at the LHC.

This is a rather modest discovery potential given the fact that octet particles are about 1.5 times heavier than the leptoquarks. TC-GIM models have 18 different color-octet particles, nine in each sector. If these octet particles are nearly degenerate in mass they may give a stronger signal. However, if the mass splittings are comparable to the invariant mass resolution of four-jet signals, the situation might be more complicated since a wider peak is more difficult to disentangle from the background. The search for the octet particles will be interesting only if the upgraded Tevatron discovers leptoquarks lighter than 250 GeV. Then, one can expect to see signals of color octet particles at the LHC.

There are several sources of single PGB production in hadron colliders. A process that gives quite a large ratio is gluon-gluon annihilation into P^0. We compute the production cross section using the narrow width approximation:

$$\frac{d\sigma}{dy}(pp \to P^0 X) = \frac{\pi^2}{8s} \frac{\Gamma(P^0 \to gg)}{m_{P^0}} f_g(\sqrt{\tau}e^y) f_g(\sqrt{\tau}e^{-y}), \tag{3.32}$$

where $\tau = \frac{m_P^2}{s}$. The cross sections of P^0 productions are depicted in Fig. 3-8. Since the width of the $P^0 \to gg$ decay is inversely proportional to f_{S-1}^2, so is the production rate. Despite the fact that the cross section is quite large, a light P^0 cannot be detected in hadron colliders. A one GeV P^0 decays predominantly into pions. Such a process does not stand out from QCD background. The branching ratio for the $P^0 \to \gamma\gamma$ decay is about 2%, which still does not help much. A one GeV P^0 would decay into two almost collinear photons, which cannot be distinguished. Such a light P^0 cannot be observed at high energy hadron colliders.

PGBs can also be produced by the quark-gluon fusion. However, the relevant Feynman diagrams always involve PGBs coupling to fermion pairs. Such couplings are too small to

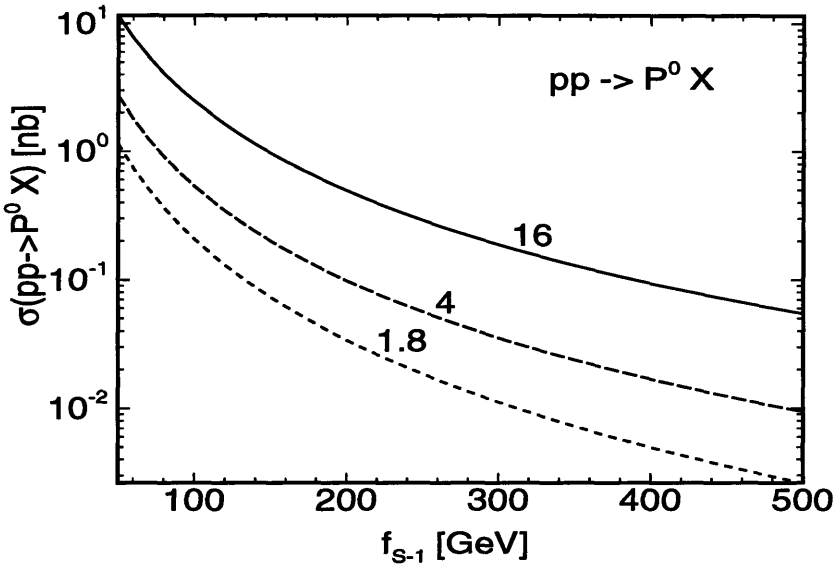

Figure 3-8: The cross section for P^0 production in pp collisions as a function of the f_{S-1} scale. The curves correspond to $\sqrt{s}$ = 1.8, 4 and 16 TeV.

give significant cross sections.

3.4.3 PGBs in TC-GIM versus other technicolor models

In this subsection we summarize the properties of PGBs in the high-scale models presented in Figs. 3-3 and 3-4a. We list their masses, dominant decay modes and recall the most suitable reactions for the detection. We compare the results with generic one-family, QCD-like model [26, 29, 49, 39] and walking technicolor [28]. This is by no means an exhaustive survey of PGBs in TC scenarios. We take two examples to show the similarities and stress the differences of TC-GIM models.

Color octet particles in TC-GIM models receive the dominant contribution to their masses from the one-gluon exchange. The masses of color octet particles can range from 190 GeV to 2 TeV if the scale f_{S-1} is large, where the dependence of the mass on the scale f_{S-1} is described by Eqs. 3.7 and 3.8. The lower bound comes from the fact that leptoquarks lighter than 130 GeV are excluded, which implies that f_{S-1} is larger than 65 GeV. The octet particles decay into two jets. Their production cross sections in pp collisions are depicted in Fig. 3-7, the cross sections are large. However, the signature of pair-produced octets is a four-jet signal that has a large QCD background [47]. The LHC will be able to observe color octet PGBs if they are lighter than 375 GeV [48], while lower energy hadron colliders have no chance of discovering octet PGBs.

Color octet particles are also present in other TC models. Their signatures are identical to the ones of TC-GIM. However, the expected mass range is not as large as in TC-GIM models because the scale of TC interactions that create PGBs is related to the scale of the electroweak symmetry breaking. In the one-family model, one expects the octet particles to have masses between 200 GeV and 400 GeV [26, 49]. In walking TC models, all PGBs receive large masses from ETC interactions. These interactions are characterized by a large scale due to walking. The octet particles in walking TC models are expected to have masses in the 200-500 GeV range [28]. The production cross section for octet particles

is dominated by the gluon-gluon fusion. Such process is governed entirely by couplings that are restricted by the gauge invariance (Eq. 3.17). Consequently, the production rate is almost model independent, so the observation of color-octet PGBs does not distinguish the models. For some choices of parameters, in walking TC models color octet PGBs can be produced more copiously than in the TC-GIM models due to techni-ρ meson decays into color octets [28]. If color-octet particles are discovered one expects the observation of leptoquarks, whose masses are 1.5 times smaller than that of octet PGBs.

Color triplet particles in TC-GIM models also receive dominant mass contribution from the one-gluon and one-photon exchanges. Their masses are bounded by Tevatron experiments to be larger than 130 GeV [43, 44], while the upper limit is as high as 2 TeV. The masses of leptoquarks are described by Eq. 3.7. Leptoquarks can be pair-produced in e^+e^- colliders and discovered up to the kinematic limit. However, since they are expected to be heavy, the best place for their discovery is a hadron collider. The production cross section in pp collisions is presented in Fig. 3-6. The upgraded Tevatron will be able to discover leptoquarks up to 440 GeV and the LHC up to 1160 GeV.

As we have already described, the right-handed parts of the down quarks and the charged leptons transform under different ETC group than the right-handed parts of up quarks and neutrinos. Similarly, there are separate copies of the light fermions, one copy for the up sector and one for the down sector. This separations of the sectors is visible from the moose diagram in Fig. 3-2. Consequently, there are two types of PGBs. The up-type bosons decay into charge 2/3 quarks and/or neutrinos, the down-type into charge 1/3 quarks and/or charged leptons. This feature is important in case of leptoquarks. TC-GIM models have two types of leptoquarks, one whose decay products always contain a charged lepton and the other type with a neutrino among its decay products. All our remarks about leptoquarks that we made so far apply to the down-type leptoquarks. The up-type leptoquarks are more difficult to observe, since their signatures are a hadronic jet and missing energy. Leptoquarks in other technicolor models can have various branching ratio for decays into neutrinos and charged leptons [26, 49].

The one-family model predicts leptoquarks in the range of 150–350 GeV, while walking TC models between 200 and 500 GeV. The discovery limit depends on the details of the model—the branching ratio of the decays into a charged lepton and a jet—and that limit is generally smaller than in TC-GIM models. Like in the octet case, the rates for pair production in hadron collisions are almost model independent. If leptoquarks are discovered, the measurements of the branching ratio into charged leptons and the masses of leptoquarks can give some hints about viable models. Moreover, in most TC models, the couplings of PGBs to the ordinary fermions have much larger magnitudes such that the leptoquarks can be singly-produced with an associated fermion pair. The expected rates of the production of single PGBs in TC-GIM models are negligibly small.

Color neutral particles are very light in TC-GIM models. Their masses range from 0.1 to 5 GeV as described in Eq. 3.12 and Table 1. In the lowest order chiral perturbation theory, their masses do not depend on the scale f_{S-1}. In QCD-like models one expects the masses of color-singlet PGBs to be in the range of 4 to 40 GeV [49]. The ETC interactions in walking TC models have large contributions to the masses of PGBs, which are between 100 and 350 GeV [28]. The majority of neutral PGBs in the TC-GIM models are unobservable in any existing or planned experiment because of the very weak couplings to ordinary fermions. The only neutral particle with anomalous couplings to gauge boson pairs is the P^0. Its mass is about 1 GeV and it decays most likely into a small number of pions or a $\mu^+\mu^-$ pair if f_{S-1} is larger than 200 GeV. The P^0 can be produced in hadron collisions, but it does

not stand out from the hadronic background. The best environment for the discovery of P^0 are e^+e^- colliders using the $e^+e^- \to P^0\gamma$ reaction. The production cross sections for this process are given by Eqs. 3.26 and 3.28. Since the P^0 mass is so small and lies in a narrow range around 1 GeV, the discovery potential depends not on the mass but on the strength of the anomalous coupling. The magnitude of the anomalous coupling is inversely proportional to f_{S-1} (Eq. 3.18), thus the production rates are proportional to $\frac{1}{f_{S-1}^2}$. The higher the collider's energy and luminosity, the larger are the values of f_{S-1} that can be probed. The LEP collaborations have collected enough data to probe f_{S-1} up to 80 GeV (not all the data has been analyzed), while the NLC will be able to probe the scale of $SU(S-1)$ interactions up to 390 GeV.

In QCD-like and walking TC models, there is usually a larger number of neutral PGBs that exhibit anomalous couplings [29, 49, 28]. These PGBs can be searched for in the same channels as the TC-GIM models: $e^+e^- \to P\gamma$ and $e^+e^- \to PZ^0$. QCD-like models generally predict low production cross sections [34]. The production rates depend on the number of technicolors, the technicolor scale and the anomaly coefficient. The rates are very close to limits LEP can place. For some models, PGBs might escape detection at LEP due to small rates. Only the NLC will provide sufficient energy and luminosity to observe neutral PGBs in the whole range of expected masses. Compared to the one-family model, the walking TC models are characterized by several low scales which greatly enhance the production rates. LEP2 has a chance of observing walking-TC bosons if their masses are about 100 GeV. The NLC with $\sqrt{s} = 500$ GeV can discover neutral PGBs as heavy as 350 GeV [28]. Obviously, the decay modes of PGBs in QCD-like and walking TC models depend on their masses. Bosons lighter than 100-150 GeV decay predominantly into $b\bar{b}$ pairs, while heavier particles into $\gamma\gamma$ pairs.

Another feature that might help distinguish the different TC scenarios are PGBs that are color neutral but carry the electric charge. Such PGBs do not exist in TC-GIM models, although many other TC models predict them. Due to the coupling to the photon, they can be pair-produced in e^+e^- colliders and discovered almost up to the kinematic limit. Future experiments may easily exclude models which predict such particles with masses that are too low.

A strong support for the TC-GIM models would be the observation of several types of PGBs predicted by the model. One could then test the ratio of the octet PGBs masses to the masses of the leptoquarks. This ratio should be very close to 1.5, which reflects the fact that the dominant contribution to the masses comes from the one-gluon exchange diagrams. The ratio of octet to triplet masses provides an indirect estimate of the size of ETC contributions to the masses of PGBs. Smaller ratio indicates large ETC contributions. For instance, the walking TC scenarios [28] predict this ratio to be around one. A ratio smaller than 1.4 would rule out TC-GIM models in their present form. Once the masses of the leptoquarks are measured, next goal would be the measurement of the P^0 production rate in e^+e^- collisions. Both the masses and the production rates depend on f_{S-1}, so it would be possible to check if they yield consistent values of f_{S-1}.

3.5 The f_{S-1} scale

In this section we discuss the scale of $SU(S-1)$ interactions. We describe theoretical constraints on that scale, summarize current experimental limits and the discovery reach of future colliders. We also comment on the possibility that the exotic fermions are heavier

than f_{S-1}. In such a case fermions do not condense. Instead of forming PGBs they form mesons resembling heavy-quark systems.

The scale of $SU(S-1)$ interactions is to a large extent a free parameter of the TC-GIM models. As long as this scale is somewhat below the scale of ETC interactions, it does not affect the pattern of symmetry breaking. Thus, all one can expect is that f_{S-1} is smaller than about 1000 GeV [22, 23]. In some models, f_{S-1} can be limited to a much smaller value. An example being the low-scale model, where condensates of fermions transforming under $SU(S-1)$ group contribute to the masses of ordinary fermions. The ETC interactions create four-fermion operators of the form

$$\frac{v_{TC}^2}{f_{ETC}^4}(\bar{q}_L q_R)(\bar{Q}_L Q_R),$$

which involve ordinary fermions q and exotic fermions Q. When Q_L and Q_R form condensates, such operators contribute to the masses of quarks and leptons by $\frac{4\pi f_{S-1}^3 v_{TC}^2}{f_{ETC}^4}$. In the low scale model, mass contribution from the $SU(S-1)$ condensates is identical for all down-type and all up-type fermions, thus it should not exceed electron mass. This means that f_{S-1} cannot be larger than 15 GeV [22].

The high-scale models avoid this limitation by arranging the fermion condensates such that they do not contribute to ordinary fermion masses. The high-scale model depicted in Fig. 3-3 leaves the vacuum alignment to be determined by the strong dynamics. It is not impossible that the way condensates form depends on fermion flavor. Some flavors may form condensates of the form $[n+12_L, S-1]$ with $[S-1, A]$ and $[A, S-1]$ with $[S-1, n+12_D]$, these do not contribute to the masses of ordinary fermions. Other flavors may form condensates $[n+12_L, S-1]$ with $[S-1, n+12_D]$ and $[A, S-1]$ with $[S-1, A]$. It is not a disaster if such condensates form for the top quark; such condensates do not limit f_{S-1} because the top quark is so heavy. Large mass contributions originating from $SU(S-1)$ condensates could explain the fermion mass hierarchy and at the same time make it possible to have a larger scale of ETC interactions. Such contributions are proportional to the cube of f_{S-1} and are of the order of the top quark mass only if $f_{S-1} \sim 1$ TeV. Numerically, the contribution equals 150 GeV$(\frac{f_{S-1}}{1\text{ TeV}})^3$.

Lack of experimental evidence for new fermions or light PGBs imposes lower limits on f_{S-1}. We summarize the reach of various experiments in Fig. 3-9. Presented results apply to the high-scale models of Figs. 3-3 and 3-4a. Currently, the best limits come from the Tevatron experiments, where one places a lower bound of 130 GeV on leptoquark masses. Thus, f_{S-1} must be larger than 65 GeV. The LEP experiments have not observed P^0, which places a limit of 38 GeV on f_{S-1}. However, this result has not been updated yet with all the data collected up to know. If all the data were analyzed, LEP could probe f_{S_1} up to 80 GeV, which would be the most competitive result available at present. The future proton colliders can greatly enhance leptoquark mass limits. The $\sqrt{s} = 4$ TeV Tevatron will probe f_{S-1} up to 215 GeV, and the LHC up to 560 GeV. LEP2 is not likely to provide any interesting information about $SU(S-1)$ interactions. One cannot fully take advantage of having energy larger than the Z^0 mass due to the small cross sections outside the Z^0 resonance peak. Limits comparable to the LHC discovery reach can be obtained by a high-energy e^+e^- collider. The NLC will be able to probe f_{S-1} up to 390 GeV by searching for the process $e^+e^- \to \gamma P^0$.

The current limits and discovery potential are not very different for the high-scale model of Fig. 3-4b. Usually the limits are at most a few GeV lower than the limits presented in

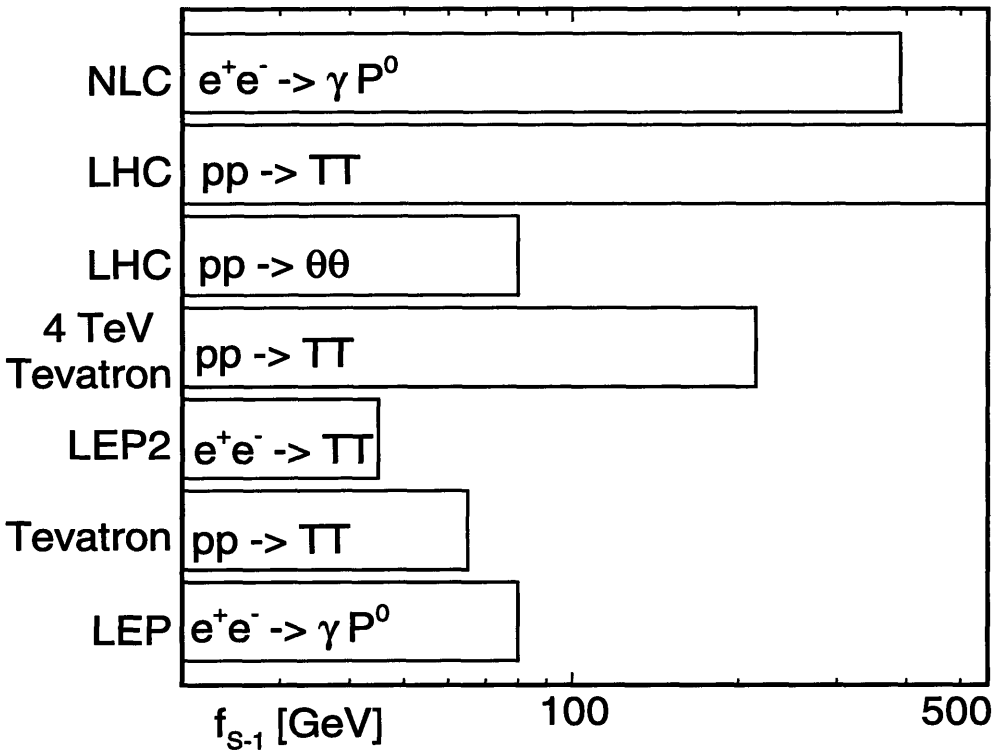

Figure 3-9: The potential of probing the scale of $SU(S-1)$ interactions at present and future colliders (the high-scale models). The most important reaction(s) for each collider is(are) indicated inside the bars.

Fig. 3-9. However, there is an exception. The process $pp \to P^0X$ can be a very sensitive probe, depending on the value of P^0 mass. In this model, P^0 can be much heavier than 1 GeV, and consequently, easier to detect. Irrespectively of the mass, the P^0 should be distinguishable from the SM Higgs boson. P^0 has large branching ratio of the decays $P^0 \to \gamma\gamma$ of about 2%. Unlike the Higgs boson, it decays mostly into light mesons, due to large $P^0 \to gg$ decay width.

It is also possible that at least some of the fermions are heavier than the scale of $SU(S-1)$ interactions. This might happen in the model of Fig. 3-3 in case of misaligned exotic top quark. Also, in the model of Fig. 3-4b, such a possibility exists if the operators providing masses to the exotic fermions are much larger than expected. In such a case, fermion condensates do not form, and observable particles are no longer Goldstone bosons of spontaneously broken symmetry. Mass terms are large enough, so that the chiral symmetry is explicitly broken at the scale where $SU(S-1)$ interactions become confining.

This situation essentially resembles heavy quark case in QCD. Heavy exotic fermions decay via four-fermion interactions connecting ordinary and exotic fermions. The operators responsible for their decays have the familiar form of current-current interaction

$$\frac{1}{f_{ETC}^2}(\bar{q}_1\gamma^\mu(1\pm\gamma^5)q_2)(\bar{Q}_2\gamma_\mu(1\pm\gamma^5)Q_1),$$

where q_i are ordinary fermions and Q_i the exotic ones. A heavy exotic fermion Q_1 decays into a lighter exotic fermion Q_2 and a pair of ordinary fermions. The lightest exotic fermions

cannot decay this way. Depending on their masses they either form PGBs, as we have described in detail, or heavy meson states that are singlets under $SU(S-1)$ interactions. Heavy mesons decays are mediated by the same four-fermion operators; here two exotic quarks annihilate into two ordinary fermions. Such heavy fermions can be searched for by means similar to searches for the fourth generation quarks and leptons. The lack of weak $SU(2)$ interactions does not play any important role in hadronic experiments. Exotic quarks are excluded up to masses comparable to the mass of the top quark. How do we know that the recently discovered [50] top quark is not an exotic quark? The top quark decays into a real $W^{\pm}$, which would not be the case of exotic quarks. LEP experiments exclude both exotic quarks and leptons up to half of the Z^0 mass.

Chapter 4

Confinement in Supersymmetric Theories[1]

In this chapter we develop a systematic approach to confinement in $N = 1$ supersymmetric theories. We identify simple necessary conditions for theories to confine without chiral symmetry breaking and to generate a superpotential non-perturbatively (s-confine). Applying these conditions we identify all $N = 1$ theories with a single gauge group and no tree-level superpotential which s-confine. We give a complete list of the confined spectra and superpotentials.

In the next section we give a short introduction to supersymmetry since investigations of supersymmetric theories will occupy both the current and the next chapter. This introduction emphasizes aspects of supersymmetric theories relevant for these two chapters. We describe fascinating results by Seiberg [53] on the low-energy behavior of supersymmetric gauge theories. These results will constitute our tools in the next chapter, where we analyze theories that break supersymmetry dynamically. In this chapter, we find an exhaustive list of supersymmetric theories with a single gauge group that confine without breaking chiral symmetries.

In Section 4.2 we introduce the idea of "s-confinement". We discuss two criteria for s-confinement in Section 4.3. It turns out that these criteria are very powerful in case of theories with a single gauge group. In Section 4.4 we apply our conditions to identify all theories with a single gauge group and no tree-level superpotential which s-confine. We gives a complete list of the confined spectra and superpotentials for all s-confining theories with an arbitrary SU, SO, Sp, or exceptional gauge group. Using the results for the s-confining theories, we then demonstrate in Section 4.5 how one can generate many more exact solutions for other models by simply integrating out matter from the s-confining theories. The models which we obtain in this way display interesting dynamics: confinement with chiral symmetry breaking, non-perturbatively generated superpotentials which drive the vacuum to infinity, and confinement with non-interacting composites.

[1]This chapter is based on research done in collaboration with Csaba Csáki and Martin Schmaltz reported in Refs. [51, 52].

4.1 Supersymmetry and exact results in supersymmetric theories

Supersymmetric theories are based on a larger set of symmetries than ordinary field theories. Usually, one assumes that the theory is invariant under the Poincaré group, whose generators include the translations, P_μ, and boost-rotation generators $M_{\mu\nu}$. The algebra of these generators is defined by the following commutators:

$$\begin{aligned}
[P^\mu, P^\nu] &= 0, \\
[M^{\mu\nu}, P^\rho] &= i(\eta^{\mu\rho}P^\nu - \eta^{\nu\rho}P^\mu), \\
[M^{\mu\nu}, M^{\rho\sigma}] &= i(\eta^{\mu\sigma}M^{\nu\rho} - \eta^{\mu\rho}M^{\nu\sigma} + \eta^{\nu\rho}M^{\mu\sigma} - \eta^{\nu\sigma}M^{\mu\rho}).
\end{aligned}$$

The famous no-go theorem by Coleman and Mandula [54] states that a symmetry larger than Poincaré is incompatible with a local, relativistic quantum field theory as long as additional bosonic generators transform non-trivially under the Lorentz group. The supersymmetric extension of the Poincaré group includes fermionic generators in addition to the bosonic ones [55]. We will be considering only $N = 1$ supersymmetry, where there are two fermionic generators: Q_α and $\bar{Q}_{\dot{\alpha}}$. Both Q's transform as Weyl fermions under the Lorentz group. The spinors are translationaly invariant

$$[Q^A_\alpha, P^\mu] = 0,$$

and transform under $M^{\mu\nu}$ in the following manner

$$[Q^A_\alpha, M^{\mu\nu}] = \frac{1}{2}\left(\sigma^\mu_{\alpha\dot{\alpha}}\bar{\sigma}^{\nu\dot{\alpha}\beta} - \sigma^\nu_{\alpha\dot{\alpha}}\bar{\sigma}^{\mu\dot{\alpha}\beta}\right)Q^A_\beta.$$

The spinors also satisfy the following anticommutation rules

$$\{Q_\alpha, \bar{Q}_{\dot{\beta}}\} = P^\mu(\sigma_\mu)_{\alpha\dot{\beta}}, \;\; \{Q^A_\alpha, Q^B_\beta\} = 0. \tag{4.1}$$

Since the fermionic generators interchange fermions and bosons, representations of SUSY-Poincaré algebra include fields with different spins. It is convenient to introduce superspace notation in order to discuss irreducible representations of supersymmetry. In this notation one includes constant Grassmann spinors θ^α, $\bar{\theta}_{\dot{\alpha}}$:

$$\{\theta^\alpha, \theta^\beta\} = \{\bar{\theta}_{\dot{\alpha}}, \bar{\theta}_{\dot{\beta}}\} = \{\theta^\alpha, \bar{\theta}_{\dot{\beta}}\} = 0$$

All fields are then written in terms of space-time coordinates and the Grassmann spinors. Because θ's anticommute with each other, any function of θ can be expanded in power series, which eventually truncates.

The two basic objects, we will be dealing with, are the chiral and the vector superfields. Both form irreducible representations of supersymmetry. A general superfield $S(x, \theta, \bar{\theta})$ does not form an irreducible representation. Irreducible representations are extracted by imposing constraints covariant under supersymmetry transformations:

$$\begin{aligned}
V &= V^\dagger, \text{ for vector superfields} \\
\text{and } \bar{D}_{\dot{\alpha}}\Phi &= 0, \text{ for chiral superfields}
\end{aligned}$$

Here, we use the notation:

$$D_\alpha = \frac{\partial}{\partial\theta^\alpha} + i\sigma^\mu_{\alpha\dot\beta}\bar\theta^{\dot\beta}\frac{\partial}{\partial x^\mu},\ \ \bar D_{\dot\alpha} = -\frac{\partial}{\partial\bar\theta^{\dot\alpha}} - i\sigma^\mu_{\beta\dot\alpha}\theta^\beta\frac{\partial}{\partial x^\mu}.$$

In terms of components, these fields can be expanded as:

$$\begin{aligned} V(x,\theta,\bar\theta) &= -\theta\sigma^\mu\bar\theta V_\mu(x) + i(\theta\theta)\bar\theta\bar\lambda(x) - i(\bar\theta\bar\theta)\theta\bar\lambda(x) + \frac{1}{2}(\theta\theta)(\bar\theta\bar\theta)D, \\ \Phi(y,\theta) &= A(y) + \sqrt{2}\theta\psi(y) + (\theta\theta)F(y), \text{ where } y^\mu = x^\mu + i\theta\sigma^\mu\bar\theta \end{aligned}$$

For the vector superfield, V, we used the so-called Wess-Zumino gauge.

Next, we identify the most general form of the Lagrangian consistent with supersymmetry. Again, it is convenient to write all expressions in terms of superfields and integrate over the Grassmann variables. There are three terms in the supersymmetric Lagrangian density:

1. $\int d^2\theta\, W(\Phi^i)$+h.c., which describes self interactions among the chiral superfields. W is an arbitrary function, called superpotential, of chiral superfields. The superpotential cannot be a function of any conjugate chiral fields, since that would be inconsistent with supersymmetry.

2. $Im[\tau\int d^2\theta f(\Phi^i)W^\alpha W_\alpha]$, which contains gauge-kinetic terms. Again, f is a function of only chiral superfields and not the antichiral ones. Function f is called the gauge-kinetic function. In the above formula we define $W^\alpha = -\frac{1}{8}(\bar D\bar D)e^{-2V}D^\alpha e^{2V}$.

3. $\int d^2\theta d^2\bar\theta K(\Phi^i, \Phi^{j\dagger}e^{2V})$, which contains kinetic terms for the chiral superfields and also interactions between the chiral and vector superfields. Function K is called the Kähler potential.

In order to construct renormalizable Lagrangians one has to restrict W to be a polynomial of order three or less. Moreover, $f(\Phi)\equiv 1$ and $K(\Phi^i, \Phi^{j\dagger}e^{2V}) = \mathrm{tr}\,\Phi^{j\dagger}e^{2V}\Phi^i$.

4.1.1 Flat directions

In order to study low-energy actions for supersymmetric gauge theories, we first need to describe their classical behavior. Supersymmetry implies that the ground state energy is zero. In the classical theory, the Kähler potential has its canonical form if the degrees of freedom are properly identified. Then, the potential for the scalar degrees of freedom is

$$V = g^2\sum_\alpha\left|\sum_i(\Phi_i)^\dagger_a(T^\alpha)^a_b\Phi^b_i\right|^2 + \sum_i\left|\frac{\partial W}{\partial\Phi_i}\right|^2, \tag{4.2}$$

the first term is called the D-term while the second contribution is called the F-term. Classically, the superpotential, W, is an arbitrary function of chiral superfields. In contrast, the D-term is determined once the gauge group and the field content are specified.

We can set $W\equiv 0$ and consider vacua of the theory without superpotential. Usually, there is a large space of solutions to $\sum_i(\Phi_i)^\dagger_a(T^\alpha)^a_b\Phi^b_i = 0$, for every α. This space, moded out by gauge transformations, is called the classical moduli space. Solving the above equations is in most cases a difficult algebraic exercise. It is very interesting that the classical moduli space can be parameterized by the vacuum expectation values of independent gauge invariant operators constructed from chiral superfields. In fact, the solutions to

$\sum_\alpha \left|\sum_i (\Phi_i)^\dagger_a (T^\alpha)^a_b \Phi^b_i\right|^2 = 0$, up to gauge invariance, are in a one-to-one correspondence with holomorphic gauge invariants [56]. In many examples it is helpful to use the holomorphic parameterization of the moduli space rather than describe it in terms of elementary fields.

Let us consider an example of supersymmetric QCD, that is an $SU(N_c)$ theory with N_f fields Q^i in the fundamental representation and N_f fields $\bar{Q}_j$ in the antifundamental. The indices $i, j = 1, \ldots, N_f$ denote flavor degrees of freedom, while the color indices are suppressed. Classically, the flat directions are parameterized by "meson" fields $M^j_i = \bar{Q}_i Q^j$, and "baryon" fields $B_{i_{N_c+1}\ldots i_{N_f}} = \epsilon_{i_1\ldots i_{N_f}} Q^{i_1}\ldots Q^{i_{N_c}}$, $\bar{B}^{i_{N_c+1}\ldots i_{N_f}} = \epsilon^{i_1\ldots i_{N_f}} \bar{Q}_{i_1}\ldots\bar{Q}_{i_{N_c}}$. Baryon fields exist only when $N_f \geq N_c$. The mesons and baryons are not independent. They obey constraints

$$\begin{aligned} B_{i_1\ldots i_{N_f-N_c}} M^{i_1}_j = 0, \quad \bar{B}^{i_1\ldots i_{N_f-N_c}} M^j_{i_1} = 0, \\ M^{i_1}_{j_1}\ldots M^{i_{N_c}}_{j_{N_c}} \epsilon_{i_1\ldots i_{N_f}} \epsilon^{j_1\ldots j_{N_f}} = B_{i_{N_c+1}\ldots i_{N_f}} \bar{B}^{i_{N_c+1}\ldots i_{N_f}}. \end{aligned} \tag{4.3}$$

These constraints are easy to verify if we express them in terms of the underlying fields Q^i and $\bar{Q}_i$. Vacuum expectation values (VEVs) of these gauge invariant polynomials, subject to constraints, describe the classical moduli space. The classical theory has a large set of degenerate vacuum states. For many of these states, the degeneracy is accidental—not protected by symmetries—and can be removed by quantum effects. The quantum-mechanical picture depends on the number of flavors N_f [53]. We outline the quantum mechanical behavior next.

4.1.2 Supersymmetric QCD

As we already mentioned, the superpotential is a holomorphic function of chiral superfields. Holomorphy proves to be quite a strong restriction on the form of allowed superpotentials. We will see that the global symmetries and the requirement of holomorphy are enough to determine effective superpotentials in many case. Any superpotential generated dynamically must obey the symmetries of the theory. In the case of supersymmetric QCD, the underlying theory has an $SU(N_f) \times SU(N_f) \times U(1) \times U(1)_R$ global symmetry under which the fields transform as follows

	$SU(N_c)$	$SU(N_f)$	$SU(N_f)$	$U(1)_B$	$U(1)_R$
Q	$\square$	$\square$	1	1	$\frac{N_f-N_c}{N_f}$
$\bar{Q}$	$\bar{\square}$	1	$\square$	-1	$\frac{N_f-N_c}{N_f}$

where the $SU(N_c)$ is the gauge symmetry.

We will now describe what happens for different number of quark flavors. When $N_f < N_c$, there is only one combination of fields, which is invariant under the non-abelian global symmetries, that is $\det M$. The R-charge of this object is $2(N_f - N_c)$. Since the superpotential must have the R-charge of two, it must be of the form:

$$W_{dyn} = \left(\frac{\Lambda^{3N_c-N_f}}{\det M}\right)^{1/(N_c-N_f)}. \tag{4.4}$$

By symmetry considerations such a term is the only one allowed in the superpotential. Yet, the coefficient of this term could be zero. It turns out that non-perturbative effects do

generate this superpotential [57]. When $N_f = N_c - 1$, the gauge group is completely broken for generic large expectation values of fields. In the regime of weak interactions instanton calculations are reliable and one can show that instantons generate this term. One can then integrate out flavors by giving masses. This way one can obtain superpotentials for $N_f < N_c - 1$ and their coefficients are indeed non-zero. The scalar potential calculated from superpotential is inversely proportional to the VEVs of chiral superfields. Therefore, supersymmetric QCD has no stable vacuum state for $0 < N_f < N_c$. It is possible to lift flat directions by adding small mass terms and have a stable vacuum state. In the ground state all fields have VEVs, and the gauge group is broken to $SU(N_c - N_f)$.

When $N_f = N_c$ all fields have zero R-charge. Therefore, no superpotential can be generated. Unlike the case just discussed, fields can have small expectation values, where the gauge coupling is strong. It turns out that the low-energy theory with $N_f = N_c$ confines. The physical degrees of freedom are N_f^2 mesons M_j^i and baryons B, $\bar{B}$. Classically, these fields obey the constraint $\det M - B\bar{B} = 0$. In the quantum regime, the constraint is modified: $\det M - B\bar{B} = \Lambda^{2N_f}$, so the classical and quantum moduli spaces are different. It is important that the origin of the moduli space—where all fields have zero expectation values—does not belong to the quantum moduli space. Quantum mechanically, some of the fields necessarily have VEVs; consequently some global symmetries are always broken. The constraint can be implemented by including it with a Lagrange multiplier μ in the superpotential:

$$W = \mu(\det M - B\bar{B} - \Lambda^{2N_f}). \tag{4.5}$$

An important consistency check on the confining picture are the 't Hooft anomaly matching conditions. Anomalies match between the high and the low-energy spectra if one takes into account modification of the quantum moduli space as compared to the classical one. For instance, anomalies do not match at the origin, since the origin does not belong to the quantum moduli space. Anomalies can be matched only for the set of symmetries preserved on the quantum moduli space, and one field has to be removed from the spectrum consistently using the constraint.

Let us discuss now the case when $N_f = N_c + 1$. The anomaly-free R-charge assignment allows for a superpotential to be generated. There are two invariants under the non-abelian global symmetries: $\det M$ and $\bar{B}^i M_i^j B_j$, they have actually R-charge of two. The combinations with correct dimensions are $\det M/\Lambda^{2N_c-1}$ and $(\bar{B}^i M_i^j B_j)/\Lambda^{2N_c-1}$. However, the theory should approach the classical limit when $\Lambda \to 0$. Classically, B's and M's obey constraints, so the constraints have to be reproduced when VEVs are large. Again, this theory is confining. In this case, the classical and quantum moduli spaces are identical. The gauge invariant operators M's, B's and $\bar{B}$'s correspond to physical degrees of freedom describing the theory at the origin. The mesons and baryons interact via a "confining superpotential"

$$W = \frac{1}{\Lambda^{2N_c-1}} \left(\bar{B}^i M_i^j B_j - \det M\right). \tag{4.6}$$

Just like before one of the consistency checks on the confining picture is that 't Hooft anomaly matching conditions between the high and low-energy degrees of freedom are satisfied. There is another check that we already mentioned: equations of motion reproduce the classical constraints of the theory. We will describe this theory in greater detail in the next section when we introduce "s-confinement".

For a larger number of flavors $N_c < N_f < 3N_c$, supersymmetric QCD is either in the free-magnetic or conformal phase. Its infrared fixed point can be described equivalently in

terms of another theory—supersymmetric QCD with $N_f - N_c$ colors. The "dual" theory has also N_f flavors of "magnetic quarks" q_i, $\bar{q}^i$; N_f^2 elementary gauge singlet "mesons" $\tilde{M}_j^i$ and the following superpotential

$$W = \tilde{M}_j^i \bar{q}^j q_i. \tag{4.7}$$

Gauge invariant operators of the original $SU(N_c)$ correspond to the gauge invariants of the dual $SU(N_f - N_c)$. The mesons $\bar{Q}Q$ are mapped into gauge singlet fields $\tilde{M}$, while baryon operators Q^{N_c} are mapped into baryons $q^{N_f - N_c}$. One of the consistency checks is anomaly matching between the original and the dual theory. The symmetries of the fields in the dual theory are

	$SU(N_f - N_c)$	$SU(N_f)$	$SU(N_f)$	$U(1)_B$	$U(1)_R$
q	$\square$	$\overline{\square}$	1	$\frac{N_c}{N_f - N_c}$	$\frac{N_c}{N_f}$
$\bar{q}$	$\overline{\square}$	1	$\overline{\square}$	$-\frac{N_c}{N_f - N_c}$	$\frac{N_c}{N_f}$
$\tilde{M}$	1	$\square$	$\square$	0	$2\frac{N_f - N_c}{N_f}$

Supersymmetric QCD is infrared free for $N_f \geq 3N_c$ and has no interesting non-perturbative dynamics.

4.2 What is s-confinement?

The number of $N = 1$ supersymmetric gauge theories for which we know exact results on their vacuum structure has been growing steadily in the last two years. The great progress was sparked by Seiberg's conjectures about the infrared properties and phase structure of supersymmetric QCD [53]. Following in his footsteps, others have obtained results on a whole zoo of theories [57-69]. Most of the discovered phenomena follow similar patterns in the different theories, and one is tempted to ask if there is maybe a more general approach than the model-specific trial and error procedure that has been customary thus far.

Whereas a completely general approach that allows one to understand all the obtained results seems impossibly difficult to find, we can make much progress by focusing on the particular phenomenon of confinement. In fact, a frequently occuring and relatively easily identified infrared behavior is "s-confinement". An s-confining theory is defined as a theory for which all the degrees of freedom in the infrared are gauge invariant composites of the fundamental fields [51]. Furthermore, we demand that the infrared physics is described by a smooth effective theory in terms of these gauge invariants. This description should be valid everywhere on the moduli space of vacua, including the origin of field space. Finally, we also demand that an s-confining theory generates a dynamical superpotential. At the origin of moduli space all global symmetries of the theory are unbroken and the global anomalies of the microscopic theory are matched by the macroscopic gauge invariants of the effective theory.

The best-known example of a theory which has been conjectured to be s-confining is supersymmetric QCD (SQCD) with N colors and $F = N + 1$ flavors of fundamental and antifundamental matter, Q and $\bar{Q}$ [53, 58]. The gauge invariant confined degrees of freedom are mesons $M = Q\bar{Q}$ and baryons $B = Q^N$, $\bar{B} = \bar{Q}^N$. At the origin of moduli space, all components of the mesons and baryons are massless, and they interact via the confining superpotential

$$W = \frac{1}{\Lambda^{2N-1}}(\det M - BM\bar{B}). \tag{4.8}$$

This description is also valid far from the origin of the moduli space where the large expec-

tation values of the fields completely break the gauge group. In such a vacuum the theory is in the Higgs phase. A smooth gauge invariant description of both the Higgs and confining vacua of the theory can only exist if there is no phase transition between the two regions in moduli space. In particular, there should be no gauge invariant order parameter that distinguishes the two phases.

To understand this in the example of SQCD, note that the quarks transform in a faithful representation of the gauge group $SU(N)$. This implies that arbitrary test charges can be screened by the dynamical quarks because the vacuum can disgorge quark-antiquark pairs to screen charges transforming in any representation of the gauge group. Thus a Wilson loop will always obey a perimeter law because any charges we might want to use to define the Wilson loop can be screened. Our definition of s-confinement above necessitates that an s-confining theory is in such a "screening-confining" phase.

This situation should be contrasted with $SU(N)$ with only adjoint matter or $SO(N)$ with vector matter. In both these cases the matter does not transform in a faithful representation of the gauge group. Now there are charges that cannot be screened by the dynamical quarks, and a Wilson loop can serve as gauge invariant order parameter to distinguish the Higgs and the confining phases. As a result, such theories cannot have a single smooth description of both the Higgs and confining phases of the theory, thus they are not s-confining.

In the next section we identified two criteria which allow us to decide whether a given theory can be s-confining without having to know the explicit infrared description. If we limit our attention to theories with no tree-level superpotential and only one gauge group, then the symmetries completely determine the form of any non-perturbatively generated superpotential. Demanding that this superpotential is smooth everywhere on the moduli space yields the first of our two conditions. The other condition arises from studying the theory along some flat direction in which the gauge group is broken to a subgroup, and the theory may sufficiently simplify so that we can understand its infrared physics. If we find a result that cannot be smoothly connected to a confining phase, we know that the whole theory is not s-confining either.

4.3 Necessary criteria for s-confinement

In this section we develop two necessary criteria which allow us to identify all s-confining theories with a simple gauge group and no tree-level superpotential. The first criterion follows from holomorphy of the dynamically generated superpotential, which can be determined using the global symmetries of the theory. This criterion allows us to reduce the number of theories that are candidates for s-confinement to a manageable set. Our second criterion follows from explorations of regions in moduli space which are easier to understand than the origin. As will be demonstrated in Section 4.4, these two conditions combined are sufficient to identify all s-confining theories with a single gauge group and no tree-level superpotential [52].

4.3.1 The index constraint

In this subsection, we derive a simple constraint on the matter content of s-confining theories which follows from the requirement of holomorphy of the confining superpotential. In theories with a simple gauge group G and no tree-level superpotential, the symmetries are sufficient to determine the form of any dynamically generated superpotential completely [59]. A simple way to prove this makes use of non-anomalous R-symmetries. Define a $U(1)_R$

symmetry as follows: all chiral superfields, except for one arbitrarily chosen field ϕ_i, are assigned zero R-charge. The charge q of the remaining field is determined by requiring anomaly cancelation of the mixed $G^2U(1)_R$ anomaly

$$(q-1)\mu_i - \sum_{j\neq i}\mu_j + \mu_G = q\mu_i - \sum_{\text{all } j}\mu_j + \mu_G = 0, \tag{4.9}$$

where μ_i is the Dynkin index[2] of the gauge representation of the field ϕ_i, and $(q-1)$ is the R-charge of its fermion component. These three terms arise from the contributions of the fermion components of ϕ_i, of all other matter superfields ϕ_j with $j \neq i$, and of the gauge superfields, respectively. The μ_j are the indices of the remaining matter representations, they are multiplied by the R-charges -1 of the fermion components of ϕ_j, and finally μ_G is the index of the adjoint representation of G multiplied by the R-charge $+1$ of the gauginos. R-invariance of the supersymmetric Lagrangian requires the dynamically generated superpotential to have R-charge two. This uniquely fixes the dependence of the superpotential on the field ϕ_i

$$W \propto (\phi_i{}^{\mu_i})^{2/(\sum_j \mu_j - \mu_G)}. \tag{4.10}$$

To determine the functional dependence on the other superfields, we note that the global symmetries contain a corresponding $U(1)_R$ symmetry for each of the matter superfields, and the superpotential has to have R-charge two under each such R-symmetry. Finally, the dependence on the dynamical scale Λ can be determined by dimensional analysis or using an anomalous R-symmetry [60]. The result is

$$W \propto \Lambda^3 \left(\prod_i \left(\frac{\phi_i}{\Lambda}\right)^{\mu_i}\right)^{2/(\sum_j \mu_j - \mu_G)}. \tag{4.11}$$

There may be several (or no) possible contractions of gauge indices, thus the superpotential can be a sum of several terms. We require the coefficient of this superpotential to be non-vanishing, then holomorphy at the origin implies that the exponents of all fields ϕ_i are positive integers. Strictly speaking, we should require holomorphy in the confined degrees of freedom which would imply that the exponents of composites must be positive integers. Since we do not want to have to determine all gauge invariants for this argument, we settle for the weaker constraint on exponents of the fundamental fields. Therefore,[3] $\sum_j \mu_j - \mu_G = 1$ or 2. However, in our normalization of the index, anomaly cancelation further constrains this quantity to be even, thus

$$\sum_j \mu_j - \mu_G = 2. \tag{4.12}$$

This formula summarizes our first necessary condition for s-confinement, which enables us to rule out most theories immediately. For example, for SQCD we find that the only

[2]We normalize the index of the fundamental representations of SU and Sp to 1 and of the vector of SO to 2. This definition ensures invariance of the index when decomposing representations of $SO(2N)$ under the $SU(N)$ subgroup. This is relevant to the flows discussed in Section 4.3.2.

[3]Other solutions exist if all μ_i have a common divisor d, then for $\sum_j \mu_j - \mu_G = d$ or $2d$ the superpotential Eq. 4.12 may be regular. We will argue at the end of Section 4.4.3 that these solutions generically do not yield s-confining theories. Another possibility is that the coefficient of the superpotential above vanishes. There are examples of confining theories with vanishing superpotentials in the literature [61].

candidate is the theory with $F = N+1$. Unfortunately, Eq. 4.12 is not a sufficient condition. An example for a theory which satisfies Eq. 4.12 but does not s-confine is $SU(N)$ with an adjoint superfield and one flavor. This theory is easily seen to be in an Abelian Coulomb phase for generic VEVs of the adjoint scalars and vanishing VEVs for the fundamentals. In the following section, we derive another necessary criterion which allows us to rule out theories that satisfy the "index-constraint" but do not s-confine.

4.3.2 Flows and s-confinement

The second condition is obtained from studying different regions on the moduli space of the theory under consideration. A generic supersymmetric theory with vanishing tree-level superpotential has a large moduli space of vacua. By definition, an s-confining theory has a smooth description in terms of gauge invariants everywhere on this moduli space. There should be no singularities in the superpotential or the Kähler potential and there should be no massless gauge bosons anywhere.

Thus, we can test a given theory for s-confinement by expanding around points that are far out in moduli space where the theory simplifies. In the microscopic theory the gauge group gets broken to a subgroup when we go out in moduli space by giving large ($\langle\phi\rangle \gg \Lambda$) expectation values to some fields. In this vacuum, the gauge superfields corresponding to broken symmetry generators get masses through the super-Higgs mechanism and the remaining matter fields decompose under the unbroken subgroup. This "reduced" theory has a smaller gauge group and may be easier to understand. If the original theory was s-confining then its confined description should be valid at this point in moduli space as well. Therefore, the reduced theory is s-confining if the original theory was. This statement can be applied in two directions.
Necessary condition: If the reduced theory does not have a smooth description with only gauge invariant degrees of freedom, then the original theory cannot be s-confining. Sufficient condition: If the original theory is known to be s-confining, then all possible reduced theories (with a remaining unbroken gauge group) which the original theory flows to are s-confining also. The confined spectrum and the confining superpotential of the reduced theories can be obtained by identifying the corresponding points in moduli space in the confined description of the original theory and integrating out all massive fields. In practice, this means identifying the correct gauge invariant fields which have vacuum expectation values and integrating out fields which now have mass terms in the superpotential using their equations of motion.

The reduced theories will always contain some gauge invariant fields in the high-energy description which originally transformed under the now broken gauge generators. These fields do not have any interactions and are irrelevant to the dynamics of the model. They can be removed from the theory. In the confined description the fields corresponding to these gauge singlets are only coupled through superpotential terms which scale to zero when the VEVs are taken to infinity, or which are irrelevant in the infrared.

A non-trivial application of the sufficient condition is given by the flow from $SU(4)$ with an antisymmetric tensor and 4 "flavors" of fundamentals and antifundamentals to $Sp(4)$ with 8 fundamentals. The $SU(4)$ theory is known to s-confine [63, 64]. By giving an expectation value to the antisymmetric tensor the gauge group is broken to $Sp(4)$. All components of the antisymmetric tensor field except for one singlet are "eaten" by the super-Higgs mechanism, and the 4 flavors of fundamentals and antifundamentals become 8 fundamentals of $Sp(4)$. Applying our sufficient criterion, we conclude that the Sp theory

is s-confining as well. Its confined spectrum and superpotential can be obtained from the spectrum and superpotential of the $SU(4)$ theory.

A non-trivial example of a theory which can be shown not to s-confine is $SU(4)$ with three antisymmetric tensors and two flavors. This theory satisfies our index condition, Eq. 4.12, and is therefore also a candidate for s-confinement. By giving a VEV to an antisymmetric tensor we can flow from this theory to $Sp(4)$ with two antisymmetric tensors and four fundamentals. VEVs for the other antisymmetric tensors let us flow further to $SU(2)$ with eight fundamentals which is known to be at an interacting fixed point in the infrared. We conclude that the $SU(4)$ with three tensors and $Sp(4)$ with two tensors and all theories that flow to them cannot be s-confining either. This allows us to rule out the following chain of theories, all of which are gauge anomaly free and satisfy Eq. 4.12:

$$\begin{array}{ccccccccc} SU(7) & \to & SU(6) & \to & SU(5) & \to & SU(4) & \to & Sp(4) \\ \square\!\square\, 2\square\, 4\bar{\square} & & \square\!\square\, \square\, 3\bar{\square} & & 2\square\!\square\, \bar{\square}\!\bar{\square}\, \square\, 2\bar{\square} & & 3\square\!\square\, 2\square\, 2\bar{\square} & & 2\square\!\square\, 4\square \end{array} \tag{4.13}$$

Note that a VEV for one of the quark flavors of the $SU(4)$ theory lets us flow to an $SU(3)$ theory with four flavors which is s-confining. We must therefore be careful: when we find a flow to an s-confining theory, it does not follow that the original theory is s-confining as well. The flow is only a necessary condition. However, in all our examples we find that a theory with a single gauge group and no tree-level superpotential is s-confining if it is found to flow to s-confining theories in all directions of its moduli space.

4.4 All s-confining theories

In this section, we present our results which we obtained using the two conditions derived in Section 4.3. We first created a list of all theories with a single gauge group and matter content satisfying the index constraint. Then we studied all possible flat directions of the individual theories and checked if they only flow to confining theories. We summarize these results in the first table of each subsection. In the first column we list all theories satisfying the index constraint. In the second column we indicate the result of the flows: theories which can be shown to have a branch with an unbroken Abelian gauge group we denote with "Coulomb branch", for theories which can be shown to flow to a reduced theory with a non-Abelian gauge group which is not s-confining we indicate the gauge group of the reduced theory and its matter content, all other theories are s-confining.

After identifying all s-confining theories in this way, we explicitly construct the confined spectra for each s-confining theory. The group theory used to obtain these results can be found in Refs. [73, 74, 75]. We present our results in tables where we indicate the matter content of the ultraviolet theory in the upper part of the table, and the gauge invariant infrared spectrum in the lower part. The gauge group and the Young tableaux of the representations of the matter fields are indicated in the first column. The other groups correspond to the global symmetries of the theory. In addition to the listed global symmetries, there is also a global $U(1)$ with a $G^2U(1)$ anomaly which is broken by instantons.

Finally, we also give the confining superpotentials when they are not too long. We denote gauge invariant composites by their constituents in parenthesis. The relative coefficients of the different terms can be determined by demanding that the equations of motion following from this superpotential reproduce the classical constraints of the ultraviolet theory. This also constitutes an important consistency check: in the limit of large generic expectation

values for fields, $\langle\phi\rangle \gg \Lambda$, the ultraviolet theory behaves classically and all its classical constraints need to be reproduced by the infrared description. Checking that all these constraints are reproduced and determining the coefficients is a very tedious exercise which we only performed for some theories. Since we have not determined the coefficients of the superpotential terms for several of the s-confining theories, it may turn out that some of the terms listed in the confining superpotentials have vanishing coefficients.

A more straightforward and also very powerful consistency check is provided by the 't Hooft anomaly matching conditions. We explicitly checked that all global anomalies match between the microscopic and macroscopic degrees of freedom in every theory. Other consistency checks which we performed for a subset of the theories include explorations of the moduli spaces and adding masses for some matter fields and checking consistency of the results. More details on these techniques are described in Section 4.5.

4.4.1 The s-confining $SU(N)$ theories

In this section, we present all s-confining theories based on $SU(N)$ gauge groups. We normalize the Dynkin index and the anomaly coefficient of the fundamental representation to be one. With these conventions, the dimension, index and anomaly coefficient of the smallest $SU(N)$ representations are listed below.

Irrep	Dim	μ	A
$\square$	N	1	1
Adj	N^2-1	$2N$	0
$\begin{smallmatrix}\square\\\square\end{smallmatrix}$	$\frac{N(N-1)}{2}$	$N-2$	$N-4$
$\square\square$	$\frac{N(N+1)}{2}$	$N+2$	$N+4$
$\begin{smallmatrix}\square\\\square\\\square\end{smallmatrix}$	$\frac{N(N-1)(N-2)}{6}$	$\frac{(N-3)(N-2)}{2}$	$\frac{(N-3)(N-6)}{2}$
$\square\square\square$	$\frac{N(N+1)(N+2)}{6}$	$\frac{(N+2)(N+3)}{2}$	$\frac{(N+3)(N+6)}{2}$
$\begin{smallmatrix}\square\square\\\square\end{smallmatrix}$	$\frac{N(N-1)(N+1)}{3}$	N^2-3	N^2-9
$\begin{smallmatrix}\square\square\\\square\square\end{smallmatrix}$	$\frac{N^2(N+1)(N-1)}{12}$	$\frac{N(N-2)(N+2)}{3}$	$\frac{N(N-4)(N+4)}{3}$
$\square\square\square\square$	$\frac{N(N+1)(N+2)(N+3)}{24}$	$\frac{(N+2)(N+3)(N+4)}{6}$	$\frac{(N+3)(N+4)(N+8)}{6}$
$\begin{smallmatrix}\square\square\\\square\\\square\end{smallmatrix}$	$\frac{N(N+1)(N-1)(N-2)}{8}$	$\frac{(N-2)(N^2-N-4)}{2}$	$\frac{(N-4)(N^2-N-8)}{2}$

Because the index of a representation of $SU(N)$ grows like N^{k-1} where k is the number of gauge indices, there are very few anomaly free representations which satisfy Eq. 4.12. These representations are listed in Table 4.1. In the first column, we indicate the gauge group and field content of the theory. In the second column we give the flows which allowed us to rule out s-confinement for a given theory. For those theories which do s-confine we then list the spectra and the confining superpotential in the following tables. For completeness, we also list those s-confining theories which are already known in the literature.

$SU(N)$	$(N+1)(\square+\bar{\square})$	s-confining
$SU(N)$	$\square\!\square+N\bar{\square}+4\square$	s-confining
$SU(N)$	$\square\!\square+\bar{\square}\!\bar{\square}+3(\square+\bar{\square})$	s-confining
$SU(N)$	Adj $+\square+\bar{\square}$	Coulomb branch
$SU(4)$	Adj $+\square\!\square$	Coulomb branch
$SU(4)$	$3\square\!\square+2(\square+\bar{\square})$	$SU(2)$: $8\square$
$SU(4)$	$4\square\!\square+\square+\bar{\square}$	$SU(2)$: $\square\square+4\square$
$SU(4)$	$5\square\!\square$	Coulomb branch
$SU(5)$	$3(\square\!\square+\bar{\square})$	s-confining
$SU(5)$	$2\square\!\square+2\square+4\bar{\square}$	s-confining
$SU(5)$	$2(\square\!\square+\bar{\square}\!\bar{\square})$	$Sp(4)$: $3\square\!\square+2\square$
$SU(5)$	$2\square\!\square+\bar{\square}\!\bar{\square}+2\bar{\square}+\square$	$SU(4)$: $3\square\!\square+2(\square+\bar{\square})$
$SU(6)$	$2\square\!\square+5\bar{\square}+\square$	s-confining
$SU(6)$	$2\square\!\square+\bar{\square}\!\bar{\square}+2\bar{\square}$	$SU(4)$: $3\square\!\square+2(\square+\bar{\square})$
$SU(6)$	$\begin{array}{l}\square\\\square\end{array}\!\!\square+4(\square+\bar{\square})$	s-confining
$SU(6)$	$\begin{array}{l}\square\\\square\end{array}\!\!\square+\square\!\square+3\bar{\square}+\square$	$SU(5)$: $2\square\!\square+\bar{\square}\!\bar{\square}+2\bar{\square}+\square$
$SU(6)$	$\begin{array}{l}\square\\\square\end{array}\!\!\square+\square\!\square+\bar{\square}\!\bar{\square}$	$Sp(6)$: $\begin{array}{l}\square\\\square\end{array}\!\!\square+\square\!\square+\square$
$SU(6)$	$2\begin{array}{l}\square\\\square\end{array}\!\!\square+\square+\bar{\square}$	$SU(5)$: $2(\square\!\square+\bar{\square}\!\bar{\square})$
$SU(7)$	$2(\square\!\square+3\bar{\square})$	s-confining
$SU(7)$	$\begin{array}{l}\square\\\square\end{array}\!\!\square+4\bar{\square}+2\square$	$SU(6)$: $\begin{array}{l}\square\\\square\end{array}\!\!\square+\square\!\square+3\bar{\square}+\square$
$SU(7)$	$\begin{array}{l}\square\\\square\end{array}\!\!\square+\bar{\square}\!\bar{\square}+\square$	$Sp(6)$: $\begin{array}{l}\square\\\square\end{array}\!\!\square+\square\!\square+\square$

Table 4.1: All SU theories satisfying $\sum_j \mu_j - \mu_G = 2$. This list is finite because the indices of higher index tensor representations grow very rapidly with the size of the gauge group. We list the gauge group and the field content of the theories in the first column. In the second column, we indicate which theories are s-confining. For the theories which do not s-confine we give the flows to non s-confining theories or indicate that there is a Coulomb branch on the moduli space.

$SU(N)$ with $(N+1)(\square+\overline{\square})$ (SUSY QCD) [53]

	$SU(N)$	$SU(N+1)$	$SU(N+1)$	$U(1)$	$U(1)_R$
Q	$\square$	$\square$	1	1	$\frac{1}{N+1}$
$\bar{Q}$	$\overline{\square}$	1	$\square$	-1	$\frac{1}{N+1}$
$Q\bar{Q}$		$\square$	$\square$	0	$\frac{2}{N+1}$
Q^N		$\overline{\square}$	1	N	$\frac{N}{N+1}$
$\bar{Q}^N$		1	$\overline{\square}$	$-N$	$\frac{N}{N+1}$

$$W_{dyn} = \frac{1}{\Lambda^{2N-1}}\left[(Q\bar{Q})^{N+1} - (Q^N)(Q\bar{Q})(\bar{Q}^N)\right]$$

$SU(2N)$ with $\square\!\square + 2N\ \overline{\square} + 4\ \square$ [64]

	$SU(2N)$	$SU(2N)$	$SU(4)$	$U(1)_1$	$U(1)_2$	$U(1)_R$
A	$\square\!\square$	1	1	0	$2N+4$	0
$\overline{Q}$	$\overline{\square}$	$\square$	1	4	$-2N+2$	0
Q	$\square$	1	$\square$	$-2N$	$-2N+2$	$\frac{1}{2}$
$Q\overline{Q}$		$\square$	$\square$	$4-2N$	$-4N+4$	$\frac{1}{2}$
$A\overline{Q}^2$		$\square\!\square$	1	8	$-2N+8$	0
A^N		1	1	0	$2N^2+4N$	0
$A^{N-1}Q^2$		1	$\square\!\square$	$-4N$	$2N^2-2N$	1
$A^{N-2}Q^4$		1	1	$-8N$	$2N^2-8N$	2
$\overline{Q}^{2N}$		1	1	$8N$	$-4N^2+4N$	0

$$\begin{aligned} W_{dyn} \;=\; & \frac{1}{\Lambda^{4N-1}}\Big[(A^N)(Q\overline{Q})^4(A\overline{Q}^2)^{N-2} + (A^{N-1}Q^2)(Q\overline{Q})^2(A\overline{Q}^2)^{N-1} + \\ & (A^{N-2}Q^4)(A\overline{Q}^2)^N + (\overline{Q}^{2N})(A^N)(A^{N-2}Q^4) + (\overline{Q}^{2N})(A^{N-1}Q^2)^2\Big] \end{aligned}$$

$SU(2N+1)$ with $\square\!\square + (2N+1)\ \overline{\square} + 4\ \square$ [64]

	$SU(2N+1)$	$SU(2N+1)$	$SU(4)$	$U(1)_1$	$U(1)_2$	$U(1)_R$
A	$\square\!\square$	1	1	0	$2N+5$	0
$\overline{Q}$	$\overline{\square}$	$\square$	1	4	$-2N+1$	0
Q	$\square$	1	$\square$	$-2N-1$	$-2N+1$	$\frac{1}{2}$
$Q\overline{Q}$		$\square$	$\square$	$3-2N$	$-4N+2$	$\frac{1}{2}$
$A\overline{Q}^2$		$\square\!\square$	1	8	$-2N+7$	0
A^NQ		1	$\square$	$-2N-1$	$2N^2+3N+1$	$\frac{1}{2}$
$A^{N-1}Q^3$		1	$\overline{\square}$	$-6N-3$	$2N^2-3N-2$	$\frac{3}{2}$
$\overline{Q}^{2N+1}$		1	1	$4(2N+1)$	$-4N^2+1$	0

$$W_{dyn} \;=\; \frac{1}{\Lambda^{2N}}\left[(A^NQ)(Q\overline{Q})^3(A\overline{Q}^2)^{N-1} + (A^{N-1}Q^3)(Q\overline{Q})(A\overline{Q}^2)^N + \right.$$

$$(\overline{Q}^{2N+1})(A^N Q)(A^{N-1}Q^3)\Big]$$

$SU(2N+1)$ **with** $\square\!\square + \overline{\square\!\square} + 3(\square + \overline{\square})$

	$SU(2N+1)$	$SU(3)$	$SU(3)$	$U(1)_1$	$U(1)_2$	$U(1)_3$	$U(1)_R$
A	$\square\!\square$	1	1	1	0	-3	0
$\bar{A}$	$\overline{\square\!\square}$	1	1	-1	0	-3	0
Q	$\square$	$\square$	1	0	1	$2N-1$	$\frac{1}{3}$
$\bar{Q}$	$\overline{\square}$	1	$\square$	0	-1	$2N-1$	$\frac{1}{3}$
$M_k = Q(A\bar{A})^k Q$		$\square$	$\square$	0	0	$4N-2-6k$	$\frac{2}{3}$
$H_k = \bar{A}(A\bar{A})^k Q^2$		$\square\!\square$	1	-1	2	$4N-5-6k$	$\frac{2}{3}$
$\bar{H}_k = A(A\bar{A})^k \bar{Q}^2$		1	$\square\!\square$	1	-2	$4N-5-6k$	$\frac{2}{3}$
$B_1 = A^N Q$		$\square$	1	N	1	$-N-1$	$\frac{1}{3}$
$\bar{B}_1 = \bar{A}^N \bar{Q}$		1	$\square$	$-N$	-1	$-N-1$	$\frac{1}{3}$
$B_3 = A^{N-1}Q^3$		1	1	$N-1$	3	$3N$	1
$\bar{B}_3 = \bar{A}^{N-1}\bar{Q}^3$		1	1	$-N+1$	-3	$3N$	1
$T_m = (A\bar{A})^m$		1	1	0	0	$-6m$	0

where $k = 0, \ldots, N-1$ and $m = 1, \ldots, N$. The number of terms in the confining superpotential grows quickly with the size of the gauge group. Therefore we only present the superpotential for the $SU(5)$ theory.

$$\begin{aligned} W_{dyn} \;=\; & \frac{1}{\Lambda^9}\Big(M_0^3 T_1 T_2 + M_1^3 + T_2 B_3 \bar{B}_3 + T_2 H_0 \bar{H}_0 M_0 + T_2 M_1 M_0^2 + T_1^3 M_0^3 + \\ & T_1^2 B_3 \bar{B}_3 + T_1^2 H_0 \bar{H}_0 M_0 + T_1^2 M_1 M_0^2 + T_1 B_1 \bar{B}_1 M_0^2 + T_1 H_0 \bar{H}_0 M_1 + \\ & B_1 \bar{B}_1 H_0 \bar{H}_0 + B_1 \bar{B} M_1 M_0 + H_1 \bar{H}_1 M_0 + H_1 \bar{H}_0 M_0 T_1 + \bar{H}_1 H_0 M_0 T_1 + \\ & \bar{H}_1 \bar{B}_1 B_3 + H_1 B_1 \bar{B}_3 + H_0 B_1 \bar{B}_3 T_1 + \bar{H}_0 \bar{B}_1 B_3 T_1 + H_1 \bar{H}_0 M_1 + \bar{H}_1 H_0 M_1\Big) \end{aligned}$$

Note that the term $T_1 M_1^2 M_0$ is allowed by all symmetries, however its coefficient is zero, which can be verified by requiring that the equations of motion reproduce the classical constraints.

$SU(2N)$ **with** $\square\!\square + \overline{\square\!\square} + 3(\square + \overline{\square})$

	$SU(2N)$	$SU(3)$	$SU(3)$	$U(1)_1$	$U(1)_2$	$U(1)_3$	$U(1)_R$
A	$\square\!\square$	1	1	1	0	-3	0
$\bar{A}$	$\overline{\square\!\square}$	1	1	-1	0	-3	0
Q	$\square$	$\square$	1	0	1	$2N-2$	$\frac{1}{3}$
$\bar{Q}$	$\overline{\square}$	1	$\square$	0	-1	$2N-2$	$\frac{1}{3}$
$M_k = Q(A\bar{A})^k Q$		$\square$	$\square$	0	0	$4N-4-6k$	$\frac{2}{3}$
$H_m = \bar{A}(A\bar{A})^k Q^2$		$\square\!\square$	1	-1	2	$4N-7-6m$	$\frac{2}{3}$
$\bar{H}_m = A(A\bar{A})^k \bar{Q}^2$		1	$\square\!\square$	1	-2	$4N-7-6m$	$\frac{2}{3}$
$B_0 = A^N$		1	1	N	0	$-3N$	0
$\bar{B}_0 = \bar{A}^N$		1	1	$-N$	0	$-3N$	0
$B_2 = A^{N-1}Q^2$		$\square\!\square$	1	$N-1$	2	$N-1$	$\frac{2}{3}$
$\bar{B}_2 = \bar{A}^{N-1}\bar{Q}^2$		1	$\square\!\square$	$-N+1$	-2	$N-1$	$\frac{2}{3}$
$T_n = (A\bar{A})^n$		1	1	0	0	$-6n$	0

where $k = 0, \ldots, N-1$, $m = 0, \ldots, N-2$ and $n = 1, \ldots, N-1$. The case of $SU(4)$ is different, because in $SU(4)$ the two-index antisymmetric tensor is self-conjugate. Therefore there is an additional $SU(2)$ global symmetry. The corresponding table is

	$SU(4)$	$SU(2)$	$SU(3)$	$SU(3)$	$U(1)_1$	$U(1)_2$	$U(1)_R$
A	$\square\!\square$	$\square$	1	1	0	-3	0
Q	$\square$	1	$\square$	1	1	2	$\frac{1}{3}$
$\bar{Q}$	$\overline{\square}$	1	1	$\square$	-1	2	$\frac{1}{3}$
$M_0 = QQ$		1	$\square$	$\square$	0	4	$\frac{2}{3}$
$M_2 = QA^2\bar{Q}$		1	$\square$	$\square$	0	-2	$\frac{2}{3}$
$H = AQ^2$		$\square$	$\overline{\square}$	1	2	1	$\frac{2}{3}$
$\bar{H} = A\bar{Q}^2$		$\square$	1	$\overline{\square}$	-2	1	$\frac{2}{3}$
$T = A^2$		$\square\!\square$	1	1	0	-6	0

The superpotential for the $SU(4)$ theory is

$$W_{dyn} = \frac{1}{\Lambda^7}\left(T^2 M_0^3 - 12 T H \bar{H} M_0 - 24 M_0 M_2^2 - 24 H \bar{H} M_2\right),$$

where the relative coefficients are fixed by requiring that the equations of motion reproduce the classical constraints.

$SU(6)$ **with** $\square\!\!\square\!\!\square + 4(\square + \bar{\square})$

	$SU(6)$	$SU(4)$	$SU(4)$	$U(1)_1$	$U(1)_2$	$U(1)_R$
A	$\square\!\!\square\!\!\square$	1	1	0	-4	-1
Q	$\square$	$\square$	1	1	3	1
$\bar{Q}$	$\bar{\square}$	1	$\square$	-1	3	1
$M_0 = Q\bar{Q}$		$\square$	$\square$	0	6	2
$M_2 = QA^2\bar{Q}$		$\square$	$\square$	0	-2	0
$B_1 = AQ^3$		$\bar{\square}$	1	3	5	2
$\bar{B}_1 = A\bar{Q}^3$		1	$\bar{\square}$	-3	5	2
$B_3 = A^3Q^3$		$\bar{\square}$	1	3	-3	0
$\bar{B}_3 = A^3\bar{Q}^3$		1	$\bar{\square}$	-3	-3	0
$T = A^4$		1	1	0	-16	4

$$W_{dyn} = \frac{1}{\Lambda^{11}}\Big(M_0B_1\bar{B}_1T + B_3\bar{B}_3M_0 + M_2^3M_0 + TM_2M_0^3 + \bar{B}_1B_3M_2 + B_1\bar{B}_3M_2\Big),$$

$SU(5)$ **with** $3(\square\!\!\square + \bar{\square})$

	$SU(5)$	$SU(3)$	$SU(3)$	$U(1)$	$U(1)_R$
A	$\square\!\!\square$	$\square$	1	1	0
$\bar{Q}$	$\bar{\square}$	1	$\square$	-3	$\frac{2}{3}$
$A\bar{Q}^2$		$\square$	$\bar{\square}$	-5	$\frac{4}{3}$
$A^3\bar{Q}$		$\square\!\!\square$	$\square$	0	$\frac{2}{3}$
A^5		$\square\square$	1	5	0

$$W_{dyn} = \frac{1}{\Lambda^9}\Big[(A^5)(A^3\overline{Q})(A\overline{Q}^2) + (A^3\overline{Q})^3\Big]$$

$SU(5)$ **with** $2\square\!\!\square + 4\,\bar{\square} + 2\square$

	$SU(5)$	$SU(2)$	$SU(4)$	$SU(2)$	$U(1)_1$	$U(1)_2$	$U(1)_R$
A	$\square\!\!\square$	$\square$	1	1	0	-1	0
$\bar{Q}$	$\bar{\square}$	1	$\square$	1	1	1	$\frac{1}{3}$
Q	$\square$	1	1	$\square$	-2	1	$\frac{1}{3}$
$Q\bar{Q}$		1	$\square$	$\square$	-1	2	$\frac{2}{3}$
$A\bar{Q}^2$		$\square$	$\square\!\!\square$	1	2	1	$\frac{2}{3}$
A^2Q		$\square\square$	1	$\square$	-2	-1	$\frac{1}{3}$
$A^3\bar{Q}$		$\square$	$\square$	1	1	-2	$\frac{1}{3}$
$A^2Q^2\bar{Q}$		1	$\square$	1	-3	1	1

$$W_{dyn} = \frac{1}{\Lambda^9}\Big[(A^3\overline{Q})^2(Q\overline{Q})^2 + (A^3\overline{Q})(A^2Q^2\overline{Q})(A\overline{Q}^2) + (A^3\overline{Q})(A^2Q)(A\overline{Q}^2)(Q\overline{Q}) + (A^2Q)^2(A\overline{Q}^2)^2\Big]$$

$SU(6)$ with $2\square + 5\overline{\square} + \square$

	$SU(6)$	$SU(2)$	$SU(5)$	$U(1)_1$	$U(1)_2$	$U(1)_R$
A	$\square\!\square$	$\square$	1	0	3	$\frac{1}{4}$
$\bar{Q}$	$\overline{\square}$	1	$\square$	1	-4	0
Q	$\square$	1	1	-5	-4	0
$Q\bar{Q}$		1	$\square$	-4	-8	0
$A\bar{Q}^2$		$\square$	$\square\!\square$	2	-5	$\frac{1}{4}$
A^3		$\square\square\square$	1	0	9	$\frac{3}{4}$
$A^3Q\bar{Q}$		$\square$	$\square$	-4	1	$\frac{3}{4}$
$A^4\bar{Q}^2$		1	$\square\!\square$	2	4	1

$$W_{dyn} = \frac{1}{\Lambda^{11}}\Big[(A^4\overline{Q}^2)^2(Q\overline{Q}) + (A^4\overline{Q}^2)(A^3Q\overline{Q})(A\overline{Q}^2) + (A^3)(A^3Q\overline{Q})(A\overline{Q}^2)^2 + (A^3)^2(A\overline{Q}^2)^2(Q\overline{Q})\Big]$$

Note, that the term $(A^4\overline{Q}^2)(A^3)(A\overline{Q}^2)(Q\overline{Q})$ is allowed by the $U(1)$ symmetries but not by the non-abelian global symmetries.

$SU(7)$ with $2\square + 6\overline{\square}$

	$SU(7)$	$SU(2)$	$SU(6)$	$U(1)$	$U(1)_R$
A	$\square\!\square$	$\square$	1	3	0
$\bar{Q}$	$\overline{\square}$	1	$\square$	-5	$\frac{1}{3}$
$H = A\bar{Q}^2$		$\square$	$\square\!\square$	-7	$\frac{2}{3}$
$N = A^4\bar{Q}$		$\square\square$	$\square$	7	$\frac{1}{3}$

$$W_{dyn} = \frac{1}{\Lambda^{13}}N^2H^2$$

4.4.2 The s-confining $Sp(2N)$ theories

We now discuss the s-confining $Sp(2N)$ theories. First, we again summarize the group theoretical properties of the simplest $Sp(2N)$ representations. Contrary to $SU(N)$ groups there is no chiral anomaly for $Sp(2N)$ groups. The only requirement on the field content is that there is no Witten anomaly, this is satisfied if the sum of the Dynkin indices of the matter fields is even. $Sp(2N)$ is the subgroup of $SU(2N)$ which leaves the tensor $J^{\alpha\beta} = (\mathbf{1}_{N\times N} \otimes i\sigma_2)^{\alpha\beta}$ invariant. Irreducible tensors of $Sp(2N)$ must be traceless with respect to $J^{\alpha\beta}$. One can obtain these irreducible representations by subtracting traces

$Sp(2N)$	$(2N+4)\square$	s-confining
$Sp(2N)$	$\begin{smallmatrix}\square\\\square\end{smallmatrix}+6\square$	s-confining
$Sp(2N)$	$\square\square+2\square$	Coulomb branch
$Sp(4)$	$2\begin{smallmatrix}\square\\\square\end{smallmatrix}+4\square$	$SU(2)$: $8\square$
$Sp(4)$	$3\begin{smallmatrix}\square\\\square\end{smallmatrix}+2\square$	$SU(2)$: $\square\square+4\square$
$Sp(4)$	$4\begin{smallmatrix}\square\\\square\end{smallmatrix}$	$SU(2)$: $2\square\square$
$Sp(6)$	$2\begin{smallmatrix}\square\\\square\end{smallmatrix}+2\square$	$Sp(4)$: $2\begin{smallmatrix}\square\\\square\end{smallmatrix}+4\square$
$Sp(6)$	$\begin{smallmatrix}\square\\\square\\\square\end{smallmatrix}+5\square$	$Sp(4)$: $2\begin{smallmatrix}\square\\\square\end{smallmatrix}+4\square$
$Sp(6)$	$\begin{smallmatrix}\square\\\square\\\square\end{smallmatrix}+\begin{smallmatrix}\square\\\square\end{smallmatrix}+\square$	$SU(2)$: $\square\square+4\square$
$Sp(6)$	$2\begin{smallmatrix}\square\\\square\\\square\end{smallmatrix}$	$SU(3)$: $\square\square+\overline{\square\square}$
$Sp(8)$	$2\begin{smallmatrix}\square\\\square\\\square\end{smallmatrix}$	$Sp(4)$: $5\begin{smallmatrix}\square\\\square\end{smallmatrix}$

Table 4.2: All Sp theories satisfying $\sum_j \mu_j - \mu_G = 2$. This list is finite because the indices of higher index tensor representations grow very rapidly with the size of the gauge group. We list the gauge group and the field content of the theories in the first column. In the second column, we indicate which theories are s-confining. For the remaining ones we give the flows to non-confining theories or indicate that there is a Coulomb branch on the moduli space.

from the $SU(2N)$ tensors. The properties of these representations are summarized in the table below. We use a normalization where the index of the fundamental is one. This normalization is consistent with the $Sp(2N) \subset SU(2N)$ embedding, under which $2N \to 2N$. Thus with these conventions the index of the matter fields does not change under $SU \to Sp$ decompositions. The adjoint of $Sp(2N)$ is the two-index symmetric tensor.

Irrep	Dim	μ
$\square$	$2N$	1
$\begin{smallmatrix}\square\\\square\end{smallmatrix}$	$N(2N-1)-1$	$2N-2$
$\square\square$	$N(2N+1)$	$2N+2$
$\begin{smallmatrix}\square\\\square\\\square\end{smallmatrix}$	$\frac{N(2N-1)(2N-2)}{3} - 2N$	$\frac{(2N-3)(2N-2)}{2} - 1$
$\square\square\square$	$\frac{N(2N+1)(2N+2)}{3}$	$\frac{(2N+2)(2N+3)}{2}$
$\begin{smallmatrix}\square\square\\\square\end{smallmatrix}$	$\frac{2N(2N-1)(2N+1)}{3} - 2N$	$(2N)^2 - 4$

With this knowledge one can again write down all anomaly-free theories for which the matter content satisfies Eq. 4.12. These theories are summarized in Table 4.2. In the first column, we indicate the gauge group and the field content of the theory. The second column gives a possible flow to a non-s-confining theory or if the theory is s-confining, we state that in the second column. The only s-confining theories based on $Sp(2N)$ groups are the two sequences that are already known in the literature. We give the spectra and dynamically generated superpotentials of these theories in the tables below.

$Sp(2N)$ **with** $(2N+4)$ $\square$ **[67]**

	$Sp(2N)$	$SU(2N+4)$	$U(1)_R$
Q	$\square$	$\square$	$\frac{1}{N+2}$
Q^2		$\begin{smallmatrix}\square\\\square\end{smallmatrix}$	$\frac{2}{N+2}$

$$W_{dyn} = \frac{1}{\Lambda^{2N+1}}(Q^2)^{N+2}$$

$Sp(2N)$ **with** $\begin{smallmatrix}\square\\\square\end{smallmatrix}$ $+ 6\ \square$ **[71, 72]**

	$Sp(2N)$	$SU(6)$	$U(1)$	$U(1)_R$
A	$\begin{smallmatrix}\square\\\square\end{smallmatrix}$	1	-3	0
Q	$\square$	$\square$	$N-1$	$\frac{1}{3}$
A^k		1	$-3k$	0
QA^mQ		$\begin{smallmatrix}\square\\\square\end{smallmatrix}$	$2(N-1)-3k$	$\frac{2}{3}$

Here $k = 2, 3, \ldots, N$ and $m = 0, 1, \ldots, N-1$. The number of terms in the superpotential grows quickly with N. For $Sp(4)$ the superpotential is

$$W_{dyn} = \frac{1}{\Lambda^5}\left[(A^2)(Q^2)^3 + (Q^2)(QAQ)^2\right].$$

4.4.3 The s-confining $SO(N)$ theories

$SO(N)$ theories[4] are distinct from the SU and Sp theories because contrary to those groups $SO(N)$ has representations which cannot be obtained from products of the vector representations. These are the spinorial representations. A theory can be s-confining only if all possible test charges can be screened by the matter fields. Spinors cannot be screened by matter in the vector representation of SO. Thus, theories without spinorial matter cannot be s-confining. This restricts the number of possible s-confining $SO(N)$ theories, because the Dynkin index of the spinor representation grows exponentially with the size of the gauge group. The biggest group for which Eq. 4.12 can be satisfied with matter including spinor representations is $SO(14)$.

$SO(N)$ theories (for $N > 6$) do not have either chiral or Witten anomalies. We do not consider the $N \leq 6$ theories because they can be obtained from our previous results by using the following isomorphisms: $SO(6) \sim SU(4)$, $SO(5) \sim Sp(4)$, $SO(4) \sim SU(2) \times SU(2)$, $SO(3) \sim SU(2)$, $SO(2) \sim U(1)$.

The spinor representations of $SO(N)$ have different properties depending on whether N is even or odd. For odd N, there is just one spinor representation, while for even N there are two inequivalent spinors. For $N = 4k$ the two spinors are self-conjugate while for $N = 4k+2$ the two spinors are complex conjugate to each other.

We use a normalization where the index of the vector of $SO(N)$ is 2. The reason is that under the embedding $SO(2N) \supset SU(N)$ the vector of $SO(2N)$ decomposes as $2N \to N + \overline{N}$. If we do not want the index of the matter fields to change under this decomposition we need

[4] We do not distinguish between $SO(N)$ and its covering group $Spin(N)$.

to normalize the index of the vector to two. The fundamental properties of the smallest $SO(N)$ representations are summarized in the tables below. The adjoint of $SO(N)$ is the two-index antisymmetric tensor.

$SO(2N+1)$		
Irrep	Dim	μ
$\square$	$2N+1$	2
S	2^N	2^{N-2}
$\begin{smallmatrix}\square\\\square\end{smallmatrix}$	$N(2N+1)$	$4N-2$
$\square\square$	$(N+1)(2N+1)-1$	$4N+6$

$SO(2N)$		
Irrep	Dim	μ
$\square$	$2N$	2
S	2^{N-1}	2^{N-3}
$\bar{S}, (S')$	2^{N-1}	2^{N-3}
$\begin{smallmatrix}\square\\\square\end{smallmatrix}$	$N(2N-1)$	$4N-4$
$\square\square$	$N(2N+1)-1$	$4N+4$

Since the vector and the spinors are the only representations that potentially have smaller index than the adjoint, it is clear that candidates for s-confining theories contain only vectors and spinors. For odd N we denote the field content by (s, v), where s is the number of spinors and v is the number of vectors. For even N we use the notation (s, s', v), where s and s' are the numbers of matter fields in the two inequivalent spinor representations and v is the number of vectors.

The $SO(8)$ group requires special attention. The reason is that there is a group automorphism which permutes the two spinor and the vector representations. Therefore only relative labelings of the representations are meaningful. For example $(4,3,0)$ and $(0,3,4)$ in $SO(8)$ are equivalent.

With this knowledge of group theory we can write down all theories which satisfy Eq. 4.12. These theories are listed in Table 4.3. Almost all of these theories are s-confining. The only spectrum that has been given in the literature [70] is for $SO(7)$ with $(5,1)$. Below we list the spectra and the confining superpotentials for the s-confining $SO(N)$ theories. Most of the confining superpotentials are very complicated. We only list those where the number of terms in the superpotential is reasonably small.

$SO(14)$	$(1,0,5)$	s-confining
$SO(13)$	$(1,4)$	s-confining
$SO(12)$	$(1,0,7)$	s-confining
$SO(12)$	$(2,0,3)$	s-confining
$SO(12)$	$(1,1,3)$	s-confining
$SO(11)$	$(1,6)$	s-confining
$SO(11)$	$(2,2)$	s-confining
$SO(10)$	$(4,0,1)$	s-confining
$SO(10)$	$(3,0,3)$	s-confining
$SO(10)$	$(2,0,5)$	s-confining
$SO(10)$	$(3,1,1)$	s-confining
$SO(10)$	$(2,1,3)$	s-confining
$SO(10)$	$(1,1,5)$	s-confining
$SO(10)$	$(2,2,1)$	s-confining
$SO(10)$	$(1,0,7)$	$SU(4)$ with $3\,\square\!\square + 2\,(\square + \overline{\square})$
$SO(9)$	$(4,0)$	s-confining
$SO(9)$	$(3,2)$	s-confining
$SO(9)$	$(2,4)$	s-confining
$SO(9)$	$(1,6)$	$SU(4)$ with $3\,\square\!\square + 2\,(\square + \overline{\square})$
$SO(8)$	$(7,0,0)$	Coulomb branch
$SO(8)$	$(6,1,0)$	Coulomb branch
$SO(8)$	$(5,2,0)$	$SU(4)$ with $3\,\square\!\square + 2\,(\square + \overline{\square})$
$SO(8)$	$(5,1,1)$	$SU(4)$ with $3\,\square\!\square + 2\,(\square + \overline{\square})$
$SO(8)$	$(4,3,0)$	s-confining
$SO(8)$	$(4,2,1)$	s-confining
$SO(8)$	$(3,3,1)$	s-confining
$SO(8)$	$(3,2,2)$	s-confining
$SO(7)$	$(6,0)$	s-confining
$SO(7)$	$(5,1)$	s-confining
$SO(7)$	$(4,2)$	s-confining
$SO(7)$	$(3,3)$	s-confining
$SO(7)$	$(2,4)$	$SU(4)$ with $3\,\square\!\square + 2\,(\square + \overline{\square})$
$SO(7)$	$(1,5)$	Coulomb branch

Table 4.3: All $SO(N)$ theories which contain at least one spinor and satisfy $\sum_j \mu_j - \mu_G = 2$. This list is finite because the index of the spinor representations grows exponentially with N. We list the gauge group of the theory in the first column and the matter content in the second column. As explained in the text, for odd N (s, v) denotes the number of spinors and the number of vectors, while for even N (s, s', v) denotes the numbers of the two inequivalent spinors and vectors. In the third column, we indicate which theories are s-confining. For the remaining ones we give the flows to non-confining theories or indicate that there is a Coulomb branch on the moduli space.

$SO(14)$ with (1,0,5)

	$SO(14)$	$SU(5)$	$U(1)$	$U(1)_R$
S	64	1	5	$\frac{1}{8}$
Q	$\square$	$\square$	-8	0
Q^2		$\square\square$	-16	0
S^2Q^3		$\begin{smallmatrix}\square\\\square\end{smallmatrix}$	-14	$\frac{1}{4}$
S^4Q^2		$\square\square$	4	$\frac{1}{2}$
S^4Q^4		$\overline{\square}$	-12	$\frac{1}{2}$
S^6Q^3		$\begin{smallmatrix}\square\\\square\end{smallmatrix}$	6	$\frac{3}{4}$
S^8		1	40	1
S^8Q^4		$\overline{\square}$	8	1

$$
\begin{aligned}
W_{dyn} \;=\; & \frac{1}{\Lambda^{23}}\Big[(S^8Q^4)^2(Q^2)+(S^8Q^4)(S^6Q^3)(S^2Q^3)+(S^8Q^4)(S^4Q^4)(S^4Q^2) \\
& +(S^8)^2(Q^2)^5+(S^8)(S^6Q^3)(S^2Q^3)(Q^2)^2+(S^4Q^2)^4(Q^2)+(S^6Q^3)^2(S^4Q^2)(Q^2) \\
& +(S^8)(S^4Q^4)^2(Q^2)+(S^8)(S^4Q^2)^2(Q^2)^3 \\
& +(S^6Q^3)(S^2Q^3)(S^4Q^2)^2+(S^6Q^3)^2(S^4Q^4)\Big]
\end{aligned}
$$

Note that several terms allowed by $U(1)$ symmetries are not allowed by the full set of global symmetries. For example, the $SU(5)$ contraction in the term $(S^8Q^4)(S^8)(Q^2)^3$ vanishes, since it is not possible to make an $SU(5)$ invariant from the third power of a symmetric tensor and one field in the antifundamental representation. There are more examples of such terms prohibited by non-abelian global symmetries in other theories in this section.

$SO(13)$ with (1,4)

	$SO(13)$	$SU(4)$	$U(1)$	$U(1)_R$
S	64	1	1	$\frac{1}{8}$
Q	$\square$	$\square$	-2	0
Q^2		$\square\square$	-4	0
S^2Q^3		$\overline{\square}$	-4	$\frac{1}{4}$
S^2Q^2		$\begin{smallmatrix}\square\\\square\end{smallmatrix}$	-2	$\frac{1}{4}$
S^4Q^4		1	-4	$\frac{1}{2}$
S^4Q^3		$\overline{\square}$	-2	$\frac{1}{2}$
S^4Q^2		$\square\square$	0	$\frac{1}{2}$
S^4Q		$\square$	2	$\frac{1}{2}$
S^4		1	4	$\frac{1}{2}$
S^6Q^3		$\overline{\square}$	0	$\frac{3}{4}$
S^6Q^2		$\begin{smallmatrix}\square\\\square\end{smallmatrix}$	2	$\frac{3}{4}$
S^8Q^3		$\overline{\square}$	2	1
S^8		1	8	1

Note, that one could add the operator S^8Q^4 to the above list without affecting anomaly matching. However, there is a mass term allowed for this operator, and by flowing to this

theory from $SO(14)$ with $(1,0,5)$ one finds that this mass term is generated. Thus S^8Q^4 is not in the IR spectrum. Similar operators appear in many other s-confining $SO(N)$ theories. Since a mass term is always generated for such operators, we do not include them in any of the forthcoming s-confining spectra.

$SO(12)$ with (1,0,7)

	$SO(12)$	$SU(7)$	$U(1)$	$U(1)_R$
S	32	1	7	$\frac{1}{4}$
Q	$\square$	$\square$	-4	0
Q^2		$\square\square$	-8	0
S^2Q^2		$\begin{smallmatrix}\square\\\square\end{smallmatrix}$	6	$\frac{1}{2}$
S^2Q^6		$\bar{\square}$	-10	$\frac{1}{2}$
S^4		1	28	1
S^4Q^6		$\bar{\square}$	4	1

$$W_{dyn} = \frac{1}{\Lambda^{19}}\Big[(S^4Q^6)^2(Q^2)+(S^4Q^6)(S^2Q^6)(S^2Q^2)+(S^4)(S^2Q^2)^2(Q^2)^5 +(S^4)(S^2Q^6)^2(Q^2)+(S^2Q^2)^4(Q^2)^3+(Q^2)^7(S^4)^2\Big]$$

$SO(12)$ with (2,0,3)

	$SO(12)$	$SU(2)$	$SU(3)$	$U(1)$	$U(1)_R$
S	32	$\square$	1	3	$\frac{1}{8}$
Q	$\square$	1	$\square$	-8	0
Q^2		1	$\square\square$	-16	0
S^2		1	1	6	$\frac{1}{4}$
S^2Q^2		$\square\square$	$\bar{\square}$	-10	$\frac{1}{4}$
S^4		$\square\square\square\square$	1	12	$\frac{1}{2}$
S^4Q^2		1	$\square\square$	-4	$\frac{1}{2}$
$S^4Q^{2'}$		$\square\square$	$\bar{\square}$	-4	$\frac{1}{2}$
S^6		1	1	18	$\frac{3}{4}$
S^6Q^2		$\square\square$	$\bar{\square}$	2	$\frac{3}{4}$
S^8Q^2		1	$\square\square$	8	1

$SO(12)$ **with (1,1,3)**

	$SO(12)$	$SU(3)$	$U(1)_1$	$U(1)_2$	$U(1)_R$
S	32	1	1	3	$\frac{1}{8}$
S'	$32'$	1	-1	3	$\frac{1}{8}$
Q	$\square$	$\square$	0	-8	0
Q^2		$\square\square$	0	-16	0
$SS'Q^3$		1	0	-18	$\frac{1}{4}$
S^2Q^2		$\overline{\square}$	2	-10	$\frac{1}{4}$
S'^2Q^2		$\overline{\square}$	-2	-10	$\frac{1}{4}$
$SS'Q$		$\square$	0	-2	$\frac{1}{4}$
S^4		1	4	12	$\frac{1}{2}$
S'^4		1	-4	12	$\frac{1}{2}$
$S^2S'^2$		1	0	12	$\frac{1}{2}$
$S^3S'Q^3$		1	2	-12	$\frac{1}{2}$
S'^3SQ^3		1	-2	-12	$\frac{1}{2}$
$S^2S'^2Q^2$		$\square\square$	0	-4	$\frac{1}{2}$
$S^2S'^2Q^{2'}$		$\overline{\square}$	0	-4	$\frac{1}{2}$
$S^3S'Q$		$\square$	2	4	$\frac{1}{2}$
S'^3SQ		$\square$	-2	4	$\frac{1}{2}$
$S^3S'^3Q^3$		1	0	-6	$\frac{3}{4}$
$S^3S'^3Q$		$\square$	0	10	$\frac{3}{4}$
$S^4S'^2Q^2$		$\overline{\square}$	2	2	$\frac{3}{4}$
$S'^4S^2Q^2$		$\overline{\square}$	-2	2	$\frac{3}{4}$
$S^4S'^4$		1	0	24	1
$S^4S'^4Q^2$		$\overline{\square}$	0	8	1

$SO(11)$ **with (1,6)**

	$SO(11)$	$SU(6)$	$U(1)$	$U(1)_R$
S	32	1	3	$\frac{1}{4}$
Q	$\square$	$\square$	-2	0
Q^2		$\square\square$	-4	0
S^2Q^2		$\begin{smallmatrix}\square\\\square\end{smallmatrix}$	2	$\frac{1}{2}$
S^2Q^5		$\overline{\square}$	-4	$\frac{1}{2}$
S^4		1	12	1
S^4Q^5		$\overline{\square}$	2	1
S^2Q		$\square$	4	$\frac{1}{2}$
S^2Q^6		1	-6	$\frac{1}{2}$

$SO(11)$ **with (2,2)**

	$SO(11)$	$SU(2)$	$SU(2)$	$U(1)$	$U(1)_R$
S	32	$\square$	1	1	0
Q	$\square$	1	$\square$	-4	$\frac{1}{2}$
Q^2		1	$\square\square$	-8	1
S^2Q^2		$\square\square$	1	-6	1
S^2Q		$\square\square$	$\square$	-2	$\frac{1}{2}$
S^2		1	1	2	0
S^4		$\square\square\square\square$	1	4	0
$S^{4'}$		1	1	4	0
S^4Q^2		1	$\square\square$	-4	1
$S^4Q^{2'}$		$\square\square$	1	-4	1
S^4Q		$\square\square$	$\square$	0	$\frac{1}{2}$
S^6Q^2		$\square\square$	1	-2	1
S^6Q		$\square\square$	$\square$	2	$\frac{1}{2}$
S^8		1	1	8	0
S^8Q		1	$\square$	4	$\frac{1}{2}$
S^4Q		1	$\square$	0	$\frac{1}{2}$
S^6		1	1	6	0

$SO(10)$ **with (4,0,1)**

	$SO(10)$	$SU(4)$	$U(1)$	$U(1)_R$
S	16	$\square$	1	0
Q	$\square$	1	-8	1
Q^2		1	-16	2
S^2Q		$\square\square$	-6	1
S^4		$\begin{smallmatrix}\square\square\\\square\square\end{smallmatrix}$	4	0
S^6Q		$\square\square$	-2	1

$$W_{dyn} = \frac{1}{\Lambda^{15}}\left[(S^6Q)^2(S^4) + (S^6Q)(S^2Q)(S^4)^2 + (S^2Q)^2(S^4)^3 + (S^4)^4(Q^2)\right]$$

$SO(10)$ **with (3,0,3)**

	$SO(10)$	$SU(3)$	$SU(3)$	$U(1)$	$U(1)_R$
S	16	$\square$	1	1	0
Q	$\square$	1	$\square$	-2	$\frac{1}{3}$
Q^2		1	$\square\square$	-4	$\frac{2}{3}$
S^2Q		$\square\square$	$\square$	0	$\frac{1}{3}$
S^2Q^3		$\overline{\square}$	1	-4	1
S^4		$\overline{\square\square}$	1	4	0
S^4Q^2		$\square$	$\overline{\square}$	0	$\frac{2}{3}$

$$
\begin{aligned}
W_{dyn} \;=\; & \frac{1}{\Lambda^{15}}\Big[(S^4Q^2)^3+(S^4Q^2)^2(S^2Q)^2+(S^4Q^2)^2(S^4)(Q^2)+(S^2Q^3)^2(S^4)^2 \\
& +(S^2Q)^2(Q^2)^2(S^4)^2+(S^2Q)^4(Q^2)(S^4)+(Q^2)^3(S^4)^3+(S^2Q)^6 \\
& +(S^4)(S^2Q^3)(S^4Q^2)(S^2Q)+(S^4Q^2)(S^4)(S^2Q)^2(Q^2) \\
& +(S^4Q^2)(S^4Q)^4+(S^2Q^3)(S^2Q)^3(S^4)\Big]
\end{aligned}
$$

$SO(10)$ **with (2,0,5)**

	$SO(10)$	$SU(2)$	$SU(5)$	$U(1)$	$U(1)_R$
S	16	$\square$	1	5	$\frac{1}{4}$
Q	$\square$	1	$\square$	-4	0
Q^2		1	$\square\square$	-8	0
S^2Q		$\square\square$	$\square$	6	$\frac{1}{2}$
S^2Q^3		1	$\begin{smallmatrix}\square\\\square\end{smallmatrix}$	-2	$\frac{1}{2}$
S^2Q^5		$\square\square$	1	-10	$\frac{1}{2}$
S^4		1	1	20	1
S^4Q^4		1	$\overline{\square}$	4	1

$SO(10)$ **with (3,1,1)**

	$SO(10)$	$SU(3)$	$U(1)_1$	$U(1)_2$	$U(1)_R$
S	16	$\square$	1	0	0
$\bar{S}$	$\overline{16}$	1	-3	1	0
Q	$\square$	1	0	-2	1
Q^2		1	0	-4	2
S^2Q		$\square\square$	2	-2	1
$S\bar{S}$		$\square$	-2	1	0
$S^3\bar{S}Q$		$\begin{smallmatrix}\square\square\\\square\end{smallmatrix}$	0	-1	1
$S^2\bar{S}^2$		$\square\square$	-4	2	0
S^4		$\overline{\square\square}$	4	0	0
$S^5\bar{S}$		$\square\square$	2	1	0
$S^4\bar{S}^2Q$		$\square$	-2	0	1
$\bar{S}^2Q$		1	-6	0	1
$S^3\bar{S}^3Q^2$		1	-6	-1	2

$SO(10)$ **with (2,1,3)**

	$SO(10)$	$SU(2)$	$SU(3)$	$U(1)_1$	$U(1)_2$	$U(1)_R$
S	16	$\square$	1	1	1	0
$\bar{S}$	$\overline{16}$	1	1	-2	1	$\frac{1}{2}$
Q	$\square$	1	$\square$	0	-2	0
Q^2		1	$\square\square$	0	-4	0
S^2Q		$\square\square$	$\square$	2	0	0
$\bar{S}^2Q$		1	$\square$	-4	0	1
$S\bar{S}$		$\square$	1	-1	2	$\frac{1}{2}$
$S^2\bar{S}^2$		$\square\square$	1	-2	4	1
S^2Q^3		1	1	2	-4	0
$S^3\bar{S}Q$		$\square$	$\square$	1	2	$\frac{1}{2}$
S^4		1	1	4	4	0
$S\bar{S}Q^2$		$\square$	$\overline{\square}$	-1	-2	$\frac{1}{2}$
$S^2\bar{S}^2Q^2$		1	$\overline{\square}$	-2	0	1
$S^3\bar{S}Q^3$		$\square$	1	1	-2	$\frac{1}{2}$

$SO(10)$ **with (1,1,5)**

	$SO(10)$	$SU(5)$	$U(1)_1$	$U(1)_2$	$U(1)_R$
S	16	1	1	5	$\frac{1}{4}$
$\overline{S}$	$\overline{16}$	1	-1	5	$\frac{1}{4}$
Q	$\square$	$\square$	0	-4	0
Q^2		$\square\square$	0	-8	0
S^2Q		$\square$	2	6	$\frac{1}{2}$
$\overline{S}^2Q$		$\square$	-2	6	$\frac{1}{2}$
$S\overline{S}$		1	0	10	$\frac{1}{2}$
S^2Q^5		1	2	-10	$\frac{1}{2}$
$\overline{S}^2Q^5$		1	-2	-10	$\frac{1}{2}$
$S\overline{S}Q^2$		$\begin{smallmatrix}\square\\\square\end{smallmatrix}$	0	2	$\frac{1}{2}$
$S\overline{S}Q^4$		$\overline{\square}$	0	-6	$\frac{1}{2}$
$S^2\overline{S}^2$		1	0	20	1
$S^2\overline{S}^2Q^4$		$\overline{\square}$	0	4	1

$SO(10)$ **with (2,2,1)**

	$SO(10)$	$SU(2)$	$SU(2)$	$U(1)_1$	$U(1)_2$	$U(1)_R$
S	16	$\square$	1	1	1	0
$\overline{S}$	$\overline{16}$	1	$\square$	-1	1	0
Q	$\square$	1	1	0	-8	1
Q^2		1	1	0	-16	2
S^2Q		$\square\square$	1	2	-6	1
$\overline{S}^2Q$		1	$\square\square$	-2	-6	1
$S\overline{S}$		$\square$	$\square$	0	2	0
S^4		1	1	4	4	0
$\overline{S}^4$		1	1	-4	4	0
$S^2\overline{S}^2$		$\square\square$	$\square\square$	0	4	0
$S^3\overline{S}Q$		$\square$	$\square$	2	-4	1
$\overline{S}^3SQ$		$\square$	$\square$	-2	-4	1
$S^2\overline{S}^2Q^2$		1	1	0	-12	2
$S^4\overline{S}^2Q$		$\square\square$	1	2	-2	1
$\overline{S}^4S^2Q$		1	$\square\square$	-2	-2	1
$S^3\overline{S}^3$		$\square$	$\square$	0	6	0
$S^6\overline{S}^2$		1	1	4	8	0
$\overline{S}^6S^2$		1	1	-4	8	0

$SO(9)$ **with (4,0)**

	$SO(9)$	$SU(4)$	$U(1)_R$
S	16	$\square$	$\frac{1}{8}$
S^2		$\square\square$	$\frac{1}{4}$
S^4		$\begin{smallmatrix}\square\\\square\end{smallmatrix}$	$\frac{1}{2}$
S^6		$\square\square$	$\frac{3}{4}$

$$W_{dyn} = \frac{1}{\Lambda^{13}}\left[(S^6)^2(S^4) + (S^6)(S^4)^2(S^2) + (S^4)^4 + (S^4)^3(S^2)^2\right]$$

$SO(9)$ **with (3,2)**

	$SO(9)$	$SU(3)$	$SU(2)$	$U(1)$	$U(1)_R$
S	16	$\square$	1	1	0
Q	$\square$	1	$\square$	-3	$\frac{1}{2}$
Q^2		1	$\square\square$	-6	1
S^2Q		$\square\square$	$\square$	-1	$\frac{1}{2}$
S^2		$\square\square$	1	2	0
S^4		$\overline{\square\square}$	1	4	0
S^2Q^2		$\overline{\square}$	1	-4	1
S^4Q^2		$\square$	1	-2	1
S^4Q		$\square$	$\square$	1	$\frac{1}{2}$

$SO(9)$ **with (2,4)**

	$SO(9)$	$SU(2)$	$SU(4)$	$U(1)$	$U(1)_R$
S	16	$\square$	1	1	$\frac{1}{4}$
Q	$\square$	1	$\square$	-1	0
Q^2		1	$\square\square$	-2	0
S^2Q		$\square\square$	$\square$	1	$\frac{1}{2}$
S^2		$\square\square$	1	2	$\frac{1}{2}$
S^2Q^3		1	$\overline{\square}$	-1	$\frac{1}{2}$
S^2Q^2		1	$\begin{smallmatrix}\square\\\square\end{smallmatrix}$	0	$\frac{1}{2}$
S^4Q^3		1	$\overline{\square}$	1	1
S^2Q^4		$\square\square$	1	-2	$\frac{1}{2}$
S^4		1	1	4	1

$SO(8)$ **with (4,3,0)**

	$SO(8)$	$SU(4)$	$SU(3)$	$U(1)$	$U(1)_R$
Q	8_v	$\square$	1	3	$\frac{1}{4}$
S	8_s	1	$\square$	-4	0
Q^2		$\square\square$	1	6	$\frac{1}{2}$
S^2		1	$\square\square$	-8	0
S^2Q^2		$\begin{smallmatrix}\square\\\square\end{smallmatrix}$	$\overline{\square}$	-2	$\frac{1}{2}$
S^2Q^4		1	$\square\square$	4	1

$$W_{dyn} = \frac{1}{\Lambda^{11}}\Big[(S^2Q^4)^2(S^2)+(S^2Q^4)(S^2Q^2)^2+(S^2Q^2)^3(Q^2)+(S^2)^3(Q^2)^4 +(S^2Q^2)^2(S^2)(Q^2)^2\Big]$$

$SO(8)$ **with (4,2,1)**

	$SO(8)$	$SU(4)$	$SU(2)$	$U(1)$	$U(1)$	$U(1)_R$
Q	8_v	$\square$	1	1	0	$\frac{1}{4}$
S	8_s	1	$\square$	-2	1	0
S'	8_c	1	1	0	-2	0
Q^2		$\square\square$	1	2	0	$\frac{1}{2}$
S^2		1	$\square\square$	-4	2	0
S'^2		1	1	0	-4	0
S^2Q^2		$\begin{smallmatrix}\square\\\square\end{smallmatrix}$	1	-2	2	$\frac{1}{2}$
S^2Q^4		1	$\square\square$	0	2	1
S'^2Q^4		1	1	4	-4	1
$SS'Q$		$\square$	$\square$	-1	-1	$\frac{1}{4}$
$SS'Q^3$		$\overline{\square}$	$\square$	1	-1	$\frac{3}{4}$

$SO(8)$ **with (3,3,1)**

	$SO(8)$	$SU(3)$	$SU(3)$	$U(1)_1$	$U(1)_2$	$U(1)_R$
Q	8_v	1	1	0	6	1
S	8_s	$\square$	1	1	-1	0
S'	8_c	1	$\square$	-1	-1	0
Q^2		1	1	0	12	2
S^2		$\square\square$	1	2	-2	0
S'^2		1	$\square\square$	-2	-2	0
$SS'Q$		$\square$	$\square$	0	4	1
$S^3S'Q$		1	$\square$	2	2	1
S'^3SQ		$\square$	1	-2	2	1
$S^2S'^2$		$\overline{\square}$	$\overline{\square}$	0	-4	0

$SO(8)$ **with (3,2,2)**

	$SO(8)$	$SU(3)$	$SU(2)$	$SU(2)$	$U(1)_1$	$U(1)_2$	$U(1)_R$
Q	8_v	$\square$	1	1	0	4	0
S	8_s	1	$\square$	1	1	-3	$\frac{1}{4}$
S'	8_c	1	1	$\square$	-1	-3	$\frac{1}{4}$
Q^2		$\square\square$	1	1	0	8	0
S^2		1	$\square\square$	1	2	-6	$\frac{1}{2}$
S'^2		1	1	$\square\square$	-2	-6	$\frac{1}{2}$
$SS'Q$		$\square$	$\square$	$\square$	0	-2	$\frac{1}{2}$
S^2Q^2		$\overline{\square}$	1	1	2	2	$\frac{1}{2}$
S'^2Q^2		$\overline{\square}$	1	1	-2	2	$\frac{1}{2}$
$SS'Q^3$		1	$\square$	$\square$	0	6	$\frac{1}{2}$
$S^2S'^2$		1	1	1	0	-12	1
$S^2S'^2Q^2$		$\overline{\square}$	1	1	0	-4	1

$SO(7)$ **with (6,0)**

	$SO(7)$	$SU(6)$	$U(1)_R$
S	8	$\square$	$\frac{1}{6}$
S^2		$\square\square$	$\frac{1}{3}$
S^4		$\begin{array}{c}\square\\\square\end{array}$	$\frac{2}{3}$

$$W_{dyn} = \frac{1}{\Lambda^9}\left[(S^4)^3 + (S^4)^2(S^2)^2 + (S^4)(S^2)^4\right]$$

$SO(7)$ **with (5,1) [70]**

	$SO(7)$	$SU(5)$	$U(1)$	$U(1)_R$
S	8	$\square$	1	0
Q	$\square$	1	-5	1
Q^2		1	-10	2
S^2		$\square\square$	2	0
S^4		$\begin{array}{c}\square\\\square\end{array}$	4	0
S^2Q		$\begin{array}{c}\square\\\square\end{array}$	-3	1
S^4Q		$\square$	-1	1

$$W_{dyn} = \frac{1}{\Lambda^9}\left[(S^4Q)^2(S^2) + (S^4Q)(S^2Q)(S^4) + (S^2Q)^2(S^4)(S^2)\right.$$
$$\left.+(Q^2)(S^2)(S^4)^2 + (S^2)^5(Q^2)\right]$$

$SO(7)$ **with (4,2)**

	$SO(7)$	$SU(4)$	$SU(2)$	$U(1)$	$U(1)_R$
S	8	$\square$	1	1	0
Q	$\square$	1	$\square$	-2	$\frac{1}{2}$
Q^2		1	$\square\square$	-4	1
S^2		$\square\square$	1	2	0
S^2Q		$\begin{array}{c}\square\\\square\end{array}$	$\square$	0	$\frac{1}{2}$
S^2Q^2		$\begin{array}{c}\square\\\square\end{array}$	1	-2	1
S^4		1	1	4	0
S^4Q		1	$\square$	2	$\frac{1}{2}$

$$W_{dyn} = \frac{1}{\Lambda^9}\left[(S^4Q)^2(Q^2) + (S^4Q)(S^2Q)(S^2Q^2) + (S^2Q)^2(S^2Q^2)(S^2)\right.$$
$$\left.+(S^4)(S^2Q^2)^2 + (S^2Q)^2(S^2)^2(Q^2) + (S^2Q^2)^2(S^2)^2 + (S^2)^4(Q^2)^2\right]$$

$SO(7)$ **with (3,3)**

	$SO(7)$	$SU(3)$	$SU(3)$	$U(1)$	$U(1)_R$
S	8	$\square$	1	1	0
Q	$\square$	1	$\square$	-1	$\frac{1}{3}$
Q^2		1	$\square\square$	-2	$\frac{2}{3}$
S^2		$\square\square$	1	2	0
S^2Q		$\bar{\square}$	$\square$	1	$\frac{1}{3}$
S^2Q^2		$\bar{\square}$	$\bar{\square}$	0	$\frac{2}{3}$
S^2Q^3		$\square\square$	1	-1	1

$$W_{dyn} = \frac{1}{\Lambda^9}\Big[(S^2Q^3)^2(S^2)+(S^2Q^3)(S^2Q^2)(S^2Q)+(S^2Q^2)^3+(S^2)^3(Q^2)^3 +(S^2Q^2)^2(S^2)(Q^2)+(S^2Q)^2(S^2)(Q^2)^2+(S^2Q)^2(S^2Q^2)(Q^2)\Big]$$

The $SO(N)$ theories with $\sum\mu_i - \mu_G = 4$

Our normalization for the indices of SO groups is somewhat non-standard. It follows from demanding that the index is invariant under flows from $SO(2N)$ groups to their $SU(N)$ subgroups. In the normalization where the index of the vector is one rather than two, it is obvious that one can obtain a superpotential that is regular at the origin for $\sum\mu_i - \mu_G = 1$ or 2. In our normalization, this corresponds to $\sum\mu_i - \mu_G = 2$ or 4. We have explicitly checked that none of the $\sum\mu_i - \mu_G = 4$ theories are s-confining by identifying flows to non-s-confining theories.

The $\sum\mu_i - \mu_G = 4$ $SO(N)$ theories are examples of the special case where the confining superpotential can be holomorphic at the origin without Eq. 4.12 being satisfied. This can only happen when μ_G and all μ_i have a common divisor. Just like the previously mentioned $\sum\mu_i - \mu_G = 4$ $SO(N)$ theories, such theories are unlikely to s-confine. The reason is that while Eq. 4.12 is preserved under most flows along flat directions, the property that μ_G and all μ_i have a common divisor is not. Thus for most such theories one should be able to find a flow to a non-s-confining theory. We expect that none of these "common divisor" theories s-confine.

4.4.4 Exceptional groups

The analysis for exceptional groups G_2, F_4, E_6, E_7, and E_8 is surprisingly simple. The s-confined spectrum of a G_2 gauge theory with 5 fundamentals has already been worked out in Ref. [69, 70]. The representations of G_2 are real, thus the invariant tensors include the two index symmetric tensor. Furthermore, there are two totally antisymmetric tensors with three and four indices, respectively. Therefore, the confined spectrum is

G_2 with 5 $\square$ [69]

	G_2	$SU(5)$	$U(1)_R$
Q	7	$\square$	$\frac{1}{5}$
$M = Q^2$		$\square\square$	$\frac{2}{5}$
$A = Q^3$		$\begin{smallmatrix}\square\\\square\end{smallmatrix}$	$\frac{3}{5}$
$B = Q^4$		$\overline{\square}$	$\frac{4}{5}$

$$W_{dyn} = \frac{1}{\Lambda^7}\left[M^5 + M^2A^2 + MB^2 + A^2B\right]$$

The F_4, E_6, E_7 and E_8 theories

Theories based on any of the other exceptional gauge groups can be shown to flow to theories which are not s-confining. This is derived most easily by starting with the real group F_4. The lowest dimensional representations of F_4 are the 26 dimensional fundamental representation and the 52 dimensional adjoint. Since any theory with adjoint matter has a Coulomb branch on its moduli space, we can restrict our attention to theories with only fundamentals. By giving an expectation value to a fundamental one can break F_4 to its maximal subgroup $SO(9)$. Under $SO(9)$ the representations decompose as follows: $26 \to 1 + 9 + 16$ and $52 \to 16 + 36$. The 9, 16, 36 are the fundamental, spinor, and adjoint of $SO(9)$. When giving an expectation value to a fundamental of F_4, the spinor component of its $SO(9)$ decomposition is eaten. Thus an F_4 theory with N_f fundamentals flows to an $SO(9)$ theory with N_f fundamentals and $N_f - 1$ spinors. For no N_f is this $SO(9)$ theory s-confining, therefore no F_4 theory s-confines.

Using this result, it is easy to show that none of the groups E_6, E_7, and E_8 s-confine. The lowest dimensional representations of E_6 are the (complex) fundamental and the adjoint. By giving an expectation value to a fundamental, one can flow to F_4, whereas expectation values for an adjoint lead to a Coulomb branch. Thus, E_6 theories cannot be s-confining either.

By giving an expectation value to a field in the 56 dimensional fundamental representation of E_7 one can flow to E_6, while an expectation value for the adjoint again yields a Coulomb branch. For E_8 the lowest dimensional representation is the adjoint, again leading to a Coulomb branch. Thus none of the $E_{6,7,8}$ groups with arbitrary matter are s-confining.

4.5 Obtaining new models by integrating out matter

In the previous section we obtained a low-energy description for many theories which satisfy $\sum \mu_i - \mu_G = 2$. Since a number of these theories contain matter in vector-like representations one can easily derive descriptions for theories with smaller matter content by integrating out fields. In this way we obtain confining theories with a quantum modified constraint, theories with dynamically generated superpotentials and theories with multiple branches.

4.5.1 Theories with quantum-deformed moduli spaces

In these theories a classical constraint of the form $\sum(\Pi_i X_i) = 0$ (where X_i are gauge invariant operators) is modified quantum mechanically to $\sum(\Pi_i X_i) = \Lambda^p \Pi_j X_j$. Here, the

X_j are some other combination of the gauge invariant operators, including the possibility that the quantum modification is just Λ^p. The power p must necessarily be positive to reproduce the correct classical limit. Such a modification of the classical constraint is only possible in theories where $\sum \mu_i - \mu_G = 0$. To show this, consider assigning R-charge zero to every chiral superfield. This R-symmetry is anomalous and the anomaly has to be compensated by assigning R-charge $\sum \mu_i - \mu_G$ to the scale of the gauge group raised to the power of its one loop β function coefficient $\Lambda^{(3\mu_G - \sum \mu_i)/2}$ [60]. Since the constraints have to respect this R-symmetry one immediately sees that Λ can only appear in a constraint if it has vanishing R-charge. Therefore, we conclude that only theories with $\sum \mu_i - \mu_G = 0$ may exhibit quantum deformed moduli spaces.

We can find all theories satisfying $\sum \mu_i - \mu_G = 0$ by simply leaving out a flavor from the matter contents listed in Tables 4.1 and 4.2 for SU and Sp theories and by leaving out a vector from Table 4.3 for SO theories. The theories obtained from the s-confining ones are all confining with a quantum modified constraint. It follows from the procedure of integrating out a flavor that the form of the quantum modified constraint is $\sum(\Pi_i X_i) = \Lambda^{\Sigma \mu_i}$.

In those cases where the s-confining theory contains several meson type fields (e.g. $Q\bar{Q}$, $QA^2\bar{Q}$, etc.) there will be additional constraints which are not modified quantum mechanically [71, 72]. All constraints can be implemented by adding them to the superpotential with Lagrange multipliers. Here, we list only those SU theories which were not previously known in the literature. Similar results can be obtained from the s-confining SO theories. In the case of $SO(N)$ theories there is always one quantum modified constraint, while the total number of constraints equals the number of operators containing exactly two vectors Q in a symmetric representation of the Q-flavor symmetry.

In the following superpotentials we denote Lagrange multipliers by Greek letters, the notation for the confined fields is defined in the corresponding tables in Section 4.4.

$SU(4)$ **with** $2\square\!\square + 2(\square + \overline{\square})$

$$W = \lambda\Big(3T^2M_0^2 - 12TH\bar{H} - 24M_2^2 - \Lambda^8\Big) + \mu\Big(2M_0M_2 + H\bar{H}\Big)$$

$SU(5)$ **with** $\square\!\square + \overline{\square\!\square} + 2(\square + \overline{\square})$

$$\begin{aligned} W \;=\; & \lambda\Big(3M_0^2T_1T_2 + T_2H_0\bar{H}_0 + 2T_2M_0M_1 + 3T_1^3M_0^2 + T_1^2H_0\bar{H}_0 + \\ & 2T_1^2M_0M_1 + 2T_1B_1\bar{B}_1M_0 + B_1\bar{B}_1M_1 + H_1\bar{H}_1 + \bar{H}_0H_1T_1 + \\ & H_0\bar{H}_1T_1 - \Lambda^{10}\Big) + \mu\Big(3M_1^2 + T_2M_0^2 + T_1^2M_0^2 + T_1H_0\bar{H}_0 + \\ & B_1\bar{B}_1M_0 + H_0\bar{H}_1 + \bar{H}_0H_1\Big) \end{aligned}$$

$SU(5)$ **with** $2\square\!\square + \square + 3\overline{\square}$

$$W = \lambda\Big[(A^3\bar{Q})^2(Q\bar{Q}) + (A^3\bar{Q})(A^2Q)(A\bar{Q}^2) - \Lambda^{10}\Big]$$

$SU(6)$ **with** $2\square + 4\overline{\square}$

$$W = \lambda\left[(A^4\bar{Q}^2)^2 + (A^3)^2(A\bar{Q}^2)^2 - \Lambda^{12}\right] + \mu\left[(A^4\bar{Q}^2)(A\bar{Q}^2) + (A^3)(A\bar{Q}^2)^2\right]$$

$SU(6)$ **with** $\begin{smallmatrix}\square\\\square\end{smallmatrix} + 3(\square + \overline{\square})$

$$\begin{aligned} W &= \lambda\left(B_1\bar{B}_1T + B_3\bar{B}_3 + M_2^3 + TM_2M_0^2 - \Lambda^{12}\right) + \\ &\quad \mu\left(M_2^2M_0 + TM_0^3 + \bar{B}_1B_3 + B_1\bar{B}_3\right) \end{aligned}$$

We have seen that all s-confining $\sum \mu_i - \mu_G = 2$ theories result in confining $\sum \mu_i - \mu_G = 0$ theories with a quantum modified constraint after integrating out a flavor. This does not imply that $\sum \mu_i - \mu_G = 2$ theories which do not s-confine cannot result in confining theories with quantum modified constraints after eliminating one flavor.

As an example we consider $SU(4)$ with $3\begin{smallmatrix}\square\\\square\end{smallmatrix} + \square + \overline{\square}$. The theory with an additional flavor is not s-confining, it flows to $SU(2)$ with $8\square$. Moreover, one can explicitly construct a dual description for $SU(4)$ with $3\begin{smallmatrix}\square\\\square\end{smallmatrix} + 2(\square + \overline{\square})$ by noting that this theory is equivalent to an $SO(6)$ theory with $3\square + 2(S + \bar{S})$, where S and $\bar{S}$ denote a spinor and its conjugate. This dual can be obtained from the dual of $SO(10)$ with one spinor and 7 vectors [70]. The confining description with one less flavor is obtained from the $SO(8)$ theory with a spinor and 5 vectors [70]. The confining spectrum is given in the table below.

	$SU(4)$	$SU(3)$	$U(1)_1$	$U(1)_2$	$U(1)_R$
A	$\begin{smallmatrix}\square\\\square\end{smallmatrix}$	$\square$	0	1	0
Q	$\square$	1	1	-3	0
$\bar{Q}$	$\overline{\square}$	1	-1	-3	0
A^2		$\square\square$	0	2	0
$QA^2\bar{Q}$		$\overline{\square}$	0	-4	0
$Q\bar{Q}$		1	0	-6	0
A^3Q^2		1	2	-3	0
$A^3\bar{Q}^2$		1	-2	-3	0

The quantum modified constraint is

$$W = \lambda\left[(Q\bar{Q})^2(A^2)^3 + (A^2)(QA^2\bar{Q})^2 + (A^3Q^2)\,(A^3\bar{Q}^2) - \Lambda^8(Q\bar{Q})\right]$$

Note that one can eliminate the field $(Q\bar{Q})$ from the theory by solving the quantum modified constraint. The remaining fields match all anomalies of the ultraviolet theory. It would be interesting to determine which of the remaining $\sum \mu_i - \mu_G = 0$ theories are confining with a quantum modified constraint.

4.5.2 Dynamically generated runaway superpotentials

Starting from the confining theories with a quantum deformed moduli space one obtains theories with dynamically generated run-away superpotentials by integrating out more flavors. Here we only list the dynamical superpotentials which one finds by starting with the s-confining SU theories and which are not already in the literature. It is straightforward

to obtain similar results from the s-confining SO theories by integrating out vectors. Our notation for the composites in the following superpotentials is defined in the corresponding tables in Section 4.4.

$SU(4)$ **with** $2\square + F(\square + \bar{\square})$

$$\begin{aligned} W_{F=1} &= \frac{\Lambda^9 M_0}{6T^2 M_0^2 + 48 M_2^2}, \\ W_{F=0} &= 0 \text{ or } W_{F=0} = \frac{\Lambda^5}{\sqrt{T^2}}. \end{aligned}$$

$SU(5)$ **with** $\square + \bar{\square} + F(\square + \bar{\square})$

$$\begin{aligned} W_{F=1} &= \Big(\Lambda^{11} M_1\Big) \Big/ \Big(M_1 M_0 T_1 T_2 + T_2 M_1^2 + T_1^3 M_0 M_1 + T_1^2 M_1^2 + \\ &\quad T_1 B_1 \bar{B}_1 M_1 - (T_2 M_0 + T_1^2 M_0 + B_1 \bar{B}_1)^2\Big), \\ W_{F=0} &= \pm \frac{\Lambda^6}{\sqrt{(T_2 + T_1^2)(T_1 \pm \sqrt{T_2 + T_1^2})}}. \end{aligned}$$

$SU(5)$ **with** $2\square + 2\bar{\square}$ **[76]**

$$W = \frac{\Lambda^{11}}{(A^3 \bar{Q})^2}.$$

$SU(6)$ **with** $\begin{smallmatrix}\square\\\square\end{smallmatrix} + F(\square + \bar{\square})$

$$\begin{aligned} W_{F=2} &= \frac{\Lambda^{13} M_2 M_0}{T(M_2 M_0)^2 - (M_2^2 + T M_0^2)^2}, \\ W_{F=1} &= \pm \frac{\Lambda^3 \sqrt{x_\pm}}{\frac{x_+^2 x_\pm T^2}{M_0^2 z^3 y^2} + \frac{x_\pm}{z}}, \\ W_{F=0} &= 0 \text{ or } W_{F=0} = \frac{\Lambda^5}{\sqrt{T}}, \end{aligned}$$

where

$$x = \tfrac{8M_2^5}{T} - 10 M_0^2 M_2^3 + 2 M_0^4 M_2 T, \quad y = M_2^2 - M_0^2 T,$$
$$z = 4M_2^2 - M_0^2 T, \quad x_\pm = x \pm \tfrac{y z^{3/2}}{T}.$$

4.5.3 Theories with multiple branches

When integrating out flavors from a few of the s-confining theories we find that there are multiple possible solutions for the superpotential: one or more solutions with a dynamically generated term, and a solution with vanishing superpotential. This indicates that such

theories have several branches of vacua. There is not only a moduli space with a smooth continuous parameterization but there is also a discrete parameter distinguishing a discrete set of vacua. In our examples there are two sets of vacua which are characterized by $W = 0$ with a non-trivial moduli space, and $W \propto \frac{1}{\text{fields}}$ without a stable vacuum [66, 71, 72]. A consistency check on the assumption that the branch with vanishing superpotential describes a confining theory is that the 't Hooft anomaly matching conditions are satisfied. In addition to the previously described $SU(4)$ with $2\square$ $SU(6)$ with $\begin{smallmatrix}\square\\\square\end{smallmatrix}$, also $SO(14)$ with one spinor field has multiple branches.

Chapter 5

Dynamical Supersymmetry Breaking[1]

In this chapter we introduce a new class of theories which dynamically break supersymmetry based on the gauge group $SU(n) \times SU(3) \times U(1)$ for even n. These theories are interesting in that no dynamical superpotential is generated in the absence of perturbations. For the example $SU(4) \times SU(3) \times U(1)$ we explicitly demonstrate that all flat directions can be lifted through a renormalizable superpotential and that supersymmetry is dynamically broken. We derive the exact superpotential for this theory, which exhibits new and interesting dynamical phenomena. For example, modifications to classical constraints can be field dependent. We also consider the generalization to $SU(n) \times SU(3) \times U(1)$ models (with even $n > 4$). We present a renormalizable superpotential which lifts all flat directions. Because $SU(3)$ is not confining in the absence of perturbations, the analysis of supersymmetry breaking is very different in these theories from the $n = 4$ example. When the $SU(n)$ gauge group confines, the Yukawa couplings drive the $SU(3)$ theory into a regime with a dynamically generated superpotential. By considering a simplified version of these theories we argue that supersymmetry is probably broken. We also show that theories in the confining, free magnetic, and conformal phases can break supersymmetry through dynamical effects. To illustrate this, we present theories based on the gauge groups $SU(n) \times SU(4) \times U(1)$ and $SU(n) \times SU(5) \times U(1)$ with the field content obtained by decomposing an $SU(m)$ theory with an antisymmetric tensor and $m - 4$ antifundamentals.

Supersymmetry breaking is an inherent part of any realistic supersymmetric theory. One of the motivations for supersymmetry is that it stabilizes the ratio of the electroweak scale to the Planck scale against large radiative corrections. If supersymmetry is broken dynamically, logarithmic running of a gauge coupling would also provide an explanation for the smallness of the ratio of the electroweak and Planck scales.

Almost all phenomenologically viable models consist of two sectors: the Minimal Supersymmetric Standard Model (MSSM) and the supersymmetry breaking sector. The information about supersymmetry breaking is transmitted to the MSSM either by gravitational or by gauge interactions, or a combination thereof. In the case of gravity mediated supersymmetry breaking, the electroweak scale, M_{weak}, is proportional to $\frac{\Lambda_{SB}^2}{M_{Planck}}$, where Λ_{SB} is the scale of supersymmetry breaking and M_{Planck} is the Planck scale. When supersymme-

[1]This chapter is based on research done in collaboration with Csaba Csáki, Lisa Randall and Robert Leigh reported in Refs. [77, 78, 79].

try breaking is mediated by gauge interactions, $M_{weak} \propto \alpha^n \Lambda_{SB}$, where α is the structure constant of the relevant gauge group. In any scenario, the electroweak scale is tied to the supersymmetry breaking scale. If the scale of supersymmetry breaking is naturally small, so is the electroweak scale.

The scale of supersymmetry breaking can be small naturally because of the supersymmetric non-renormalization theorem [80]. Since the superpotential receives no radiative corrections, if supersymmetry is unbroken at the tree-level, it remains unbroken at any order of perturbation theory. Therefore, only non-perturbative effects can be responsible for dynamical supersymmetry breaking. Such effects in asymptotically-free gauge theories are only relevant at low energies.

In the next section, we discuss general conditions that help to identify potential candidate theories for DSB. We explain the necessary and the sufficient criteria for supersymmetry breaking. We also outline the mechanism of supersymmetry breaking in two classic examples. In Section 5.2 we describe the $SU(4) \times SU(3) \times U(1)$ model. We first describe the theory classically, in particular, we show that the model has no classical flat directions. Then, we analyze the quantum mechanical theory in the strongly interacting regime. At the end of that section we show that the model breaks supersymmetry [77]. In Section 5.3, we discuss generalizations to $SU(n) \times SU(3) \times U(1)$ and argue that these models break supersymmetry as well. Finally, in Section 5.4 we discuss theories that have to be analyzed using dual gauge dynamics [78].

5.1 Basics of dynamical supersymmetry breaking

In this section, we summarize both the necessary and sufficient conditions for dynamical supersymmetry breaking. It is necessary for the theories to be chiral to break supersymmetry dynamically [81]. It is sufficient for supersymmetry breaking that a theory without flat directions has a spontaneously broken global symmetry [59, 82]. We will also review an observation by Dine, Nelson, Nir and Shirman [83].

The Witten index $\mathrm{Tr}(-1)^F$ measures the number of bosonic states of zero energy minus the number of fermionic ones. Since unbroken supersymmetry implies that the vacuum energy is zero, the Witten index counts the difference between the number of supersymmetric bosonic and fermionic vacua. If the index is nonzero, then there are certainly supersymmetric vacua, so supersymmetry is preserved in the ground state. It turns out that pure Yang-Mills theories have a non-zero index [81].

The index does not change when the parameters of a theory vary continuously. If it is possible to write the mass terms for all matter fields in the theory, then all mass parameters can be adjusted to take large values. Consequently, all matter fields can be decoupled from the theory. The low-energy theory is pure Yang-Mills, which cannot break supersymmetry. We will therefore consider chiral theories as candidates for DSB. However, the index can change discontinuously when a change of parameters alters the asymptotic behavior of the theory.

We now turn to the second criterion for DSB. A generic supersymmetric gauge theory without tree-level superpotential has a large set of possible vacuum states. These are the points where the D-terms vanish, the so-called flat directions. We explained what flat directions are in the first section of the previous chapter. When the superpotential is added, some flat directions are lifted, meaning that the F-terms are usually non-zero along D-flat directions.

Suppose a theory does not have flat directions either because it does not have any gauge invariants constructed from chiral superfields or because flat directions are lifted by appropriate choice of tree-level superpotential. If such a theory has a continuous global symmetry which is spontaneously broken, then supersymmetry is also spontaneously broken [59, 82]. A spontaneously broken global symmetry implies the presence of a Goldstone boson. In a supersymmetric theory, this Goldstone boson has to combine with another massless scalar particle to form a supersymmetric multiplet. Since we assume that there are no non-compact flat directions, then there cannot be another massless scalar in the theory. Hence, supersymmetry must be broken.

Unfortunately, finding theories which break supersymmetry dynamically is not an easy task. An interesting observation by Dine, Nelson, Nir and Shirman helps to find such theories [83]. Suppose one knows a theory that breaks supersymmetry dynamically. Instead of the original theory consider a theory with the gauge group reduced to a subgroup. The matter fields are the same, except that the representations they transform in are obtained by decomposing the original representations into those of the subgroup. Such a theory is guaranteed to be anomaly-free just as the the original one was. Moreover, it is frequently possible to lift all flat directions while preserving a global symmetry. We should stress here that we do not imply a physical procedure of breaking the gauge group by the Higgs mechanism. Also, the superpotential in the new theory is not derived from the original one. The theory with reduced gauge group has fewer D-terms, while the same number of chiral superfields. Usually, lifting flat directions in the new theory requires additional terms in the tree-level superpotential.

5.1.1 Two classic examples

In this section, we briefly explain the mechanism for supersymmetry breaking in two models. The first theory—an $SU(5)$ theory with one antisymmetric tensor and one antifundamental [82] is a necessary step in explaining how the second model works. The second one an $SU(N)$ theory with an antisymmetric tensor A and $N-4$ antifundamentals $\bar{F}_i$, will be the starting point for all theories considered in the rest of this chapter.

The $SU(5)$ theory with one antisymmetric tensor and one antifundamental [82] breaks supersymmetry because of strong dynamics. This theory has no flat directions since there are no invariants that can be constructed out of single **10** and single $\bar{\mathbf{5}}$ of $SU(5)$. This theory has two $U(1)$ symmetries. The authors of Ref. [82] argued that one of these symmetries must be broken in the ground state. Thus, supersymmetry is broken as well since the theory has no flat directions. The theory has been analyzed recently by adding fields in vector-like representations. It is then possible to find low-energy description of these $SU(5)$ theories with extra fields. Theories with mass terms for the additional fields break supersymmetry [63, 64]. A similar theory is $SO(10)$ with one spinor field. It also does not have flat directions and breaks supersymmetry [82]. This model has also been studied with larger matter content and appropriate mass terms [65, 70].

In the next sections we will analyze theories whose field content is obtained by decomposing an $SU(N)$ theory with an antisymmetric tensor A and $N-4$ antifundamentals $\bar{F}_i$, N is odd and larger than 5. Let us outline the mechanism of supersymmetry breaking in the $SU(N)$ theory with an antisymmetric tensor and $N-4$ antifundamentals [59]. Without tree-level superpotential this theory has flat directions described by the gauge invariants $A\bar{F}_i\bar{F}_j$. Along a generic flat direction, the $SU(N)$ gauge group is broken to $SU(5)$. The uneaten fields are **10** and $\bar{\mathbf{5}}$ of $SU(5)$. The vacuum energy in the $SU(5)$ theory is proportional

to the dynamical scale of $SU(5)$: $E_{vac} \propto \Lambda_5$.

When $SU(N)$ is broken to $SU(5)$ by VEVs of order $\langle\phi\rangle$ the scales of $SU(N)$ and $SU(5)$ are related by matching:

$$\Lambda_5 = \Lambda_N^{(2N+3)/13} \langle\phi\rangle^{-(2N-10)/13}. \tag{5.1}$$

Here, $\langle\phi\rangle$ indicates a generic value of a VEV for either A or $\bar{F}$ [2]. Therefore, the vacuum energy as a function of the VEVs is $E_{vac} \propto \langle\phi\rangle^{-(2N-10)/13}$. This resembles the situation in models with a dynamically generated superpotentials. The low-energy $SU(5)$ generates a potential which decreases to zero at large VEVs. When flat directions are lifted by the tree-level superpotential $W = \lambda^{ij} A \bar{F}_i \bar{F}_j$, the theory breaks supersymmetry [59]. Here, λ^{ij} is a matrix of rank $N - 5$.

5.2 The $SU(4) \times SU(3) \times U(1)$ model

In this section, we present an interesting nontrivial application of exact methods to analyze a model which spontaneously breaks supersymmetry. The theories that we analyze are based on the gauge group $SU(n) \times SU(3) \times U(1)$. Because the gauge dynamics are very different for $n = 4$ and $n > 4$, we first consider the gauge group $SU(4) \times SU(3) \times U(1)$. The particular models we explore in this section are based on an idea discussed in Ref. [83], where it was suggested to search for models which dynamically break supersymmetry by taking a known model and removing generators to reduce the gauge group. We explained this idea earlier in Section 5.1. In that section we also outlined why the $SU(n+3)$ theories with an antisymmetric tensor and $n-1$ antifundamentals break supersymmetry dynamically when n is even [59]. In this and the following section we consider models based on the reduced gauge group $SU(n) \times SU(3) \times U(1)$.

Unlike previous models in the literature, neither of the nonabelian gauge groups generates a dynamical superpotential in the absence of the perturbations added at tree level. Because neither factor generates a dynamical superpotential, there is no limit in which the theory can be analyzed perturbatively. Therefore, we derive the exact superpotential for the $n = 4$ case which we use to show supersymmetry is broken in the strongly interacting theory.

The $SU(4) \times SU(3) \times U(1)$ model is interesting for several reasons. First, the demonstration of supersymmetry breaking involves a subtle interplay between the confining dynamics and the tree-level superpotential of the theory. Second, this model implements the mechanism of [84, 85] without introducing additional singlets or potential runaway directions. Third, we can lift all the flat directions by a renormalizable superpotential. Fourth, none of the gauge groups generates a dynamical superpotential; the fields are kept from the origin solely by a quantum modified constraint.

In addition, the exact superpotential exhibits several novel features. First, fields with quantum numbers corresponding to classically vanishing gauge invariant operators emerge, and play the role of Lagrange multipliers for known constraints. Second, we find that classical constraints can be modified not only by a constant, but by field dependent terms which vanish in the classical limit. Third, fields which are independent in the classical theory satisfy linear constraints in the quantum theory. By explicitly substituting the solution to the equation of motion for these fields, we show that quantum analogs of the classical constraints are still satisfied.

[2] These VEVs are related because of the D-flatness conditions.

The $SU(n) \times SU(3) \times U(1)$ theories for $n > 4$, presented in the next section, are less tractable but nonetheless very interesting. We show that it is possible to introduce Yukawa couplings which lift all classical flat directions. We then consider the low-energy limit of this theory. The $SU(3)$ gauge group without the perturbative superpotential is not confining. However, the $SU(n)$ confined theory in the presence of Yukawa couplings induces masses for sufficiently many flavors that there is a dynamical superpotential associated with both the $SU(3)$ and $SU(n)$ dynamics. This low-energy superpotential depends non-trivially on both the strong dynamical scales of the low-energy theory and the Yukawa couplings of the microscopic theory. We consider this model with and without Yukawa couplings which lift the baryon flat directions. In the first case, the theory is too complicated to solve. The form of the low-energy superpotential permitted by the symmetries is nonetheless quite interesting in that it mixes the perturbative and strong dynamics. In the second case, we can explicitly derive that supersymmetry is broken. In either case, there is a spontaneously broken global $U(1)$ symmetry, so we conclude this theory probably breaks supersymmetry and has no dangerous runaway directions when all required Yukawa couplings are nonvanishing.

5.2.1 Analysis of the classical theory

The field content of the model we study is obtained by decomposing the chiral multiplets of an $SU(7)$ theory with the field content consisting of an antisymmetric tensor and three anti-fundamentals into its $SU(4) \times SU(3) \times U(1)$ subgroup. The fields are:

$$A^{\alpha\beta}(6,1)_6,\ \bar{Q}_a(1,\bar{3})_{-8},\ T^{\alpha a}(4,3)_{-1},\ \bar{F}_{\alpha I}(\bar{4},1)_{-3},\ \bar{Q}_{ai}(1,\bar{3})_4,$$

where $i, I = 1,2,3$ are flavor indices, while Greek letters denote $SU(4)$ indices and Latin ones correspond to $SU(3)$. In this notation $(n,m)_q$ denotes a field that transforms as an n under $SU(4)$, m under $SU(3)$ and has $U(1)$ charge q.

We take the classical superpotential to be

$$\begin{aligned} W_{cl} \;=\; & A^{\alpha\beta}\bar{F}_{\alpha 1}\bar{F}_{\beta 2} + T^{\alpha a}\bar{Q}_{a1}\bar{F}_{\alpha 1} + T^{\alpha a}\bar{Q}_{a2}\bar{F}_{\alpha 2} + T^{\alpha a}\bar{Q}_{a3}\bar{F}_{\alpha 3} + \\ & \bar{Q}_a\bar{Q}_{b2}\bar{Q}_{c1}\epsilon^{abc}. \end{aligned} \tag{5.2}$$

We will show shortly that this superpotential lifts all D-flat directions.

From the fundamental fields we can construct operators which are invariant under the gauge symmetries of the theory. We first list those which are invariant under $SU(4) \times SU(3)$ and subsequently construct operators which are also $U(1)$ invariant. Later on it will be important to distinguish operators invariant under the confining gauge groups but which carry $U(1)$ charge.

$$\begin{aligned} M_{iI} &= T^{\alpha a}\bar{Q}_{ai}\bar{F}_{\alpha I} && 0 \\ M_{4I} &= T^{\alpha a}\bar{Q}_a\bar{F}_{\alpha I} && -12 \\ X_{IJ} &= A^{\alpha\beta}\bar{F}_{\alpha I}\bar{F}_{\beta J} && 0 \\ X_{I4} &= \tfrac{1}{6}A^{\beta\alpha}\bar{F}_{\beta I}\epsilon_{\alpha\gamma\delta\zeta}T^{\gamma a}T^{\delta b}T^{\zeta c}\epsilon_{abc} && 0 \\ \mathrm{Pf}A &= \epsilon_{\alpha\beta\gamma\delta}A^{\alpha\beta}A^{\gamma\delta} && 12 \\ Y_{ij} &= \epsilon_{\alpha\beta\gamma\delta}A^{\alpha\beta}T^{\gamma a}\bar{Q}_{ai}T^{\delta b}\bar{Q}_{bj} && 12 \\ Y_{i4} &= \epsilon_{\alpha\beta\gamma\delta}A^{\alpha\beta}T^{\gamma a}\bar{Q}_{ai}T^{\delta b}\bar{Q}_b && 0 \\ \bar{B} &= \tfrac{1}{6}\bar{F}_{\alpha I}\bar{F}_{\beta J}\bar{F}_{\gamma K}\epsilon^{IJK}T^{\alpha a}T^{\beta b}T^{\gamma c}\epsilon_{abc} && -12 \end{aligned} \tag{5.3}$$

$$\begin{aligned} \bar{b}^i = & \quad -\tfrac{1}{2}\bar{Q}_a\bar{Q}_{bj}\bar{Q}_{ck}\epsilon^{ijk}\epsilon^{abc} \quad & 0 \\ \bar{b}^4 = & \quad \tfrac{1}{6}\bar{Q}_{ai}\bar{Q}_{bj}\bar{Q}_{ck}\epsilon^{ijk}\epsilon^{abc} \quad & 12 \end{aligned}$$

The right hand side column indicates the charges of the operators under the $U(1)$ gauge group. All other $SU(4) \times SU(3)$ invariants can be obtained as products of these operators. The classical constraints obeyed by these fields are:

$$\begin{aligned} & 4\,X_{I4}X_{JK}\epsilon^{IJK} - \bar{B}\,\mathrm{Pf}A = 0 \\ & \epsilon^{ijk}\epsilon^{IJK}\,(\mathrm{Pf}A\,M_{iI}M_{jJ}M_{kK} - 6Y_{ij}M_{kI}X_{JK}) = 0 \\ & \epsilon^{ijk}\epsilon^{IJK}\,(\mathrm{Pf}A\,M_{4I}M_{jJ}M_{kK} - 2Y_{jk}M_{4I}X_{JK} + 4Y_{j4}M_{kI}X_{JK}) = 0 \\ & Y_{i4}\bar{b}^i = 0 \\ & \bar{B}\bar{b}^4 - \frac{1}{6}\epsilon^{ijk}\epsilon^{IJK}M_{iI}M_{jJ}M_{kK} = 0 \\ & \bar{B}\epsilon^{kij}Y_{ij} - 2\,\epsilon^{kij}\epsilon^{IJK}M_{iI}M_{jJ}X_{K4} = 0 \\ & M_{4I}\bar{b}^4 + M_{iI}\bar{b}^i = 0 \\ & \epsilon^{ijk}Y_{jk}M_{4I} + 2\,\epsilon^{ijk}M_{jI}Y_{k4} + 4\,X_{I4}\bar{b}^i = 0 \\ & \epsilon^{IJK}\epsilon^{ijk}M_{iI}M_{jJ}M_{4K}Y_{k4} = 0. \end{aligned} \tag{5.4}$$

The completely gauge invariant fields can be formed by taking products of the above $U(1)$ charged fields. However, most of these combinations turn out to be products of other completely gauge invariant operators. As an operator basis we can use the neutral fields from Eq. 5.3 and $E_I = M_{4I}\mathrm{Pf}A$. These operators are subject to the following classical constraints:

$$\begin{aligned} & \epsilon^{IJK}E_JM_{iK}\bar{b}^i = 0 \\ & Y_{i4}\bar{b}^i = 0 \\ & \epsilon^{IJK}\epsilon^{ijk}M_{iI}M_{jJ}E_KY_{k4} = 0 \\ & \epsilon^{IJK}\epsilon^{ijk}M_{iI}M_{jJ}Y_{k4}M_{lK}\bar{b}^l = 0 \end{aligned} \tag{5.5}$$

These constraints follow from Eq. 5.4. We have omitted the linear constraints following from Eq. 5.4 which define additional unnecessary fields. These operators obeying the above constraints parameterize the D-flat directions of the theory.

In terms of the invariants defined above we can express the superpotential as

$$W_{cl} = X_{12} + M_{11} + M_{22} + M_{33} + \bar{b}^3. \tag{5.6}$$

We now show that this superpotential suffices to lift all D-flat directions. It is easiest to show this (using the results of Ref. [56]) by demonstrating that the holomorphic invariants which parameterize the flat directions are all determined by the equations of motion (as opposed to parameterizing the flat directions in terms of the fundamental fields). If all holomorphic invariants are determined, we can conclude that all potential flat directions are lifted.

We consider the equations of motion corresponding to the classical superpotential of Eq. 5.2. The equation $\frac{\partial W}{\partial A}$ sets X_{12} to zero if we multiply by A. Forming all gauge invariant combinations from $\frac{\partial W}{\partial \bar{Q}_{ai}}$ we obtain the following. Multiplying $\frac{\partial W}{\partial \bar{Q}_{a3}}$ by $\bar{Q}_{aj}$ gives

$$M_{j3} = 0,$$

similarly for $\frac{\partial W}{\partial \bar{Q}_{a1,2}}$ we obtain

$$M_{12} = 0 \quad M_{22} + \bar{b}^3 = 0 \quad M_{32} - \bar{b}^2 = 0$$
$$M_{21} = 0 \quad M_{11} + \bar{b}^3 = 0 \quad M_{31} - \bar{b}^1 = 0.$$

Next, we multiply the same equations by $\epsilon_{abc}T^{\beta b}T^{\gamma c}A^{\delta\rho}\epsilon_{\beta\gamma\delta\rho}$ to obtain

$$X_{34} = 0 \;\; Y_{24} + 2X_{14} = 0 \;\; Y_{14} - 2X_{24} = 0.$$

Also, by multiplying $\frac{\partial W}{\partial \bar{Q}_{ai}}$ by $\bar{Q}_a \mathrm{Pf}A$ we get

$$E_I = 0.$$

Next, from $\frac{\partial W}{\partial \bar{Q}_a}\bar{Q}_a$ we obtain that

$$\bar{b}^3 = 0.$$

We obtain the remaining equations from $\frac{\partial W}{\partial \bar{F}_{aI}}$. They are:

$$M_{13} - X_{23} = 0 \quad M_{23} + X_{13} = 0 \quad M_{3I} = 0$$
$$E_2 + 4Y_{14} = 0 \quad E_1 - 4Y_{24} = 0 \quad Y_{34} = 0$$

The only solution to these equations sets all operators to be zero. Therefore, our theory does not have flat directions.

In Ref. [82] it was argued that theories which have no flat directions, but preserve an anomaly free R symmetry break supersymmetry spontaneously if the $U(1)_R$ symmetry is spontaneously broken in the vacuum. This follows because there would be a massless pseudoscalar, which is unlikely to have a massless scalar partner. The superpotential of Eq. 5.2 preserves an R symmetry under which the R charges are $R(A) = R(\bar{F}_3) = 0$, $R(\bar{F}_1) = R(\bar{F}_2) = 1$, $R(\bar{Q}_1) = R(\bar{Q}_2) = \frac{5}{3}$, $R(\bar{Q}_3) = \frac{8}{3}$, $R(\bar{Q}) = -\frac{4}{3}$ and $R(T) = -\frac{2}{3}$. Although this symmetry is anomalous with respect to the $U(1)$ gauge group, if it is spontaneously broken, the associated Goldstone boson is nonetheless massless so the argument of Ref. [82] should still apply.

Notice that the classical equations of motion in our theory have a solution only where all fields vanish. In the next section we show that the quantum theory does not permit such a supersymmetric solution, so that supersymmetry is broken.

5.2.2 The Quantum $SU(4) \times SU(3) \times U(1)$ Theory

In this section we will derive the exact superpotential of the $SU(4) \times SU(3) \times U(1)$ theory. The fact that it is possible to determine the exact superpotential of the theory will enable us to prove that supersymmetry is dynamically broken.

Before proceeding, we list the global symmetries of the microscopic fields, which are

useful when constraining the form of the exact superpotential. The global symmetries are:

	$U(1)_A$	$U(1)_{\bar{Q}}$	$U(1)_T$	$U(1)_{\bar{F}}$	$SU(3)_{\bar{F}_I}$	$U(1)_{\bar{Q}_i}$	$SU(3)_{\bar{Q}_i}$	$U(1)_R$
A	1	0	0	0	1	0	1	0
$\bar{Q}$	0	1	0	0	1	0	1	0
T	0	0	1	0	1	0	1	0
$\bar{F}_I$	0	0	0	1	3	0	1	0
$\bar{Q}_i$	0	0	0	0	1	1	3	0
Λ_3^5	0	1	4	0	1	3	1	-2
Λ_4^8	2	0	3	3	1	0	1	0

The only invariants under all global symmetries including $U(1)_R$ are $\mathcal{A} = X_{IJ}X_{K4}\epsilon^{IJK}/\Lambda_4^8$ and $\mathcal{B} = \bar{B}\mathrm{Pf}A/\Lambda_4^8$.

We now identify the proper degrees of freedom. To do so, it is convenient to first take the limit $\Lambda_3 \gg \Lambda_4$ and construct $SU(3)$ invariant operators which are mesons and baryons formed from the $SU(3)$ charged fields, and then to construct the $SU(4)$ bound states of these fields. This gives us the spectrum which matches anomalies of the original microscopic theory, independent of the ratio Λ_3/Λ_4.

Below the $SU(3)$ scale, the theory can be described by an $SU(4)$ theory with an antisymmetric tensor and four flavors. These four flavors are

$$\begin{aligned}
\bar{F}_{\alpha 4} &= \frac{1}{6}\epsilon_{\beta\gamma\delta\alpha}T^{\beta a}T^{\gamma b}T^{\delta c}\epsilon_{abc}, \\
F_i^\alpha &= T^{\alpha a}\bar{Q}_{ai},\ i = 1,2,3 \\
F_4^\alpha &= T^{\alpha a}\bar{Q}_a,
\end{aligned} \tag{5.7}$$

The three remaining antifundamentals are $\bar{F}_{\alpha I}$, $I = 1,2,3$, the original fields. The $SU(3)$ antibaryons are the $\bar{b}^i$'s of Eq. 5.3, which are singlets under $SU(4)$.

The four-flavor theory with an antisymmetric tensor has been described in Ref. [70]. The confined states of the $SU(4)$ theory are

$$\begin{aligned}
\mathrm{Pf}A &= \epsilon_{\alpha\beta\gamma\delta}A^{\alpha\beta}A^{\gamma\delta} \\
M_{iI} &= F_i^\alpha \bar{F}_{\alpha I} \\
X_{IJ} &= A^{\alpha\beta}\bar{F}_{\alpha I}\bar{F}_{\beta J} \\
Y_{ij} &= A^{\alpha\beta}F_i^\gamma F_j^\delta \epsilon_{\alpha\beta\gamma\delta} \\
B &= \frac{1}{24}F_i^\alpha F_j^\beta F_k^\gamma F_l^\delta \epsilon_{\alpha\beta\gamma\delta}\epsilon^{ijkl} \\
\bar{B} &= \frac{1}{24}\bar{F}_{\alpha I}\bar{F}_{\beta J}\bar{F}_{\gamma K}\bar{F}_{\delta L}\epsilon^{\alpha\beta\gamma\delta}\epsilon^{IJKL}.
\end{aligned} \tag{5.8}$$

Here the indices i and I range from 1 to 4. Note that B, M_{44} and M_{i4} are fields which vanish classically. However, anomaly matching of the microscopic theory to the low-energy theory requires the presence of these fields. Fields other than B, M_{44} and M_{i4} correspond to operators introduced in Eq. 5.3. The low-energy theory consists of the fields listed in Eq. 5.3 and the new fields B, M_{44}, and M_{i4}.

In order to construct the superpotential it is again convenient to consider the limit $\Lambda_3 \gg \Lambda_4$. Below the Λ_3 scale, there is an $SU(4)$ theory with four flavors and an antisymmetric tensor together with the confining $SU(3)$ superpotential of Ref. [53]. The superpotential for

the four-flavor $SU(4)$ theory with an antisymmetric tensor has been described in Ref. [70]. We determined the coefficients in the superpotential of Ref. [70] by requiring that the equations of motion reproduce the classical constraints.

In this limit, the superpotential has to be the sum of the contributions from $SU(3)$ and $SU(4)$ dynamics. The exact superpotential is therefore of the form:

$$\begin{aligned} W \;=\; & \bar{b}^3 + X_{12} + M_{11} + M_{22} + M_{33} + \frac{1}{\Lambda_3^5}\left(M_{i4}\bar{b}^i - B\right) + \\ & f(\mathcal{A},\mathcal{B}) \cdot \frac{1}{24\,\Lambda_3^5\Lambda_4^8}\Big(24\,BX_{IJ}X_{KL}\epsilon^{IJKL} + 6\,\bar{B}Y_{ij}Y_{kl}\epsilon^{ijkl} - 24\,B\bar{B}\mathrm{Pf}A + \\ & \mathrm{Pf}A\epsilon^{ijkl}\epsilon^{IJKL}M_{iI}M_{jJ}M_{kK}M_{lL} - 12\,\epsilon^{ijkl}Y_{ij}M_{kI}M_{lJ}X_{KL}\epsilon^{IJKL}\Big), \end{aligned} \tag{5.9}$$

where f is an as yet undetermined function of the symmetry invariants $\mathcal{A}$ and $\mathcal{B}$, and $i, I = 1,\ldots,4$. Therefore, the symmetries together with the limit $\Lambda_3 \gg \Lambda_4$ restrict the superpotential up to a function of $\mathcal{A}$ and $\mathcal{B}$. However, a negative power series in $\mathcal{A}$ or $\mathcal{B}$ would imply unphysical singularities, since there is no limit in which the number of flavors in the $SU(4)$ theory is less than the number of colors. On the other hand, a positive power series in $\mathcal{A}$ or $\mathcal{B}$ would not correctly reproduce the limit where $\Lambda_4 \gg \Lambda_3$. In this limit one has an $SU(4)$ theory with an antisymmetric tensor and three flavors, which yields a quantum modified constraint [63]. Observe the amazing fact that the B equation of motion which involves the superpotential from both the $SU(3)$ and $SU(4)$ terms exactly reproduces this $SU(4)$ quantum modified constraint. This is only true with no further modification of the second term. In fact, this is what permits us to fix the relative coefficient of the two terms in parentheses. Thus we conclude that $f(\mathcal{A},\mathcal{B}) \equiv 1$.

We stress again that each of the fields B, M_{i4}, and M_{44} vanish classically. In the quantum theory, the B field acts as a Lagrange multiplier for the three flavor $SU(4)$ quantum modified constraint. The M_{i4} and M_{44} equations of motion are

$$\begin{aligned} \epsilon^{ijk}\epsilon^{IJK}\left(\mathrm{Pf}AM_{iI}M_{jJ}M_{kK} - 6Y_{ij}M_{kI}X_{JK}\right) &= 6\Lambda_4^8\bar{b}^4 \\ \epsilon^{ijk}\epsilon^{IJK}\left(\mathrm{Pf}AM_{4I}M_{jJ}M_{kK} - 2Y_{jk}M_{4I}X_{JK} + 4Y_{j4}M_{kI}X_{JK}\right) &= 2\Lambda_4^8\bar{b}^i \end{aligned} \tag{5.10}$$

The linear equations for $\bar{b}^i$ and $\bar{b}^4$ can be understood by the fact that they appear as mass terms for M_{44} and M_{i4}. The equations of motion in Eq. 5.10 can be interpreted as quantum modified constraints of a three flavor $SU(4)$ theory with the scales related through the $\bar{b}$-dependent masses.

It is a nontrivial check on the superpotential of Eq. 5.9 that all classical constraints have a quantum analog and vice versa. The quantum modified constraints involving $\bar{b}^i$ and $\bar{b}^4$ are derived by substituting in the solution to their equation of motion. The quantum modified constraints are:

$$4\,X_{I4}X_{JK}\epsilon^{IJK} - \bar{B}\mathrm{Pf}A = \Lambda_4^8 \tag{5.11}$$

$$\epsilon^{ijk}\epsilon^{IJK}\left(\mathrm{Pf}AM_{iI}M_{jJ}M_{kK} - 6Y_{ij}M_{kI}X_{JK}\right) = 6\Lambda_4^8\bar{b}^4 \tag{5.12}$$

$$\epsilon^{ijk}\epsilon^{IJK}\left(\mathrm{Pf}AM_{4I}M_{jJ}M_{kK} - 2Y_{jk}M_{4I}X_{JK} + 4Y_{j4}M_{kI}X_{JK}\right) = 2\Lambda_4^8\bar{b}^i \tag{5.13}$$

$$\epsilon^{IJK}\epsilon^{ijk}M_{iI}M_{jJ}M_{4K}Y_{k4} = 2\,BM_{4I}X_{JK}\epsilon^{IJK} \tag{5.14}$$

$$\bar{B}\epsilon^{kij}Y_{ij} - 2\,\epsilon^{kij}\epsilon^{IJK}M_{iI}M_{jJ}X_{K4} = -2\,M_{i4}M_{jI}\epsilon^{kij}X_{JK}\epsilon^{IJK} \tag{5.15}$$

while the remaining constraints are not modified. The interesting thing to observe in the

above equations is that the quantum modifications do not simply involve addition of a constant to the classical field equations. The quantum modification can be field dependent. The classical limit is recovered in Eqs. 5.14, 5.15 because B and M_{i4} are fields which vanish classically. Without a tree-level superpotential M_{i4} is set to zero by the $\bar{b}^i$ equations of motion. However, M_{i4} can be non-vanishing in the presence of a tree-level superpotential. The quantum modifications in Eqs. 5.12, 5.13 do not contain classically vanishing fields, but are proportional to Λ_4, which ensures the correct classical limit. This field dependent modification of constraints is a new feature which is not present when analyzing simple nonabelian gauge groups.

Note that five of our constraints (Eqs. 5.11, 5.12 and 5.13) can be interpreted as the quantum modified constraints on the moduli space of an $SU(4)$ gauge theory with an antisymmetric tensor and three flavors. Such a theory is obtained in several limits. If $\Lambda_4 \gg \Lambda_3$ one trivially has a three flavor $SU(4)$ theory with an antisymmetric tensor. On the other hand, if $\Lambda_3 \gg \Lambda_4$ and any single $\bar{b}$ is non-vanishing one also has a three flavor $SU(4)$ theory with its corresponding quantum modified constraint.

When deriving the constraints in Eqs. 5.11-5.15 from the exact superpotential we frequently encounter expressions containing inverse powers of Λ_4. Such terms are singular in the limit when Λ_3 is held fixed and $\Lambda_4 \to 0$. This is true even for expressions containing the fields B, M_{i4} and M_{44}, since they vanish only in the limit when $\Lambda_3 \to 0$. Therefore all such terms must and do cancel.

5.2.3 Dynamical Supersymmetry Breaking

In the low-energy description of our model the $SU(4)$ and $SU(3)$ gauge groups are confined and the only remaining gauge group is the $U(1)$. This $U(1)$ does not play any role in supersymmetry breaking; its purpose is to lift some classical flat directions. Unlike previous examples of dynamical supersymmetry breaking, the superpotential can be completely analyzed in a regime where there are no singularities, either due to a dynamically generated superpotential present in the initial theory, integrating out fields, or particular limits. If the theory breaks supersymmetry, it is simply of O'Raifeartaigh type [86]. In this section, we show that this is the case; there is no consistent solution of the F-flatness equations for the exact superpotential of Eq. 5.9.

We first assume that $\bar{B} \neq 0$. Then the $\frac{\partial W}{\partial Y_{ij}}$ equation of motion implies

$$Y_{ij} = \frac{1}{\bar{B}} X_{KL} M_{iI} M_{jJ} \epsilon^{IJKL}. \tag{5.16}$$

Plugging this expression into the $\frac{\partial W}{\partial X_{IJ}}$ equation of motion, we obtain

$$(\delta^3_S \delta^4_T - \delta^3_T \delta^4_S) + \frac{8}{\Lambda_3^5 \Lambda_4^8} B X_{ST} - \frac{2}{\Lambda_3^5 \Lambda_4^8} \frac{1}{\bar{B}} \epsilon^{ijkl} M_{iM} M_{jN} M_{kS} M_{lT} X_{KL} \epsilon^{MNKL} = 0.$$

However, by using the $\frac{\partial W}{\partial \mathrm{Pf} A} = 0$ equation in the above expression we arrive at a contradiction.

Next we assume that $\bar{B} = 0$, but $B \neq 0$. We can now solve for X using the equation $\frac{\partial W}{\partial X_{IJ}} = 0$:

$$X_{MN} = \frac{\Lambda_3^5 \Lambda_4^8}{8B} \left[(\delta^3_M \delta^4_N - \delta^3_N \delta^4_M) + 48\, \epsilon^{ijkl} Y_{ij} M_{kM} M_{lN} \right]. \tag{5.17}$$

Then we multiply this equation by $\epsilon^{ijkl}\epsilon^{IJMN}M_{kI}M_{lJ}$. The Y_{ij} equation of motion sets the left hand side to zero, while the PfA equation of motion sets the second term on the right hand side to zero. Therefore,

$$\epsilon^{ijkl}M_{iI}M_{jJ}\epsilon^{IJ34} = 0.$$

Using this fact, the PfA equation of motion, and the expression for X_{MN} in Eq. 5.17 we get that $\frac{\partial W}{\partial B} = -\frac{1}{\Lambda_3^5}$, which again means that the equations of motion are contradictory.

Finally we assume that $B = \bar{B} = 0$. Then the $\frac{\partial W}{\partial X_{IJ}}$ equation of motion implies

$$\epsilon^{ijkl}Y_{ij}M_{kI}M_{lJ} = 0$$

for all I, J except $I = 3, J = 4$. Multiplying the $\frac{\partial W}{\partial X_{IJ}}$ equation of motion by $M_{iI}M_{jJ}$ and using the $\frac{\partial W}{\partial \mathrm{Pf}A}$ equation of motion we get that

$$\epsilon^{ijkl}M_{i1}M_{j2} = 0.$$

Using these results the $\frac{\partial W}{\partial M_{i3}}$ equation of motion yields

$$\delta^{i3} - \frac{1}{\Lambda_3^5\Lambda_4^8}\epsilon^{ijkl}Y_{jk}M_{lJ}X_{KL}\epsilon^{3JKL} = 0.$$

Multiplying this equation by M_{i4} implies $M_{34} = 0$, which is in contradiction with the $\frac{\partial W}{\partial \bar{b}^3}$ equation of motion. Thus we have shown that this $SU(4) \times SU(3) \times U(1)$ model breaks supersymmetry dynamically. Since there are no classical flat directions, there should not be runaway directions in this model.

Having presented a general proof of supersymmetry breaking, we now give a simpler proof that applies only in a restricted region of parameter space. Assume that Λ_3 is the largest parameter in the theory. The effective superpotential just below the Λ_3 scale is

$$\begin{aligned} W &= \bar{b}^3 + \gamma A^{\alpha\beta}\bar{F}_{\alpha 1}\bar{F}_{\beta 2} + \lambda_1 F_1^\alpha \bar{F}_{\alpha 1} + \lambda_2 F_2^\alpha \bar{F}_{\alpha 2} + \lambda_3 F_3^\alpha \bar{F}_{\alpha 3} + \\ &\quad \frac{1}{\Lambda_3^5}\left(\bar{F}_{\alpha 4}F_i^\alpha \bar{b}^i - \det F_i^\alpha\right), \end{aligned} \tag{5.18}$$

where we use the notation from Eq. 5.7 and we introduced explicitly the Yukawa couplings γ and $\lambda_{1,2,3}$. In terms of the canonically normalized fields, $\lambda_{1,2,3}$ are mass parameters.

Next, we integrate out three of the four flavors to arrive at an $SU(4)$ theory with one flavor and a superpotential

$$W = \bar{b}^3 + \frac{1}{\Lambda_3^5}\bar{F}_{\alpha 4}F_4^\alpha \bar{b}^4. \tag{5.19}$$

To describe the dynamics of the one-flavor $SU(4)$ theory, it is useful to define the effective one-flavor $SU(4)$ scale $\tilde{\Lambda}_4^5$, which is proportional to $\lambda_1\lambda_2\lambda_3\Lambda_3^5\Lambda_4^8$. Below the effective $\tilde{\Lambda}_4$ scale there is a dynamically generated term, so the low-energy superpotential is

$$W = \bar{b}^3 + \frac{1}{\Lambda_3^5}M_{44}\bar{b}^4 + \left(\frac{\tilde{\Lambda}_4^5}{\mathrm{Pf}A\, M_{44}}\right)^{\frac{1}{2}}, \tag{5.20}$$

where $M_{44} = \bar{F}_{\alpha 4}F_4^\alpha$. There are no solutions to the equations of motion. Note that the potential runaway direction is removed by the $U(1)$ D-flatness condition. Therefore su-

persymmetry is dynamically broken. Observe that supersymmetry breaking in this limit has two sources. First the superpotential generated by the $SU(3)$ and $SU(4)$ gauge groups together does not have a supersymmetric minimum. Second, a Yukawa term in the tree level superpotential is confined into a single field which is also a source of supersymmetry breaking. In fact, the tree-level Yukawa terms have three different important roles in this analysis. They lift the flat directions, they yield mass terms for the $SU(4)$ fields after $SU(3)$ is confining, and they also contribute to supersymmetry breaking by the linear term. The fact that there is a quantum modified constraint in the $\Lambda_4 \gg \Lambda_3$ limit of the theory does not seem to play a major role in the dynamics of supersymmetry breaking.

By symmetries, it can be shown that this simpler proof neglects power corrections proportional to

$$\left(\frac{\gamma^2 \bar{b}^i \mathrm{Pf} A\, M_{44}}{\lambda^4 (\Lambda_3^5)^2}\right)^k .$$

This reflects the fact that here we are studying the effective theory treating Λ_3 as large. The $\bar{b}^4$ equation of motion together with the fact that there are no flat directions imply broken supersymmetry even with these corrections incorporated.

5.3 $SU(n) \times SU(3) \times U(1)$ Theories

In this section we generalize the $SU(4) \times SU(3) \times U(1)$ model to $SU(n) \times SU(3) \times U(1)$, with n even. There are several interesting features of the dynamics of these theories. Without a tree-level superpotential the $SU(3)$ group is not confining. However, the Yukawa couplings of the tree-level superpotential become mass terms when the $SU(n)$ group confines. These mass terms drive the $SU(3)$ group into the confining regime as well. Confinement can change chiral theories into non-chiral ones. In this example Yukawa couplings become mass terms. In fact, the quantum modified constraint associated with the $SU(n)$ group of the initial theory does not appear to play an essential role in the dynamics of supersymmetry breaking. Another interesting phenomena is that even if we remove some of the couplings from the superpotential, so that some flat directions are not lifted, these directions turn out to be lifted in the quantum theory. In particular, once the Yukawa couplings turn into mass terms, the $SU(3)$ antibaryon directions are automatically lifted.

As in Section 2, we obtain the field content for these models by decomposing the fields of the $SU(n+3)$ theory with an antisymmetric tensor and $n-1$ anti-fundamentals to $SU(n) \times SU(3) \times U(1)$:

$$\begin{array}{rcl} \square\!\square & \to & A^{\alpha\beta}(\square\!\square, 1)_6 + \bar{Q}_a(1, \bar{3})_{-2n} + T^{\alpha a}(\square, 3)_{3-n} \\ (n-1)\bar{\square} & \to & \bar{F}_{\alpha I}(\bar{\square}, 1)_{-3} + \bar{Q}_{ai}(1, \bar{3})_n, \end{array} \tag{5.21}$$

where $i, I = 1, \ldots, n-1$.

In analogy to the 4-3-1 case, $SU(n) \times SU(3) \times U(1)$ invariants are:

$$\begin{aligned} M_{iI} &= T^{\alpha a} \bar{Q}_{ai} \bar{F}_{\alpha I} \\ X_{IJ} &= A^{\alpha\beta} \bar{F}_{\alpha I} \bar{F}_{\beta J} \\ X_I &= \frac{1}{6} A^{\alpha_n \alpha_{n-1}} \ldots A^{\alpha_4 \beta} \bar{F}_{\beta I} \epsilon_{\alpha_n \ldots \alpha_1} T^{\alpha_3 a} T^{\alpha_2 b} T^{\alpha_1 c} \epsilon_{abc} \\ Y_i &= A^{\alpha_n \alpha_{n-1}} \ldots A^{\alpha_4 \alpha_3} T^{\alpha_2 a} \bar{Q}_{ai} T^{\alpha_1 b} \bar{Q}_b \end{aligned}$$

$$\begin{aligned} \bar{b}_{ij} &= \bar{Q}_a \bar{Q}_{bi} \bar{Q}_{cj} \epsilon^{abc} \\ E_I &= \epsilon_{\alpha_n \ldots \alpha_1} A^{\alpha_n \alpha_{n-1}} \ldots A^{\alpha_2 \alpha_1} T^{\beta a} \bar{Q}_a \bar{F}_{\beta I} \end{aligned} \tag{5.22}$$

We consider the following superpotential:

$$\begin{aligned} W &= X_{12} + X_{34} + \ldots + X_{n-3,n-2} + \bar{b}_{23} + \bar{b}_{45} + \ldots + \bar{b}_{n-2,1} + \\ &\quad M_{11} + M_{22} + \ldots + M_{n-1,n-1}. \end{aligned} \tag{5.23}$$

Observe the relative shifts in the indices between the X and $\bar{b}$ operators. One can check that not all flat directions are removed without such a shift in the indices.

To demonstrate that all flat directions are lifted, one can use the same method as described in Section 5.2. In this example, we require looking not only at linear equations in the flat direction fields, but also higher order equations, in order to demonstrate that no flat directions remain in the presence of the tree-level superpotential above.

We first use the $\bar{Q}_i$ and $\bar{F}_i$ equations of motion (contracted with $\bar{Q}_k$ and $\bar{F}_j$). One will then find potential flat directions which are labeled by $i = 1, 3, 5, \ldots, 2[n/4] - 1$ with equal values of $X_{2j-1,(2j-1+i)||(n-2)} = \bar{b}_{2j,(2j+i)||(n-2)}$, where $j = 1, 2, 3, \ldots, (n-2)/2$ labels nonvanishing X and $\bar{b}$ fields which are equal along the flat direction. Here, by $[x]$ we denote the greatest integer less than x, while we define $m||n \equiv 1 + (m-1)$ Mod n. There is another set of potential flat directions of the form $X_{2j,(2j+i)||(n-2)} = \bar{b}_{2j-1,(2j-1+i)||(n-2)}$, where again $j = 1, 2, 3, \ldots, (n-2)/2$ and $i = 1, 3, 5, \ldots, 2[n/4] - 1$. In the case when $n = 4k$ and $i = k$, two potential flat directions described above are equal to each other, so they represent just one flat direction. Altogether, there are $(n-2)/2$ potential flat directions. One of these flat directions is lifted trivially by the A equation of motion. To see that the remaining flat directions are lifted requires obtaining quadratic equations in the flat direction of fields by suitably contracting the T equations of motion. These equations can be shown to have only the trivial solution where all fields vanish. We have verified this explicitly in the cases $n = 6, 8, 10$, and 12, but we expect this method to generalize.

One can also verify that the superpotential above preserves two $U(1)$ symmetries, one of which is an R symmetry which is anomalous only with respect to the $U(1)$ gauge group. From the quantum modified constraint it can be shown that at least one of these $U(1)$ symmetries is spontaneously broken. Since the theory has no flat directions and spontaneously breaks a $U(1)$ symmetry, we expect that supersymmetry is broken.

There is a possibility however that in the strongly interacting regime there is a point at which supersymmetry is restored. We now consider the quantum theory and argue that it is likely that supersymmetry is broken.

Without a tree-level superpotential the $SU(3)$ group is not confining for $n > 4$ since $N_f > \frac{3}{2} N_c$. We choose to use fields transforming under $SU(3)$ instead of the $SU(3)$ invariant operators. The D-flatness conditions can then be imposed explicitly. Although in principle one could use holomorphic invariants to parameterize the D-flat directions, the naive application of this method would lead to incorrect results at points of the moduli space where these invariants vanish [87]. Although with careful choice of holomorphic invariants this problem can be circumvented, in practice it is simpler to use the charged fields when the gauge group is not confining.

The $SU(n)$ group has three flavors and an antisymmetric tensor. Therefore $SU(n)$ is confining and gives rise to a quantum modified constraint as described in Ref. [63]. The

$SU(n)$ invariants are:

$$\begin{aligned} X_{IJ} &= A^{\alpha\beta}\bar{F}_{\alpha I}\bar{F}_{\beta J} \\ m_I^a &= T^{\alpha a}\bar{F}_{\alpha I} \\ \mathrm{Pf}A &= \epsilon_{\alpha_n\ldots\alpha_1}A^{\alpha_n\alpha_{n-1}}\ldots A^{\alpha_2\alpha_1} \\ y_a &= A^{\alpha_n\alpha_{n-1}}\ldots A^{\alpha_4\alpha_3}\epsilon_{\alpha_n\ldots\alpha_1}T^{\alpha_2 b}T^{\alpha_1 c}\epsilon_{abc} \end{aligned} \tag{5.24}$$

together with the fields $\bar{Q}_a$ and $\bar{Q}_{ai}$.

The superpotential below the Λ_n scale is

$$\begin{aligned} W &= \alpha^{12}X_{12}+\ldots+\alpha^{n-3,n-2}X_{n-3,n-2}+\beta^{23}\bar{Q}_a\bar{Q}_{b2}\bar{Q}_{c3}\epsilon^{abc}+\ldots+ \\ &\beta^{n-2,1}\bar{Q}_a\bar{Q}_{b,n-2}\bar{Q}_{c1}\epsilon^{abc}+\lambda^{11}m_1^a\bar{Q}_{a1}+\ldots+\lambda^{n-1,n-1}m_{n-1}^a\bar{Q}_{a,n-1}+ \\ &\eta\Big(\frac{n-2}{3n}\epsilon_{abc}m_{I_1}^a m_{I_2}^b m_{I_3}^c X_{I_4I_5}\ldots X_{I_{n-2}I_{n-1}}\epsilon^{I_1\ldots I_{n-1}}\mathrm{Pf}A- \\ &y_a m_{I_1}^a X_{I_2I_3}\ldots X_{I_{n-2}I_{n-1}}\epsilon^{I_1\ldots I_{n-1}}+\Lambda_n^{2n}\Big), \end{aligned} \tag{5.25}$$

where η is a Lagrange multiplier and we have explicitly included the coupling constants in the tree-level superpotential. In terms of $SU(n)$ invariants, some of the terms in the above superpotential are just mass terms for $(n-1)$ flavors of $SU(3)$, which drive $SU(3)$ into the confining phase. In the presence of these perturbations, nonperturbative $SU(3)$ dynamics will generate a superpotential. Similar results are found in Ref. [88]. We stress again that in the underlying theory these interactions are Yukawa couplings and not mass terms.

To analyze the low-energy theory, we introduce an additional flavor of $SU(n)$ with mass μ. We do this because the $SU(n)$ quantum modified constraint or equivalently anomaly matching shows that $SU(3)$ must be broken below the scale Λ_n in the original theory. With an additional flavor, the origin of moduli space is permitted and $SU(3)$ can remain unbroken. This permits us to derive the confining superpotential with two massless $SU(3)$ flavors. Although the correct theory is only recovered in the limit $\mu\to\infty$, we will analyze the theory in the regime $\mu<\Lambda_n$ and hope one can extrapolate the conclusion that supersymmetry is broken [65].

The superpotential with the additional massive $SU(n)$ flavor is:

$$\begin{aligned} W &= \alpha^{12}X_{12}+\ldots+\alpha^{n-3,n-2}X_{n-3,n-2}+ \\ &\beta^{23}\bar{Q}_a\bar{Q}_{b2}\bar{Q}_{c3}\epsilon^{abc}+\ldots+\beta^{n-2,1}\bar{Q}_a\bar{Q}_{b,n-2}\bar{Q}_{c1}\epsilon^{abc}+ \\ &\lambda^{11}m_1^a\bar{Q}_{a1}+\ldots+\lambda^{n-1,n-1}m_{n-1}^a\bar{Q}_{a,n-1}+\mu m_n^4+ \\ &\frac{1}{\Lambda_n^{2n-1}}\Big(\mathrm{Pf}A\, m_{I_1}^a m_{I_2}^b m_{I_3}^c m_{I_4}^d X_{I_5I_6}\ldots X_{I_{n-1}I_n}\epsilon_{abcd}\epsilon^{I_1\ldots I_n}+ \\ &Y^{ab}m_{I_1}^c m_{I_2}^d X_{I_3I_4}\ldots X_{I_{n-1}I_n}\epsilon_{abcd}\epsilon^{I_1\ldots I_n}+BX_{I_1I_2}\ldots X_{I_{n-1}I_n}\epsilon^{I_1\ldots I_n}+ \\ &\bar{B}Y^{ab}Y^{cd}\epsilon_{abcd}+B\bar{B}\mathrm{Pf}A\Big), \end{aligned} \tag{5.26}$$

where the variables are as defined in Eq. 5.24 with an extra $SU(n)$ flavor and

$$\begin{aligned} B &= T^{\alpha_1 a}T^{\alpha_2 b}T^{\alpha_3 c}F^{\alpha_4 4}A^{\alpha_5\alpha_6}\ldots A^{\alpha_{n-1}\alpha_n}\epsilon_{abc}\,\epsilon_{\alpha_1\ldots\alpha_n} \\ \bar{B} &= \bar{F}_{\alpha_1 I_1}\ldots\bar{F}_{\alpha_n I_n}\epsilon^{I_1\ldots I_n}\epsilon^{\alpha_1\ldots\alpha_n} \\ Y^{a4} &= T^{\alpha_1 a}F^{\alpha_2 4}A^{\alpha_3\alpha_4}\ldots A^{\alpha_{n-1}\alpha_n}\epsilon_{\alpha_1\ldots\alpha_n} \\ Y^{ab} &= \epsilon^{abc}y_c. \end{aligned} \tag{5.27}$$

The extra $SU(n)$ flavor is denoted by $F^{\alpha 4}$ and $\bar{F}_{\alpha n}$, and Λ_n is the dynamical scale of the four-flavor $SU(n)$ theory. Here we have not bothered to establish the correct coefficients in the last term in parentheses, since they are irrelevant in the forthcoming analysis.

To arrive at the true low-energy theory, one would integrate out $n-3$ flavors, at which point a superpotential is generated involving Λ_3 for the four flavor theory. Upon integrating out the two remaining heavy flavors, one would generate a complicated superpotential, involving both the Yukawa couplings and the dynamical scales Λ_n and Λ_3. It is however technically difficult to explicitly perform this procedure because of the nonlinear terms induced by the baryon operators in the tree-level superpotential.

If we instead constrain the form of the low-energy superpotential with symmetries and limits, we find that the analysis remains quite complicated, because many terms are permitted by the symmetries and physical limits. We deduce the allowed terms by introducing a parameter $\tilde{\Lambda}_3$ which transforms under anomalous global symmetries associated with the rotation of each field carrying $SU(3)$ gauge charge in the initial microscopic theory. Alternatively, we can define Λ_3 for the two flavor theory, where all heavy flavors have been integrated out. The parameters $\tilde{\Lambda}_3^{9-n}\det(\lambda^{iI})/\Lambda_n^{2n-1}$ and Λ_3^7 have the same charge under all anomalous symmetries so we can describe the low energy dynamics in terms of either one. We also see that if we consider $\tilde{\Lambda}_3$ as a fundamental finite parameter of the initial theory, singularities in the Yukawa couplings λ^{iI} are permitted when we express the result in terms of the low-energy Λ_3, since the appropriate ratio is finite. In essence, the Yukawa couplings become mass terms in the $SU(n)$ confined theory, and appear in the matching of Λ_3 across mass thresholds.

Examples of terms permitted by all symmetries and limits are:

$$\frac{\Lambda_3^7}{\Lambda_n^{2n-1}}\frac{\beta^{ij}}{(\lambda^{iI})^2}(X_{IJ})^{(n-4)/2}\mathrm{Pf}A\,M_I^4\frac{1}{y_a Y^{a4}},$$
$$\frac{\Lambda_3^{14}}{\Lambda_n^{2n-1}}\frac{(\beta^{ij})^2}{(\lambda^{iI})^4}X_{In}(X_{IJ})^{(n-6)/2}\mathrm{Pf}A\frac{1}{(y_a Y^{a4})(y_a M_n^a)},$$

where β^{ij}'s are the coefficients of the baryon operators $\bar{Q}\bar{Q}_i\bar{Q}_j$, and λ^{iI} of the $T\bar{F}_I\bar{Q}_i$ terms in the tree-level superpotential, but the index structure is not specified. These terms mix the effects of the strong dynamics with the tree-level superpotential, which is purely a consequence of integrating out heavy fields. This does not violate the conjecture of Refs. [60, 89], which states that the couplings of the light fields are not mixed into the dynamically generated superpotential.

Because of the complicated superpotential, the analysis of the full theory is difficult. We will therefore consider a simpler version of the theory, in which the baryon couplings, β^{ij}, are zero. This simplified superpotential does not lift all flat directions classically, which might lead to runaway directions in the quantum theory. One can show that these remaining classical flat directions can be parameterized by the baryon operators $\bar{b}_{ij}$. However, in the $SU(n)$ confined theory, these fields are not flat, since the terms proportional to m_{iI}, which are Yukawa couplings in the classical theory, are mass terms in the confined theory. In this case, there is a potential for the baryon fields which drives them towards the origin, and the baryon flat directions are lifted in the quantum theory. This is similar in spirit to what was found in Ref. [84]. In that example however, a quadratic constraint becomes a linear constraint so the flat direction is removed; here we simply see that the $SU(n)$ confined superpotential is such that the baryon fields are not flat. However there is a caveat to this analysis which we discuss shortly.

In this limit it is simple to integrate out the heavy flavors and arrive at the low-energy theory. The resulting superpotential is

$$\begin{aligned} W &= \frac{1}{\Lambda_n^{2n-1}}\Big(y_a m_n^a m_{I_1}^4 X_{I_2 I_3}\ldots X_{I_{n-2}I_{n-1}}\epsilon^{I_1\ldots I_{n-1}} + B X_{I_1 I_2}\ldots X_{I_{n-1}I_n}\epsilon^{I_1\ldots I_n} \\ &\quad + \bar{B} Y^{a4} y_a + B\bar{B}\mathrm{Pf}A\Big) + \mu m_n^4 + \lambda^{12}X_{12} + \ldots + \lambda^{n-3,n-2}X_{n-3,n-2} \\ &\quad + \frac{\Lambda_3^7}{(Y^{a4}y_a)(m_n^b\bar{Q}_b) - (Y^{a4}\bar{Q}_a)(m_n^b y_b)}. \end{aligned} \tag{5.28}$$

This superpotential clearly breaks supersymmetry since m_n^4 appears only in the term μm_n^4. Since the scales of the $SU(n)$ theory with and without extra flavor are related by $\mu\Lambda_n^{2n-1} = \Lambda_n^{2n}$, this presumably implies that supersymmetry breaking is characterized by Λ_n^{2n-1} in the original theory.

Thus we just showed that if the $SU(n)$ gauge group is confining, supersymmetry is broken. Had supersymmetry not been broken, this would have been a good assumption, since all operators involving fields transforming under the $SU(n)$ are driven to the origin by the classical potential. Because supersymmetry is broken, it is conceivable that the true vacuum is in the Higgs, rather than the confining phase. Nonetheless, we still expect supersymmetry to be broken since there are no classically flat directions in the theory. In this case however, the $\bar{b}$ operators are not lifted by the superpotential. Once the effect of supersymmetry breaking and the Kähler potential are included, the $\bar{b}$ fields presumably have a nontrivial potential. We have not analyzed whether or not this can give rise to runaway directions, should the Higgs phase prove to be the true vacuum.

Having argued that supersymmetry is probably broken for $\beta^{ij} = 0$, we hope that by including the remaining couplings, while lifting the flat directions, does not introduce a supersymmetric minimum. We expect that the arguments presented above indicate that supersymmetry is broken in the full $SU(n) \times SU(3) \times U(1)$ theories.

5.4 $SU(n) \times SU(4) \times U(1)$ models and their generalizations

While many of the first models for breaking supersymmetry had instanton or gaugino generated terms which kept fields away from the origin [59, 83], recent work has argued that models in other phases can also break supersymmetry. In Ref. [61], it was argued that supersymmetry can be broken due to confinement. A nontrivial modification of the Kähler potential near the origin removes the supersymmetry preserving minimum. Alternatively, models with a quantum modified moduli space can also break supersymmetry [84] because the supersymmetry preserving origin is removed by the quantum modified constraint. Models in the conformal or free magnetic phase can also break supersymmetry. In the models which have been studied to now, these models broke supersymmetry through an O'Raifeartaigh mechanism in the dual theory [70] or strong dynamics in the electric theory. A class of models described below is distinguished by the fact that the dynamics can be understood only in the dual description where dynamical effects are responsible for supersymmetry breaking.

In the previous sections, a new class of models was studied which were based on a product group in which supersymmetry is broken dynamically. There it was argued that supersymmetry breaking could be understood as a collusion between separate dynamical effects from the two nonabelian gauge groups. In the first example, the 4-3-1 model based

on the gauge group $SU(4) \times SU(3) \times U(1)$, the exact superpotential could be found and the model was an O'Raifeartaigh model with both groups contributing to the final form of the superpotential. In all cases, supersymmetry breaking could be understood by taking a limit in which the gauge coupling of a confining gauge group is the biggest coupling. In this limit, Yukawa couplings which were necessary to lift flat directions turn into mass terms. Many flavors can be integrated out and the gauge dynamics of the second nonabelian gauge factor generated a superpotential which drives fields from the origin leading to the breaking of supersymmetry.

In the particular models considered in the previous section, other mechanisms of supersymmetry breaking could appear as well in the limit that one of the gauge couplings dominated. For example, in the particular case of the 4-3-1 model supersymmetry breaking occurs in the strong Λ_3 limit through confinement, analogous to the mechanism of Ref. [61]. On the other hand, if some of the tree level terms are removed, supersymmetry breaking appears due to a quantum modified constraint [84]. Because of these additional descriptions, it was not clear that the quantum modified constraint was not essential to supersymmetry breaking.

In this section, we show that analogous models in which each of the two groups is in one of a confining, free magnetic, or conformal phase (in the limit that we neglect the other coupling) also break supersymmetry, through a conspiracy of dynamical effects from the two gauge groups. Naively, it would appear that such models should allow fields to go to the origin. However, because of the tree-level superpotential and dynamics of one group, the other group can generate a dynamical superpotential in the infrared which forbids the origin and yields supersymmetry breaking.

It is interesting that models in which the theory must be analyzed at low energy in the dual phase can break supersymmetry. It is not essential for the number of flavors to be so small that a dynamical superpotential, a quantum modified constraint, or even confinement occurs in the electric theory. This suggests the possibility of a much larger class of supersymmetry breaking models because of the much less restrictive condition on the size of the initial particle content.

The two models we present in this section are obvious generalizations of the models considered in the previous section. Analogously to the n-3-1 models, supersymmetry breaking can be understood as a result of Yukawa couplings and strong dynamics which make flavors of the second gauge group heavy. In the resulting theory, the origin is forbidden because of a dynamical superpotential from the second gauge group. The mechanism is in some sense independent of the number of flavors in the initial theory. We present two classes of models to illustrate this. In the first class of models, in which one of the gauge groups is confining, supersymmetry breaking occurs through a conspiracy of gauge effects. We then consider a model which must be analyzed in the dual phase. The supersymmetry breaking dynamics for this model is remarkably similar to that of the confining theory, as we will show below.

5.4.1 n-4-1

The fields of the first model can be obtained by decomposing $SU(n+4)$ model with an antisymmetric tensor [59] into its $SU(n) \times SU(4) \times U(1)$ subgroup. The field content is

$$\begin{array}{rcl} \square\!\square & \rightarrow & A(\square\!\square, 1)_8 + a(1, \square\!\square)_{-2n} + T(\square, \square)_{4-n} \\ n \cdot \bar{\square} & \rightarrow & \bar{F}_I(\bar{\square}, 1)_{-4} + \bar{Q}_i(1, \bar{\square})_n, \end{array} \tag{5.29}$$

where $i, I = 1, \ldots, n$. We take the tree-level superpotential to be

$$W_{tree} = A\bar{F}_1\bar{F}_2 + A\bar{F}_3\bar{F}_4 + \ldots + A\bar{F}_{n-2}\bar{F}_{n-1}$$
$$+a\bar{Q}_2\bar{Q}_3 + a\bar{Q}_4\bar{Q}_5 + \ldots + a\bar{Q}_{n-1}\bar{Q}_1 + T\bar{F}_1\bar{Q}_1 + \ldots + T\bar{F}_n\bar{Q}_n. \tag{5.30}$$

A detailed analysis along the lines presented in Section 5.2 shows that this superpotential lifts all flat directions. The relative shift of the indices in the $A\bar{F}\bar{F}$ and $a\bar{Q}\bar{Q}$ terms is important. Without this shift not all flat directions are lifted. This superpotential preserves an R-symmetry which is anomalous only under the $U(1)$ gauge group.

We analyze this theory in the limit where $\Lambda_n \gg \Lambda_4$. The $SU(n)$ field content is an antisymmetric tensor, four fundamentals and n antifundamentals which give confining gauge dynamics. Below Λ_n, the effective degrees of freedom are the $SU(n)$ invariants [70]

$$\begin{aligned}
X_{IJ} &= A^{\alpha\beta}\bar{F}_{\alpha I}\bar{F}_{\beta J} \\
\bar{B} &= \bar{F}_{\alpha_1 1}\ldots\bar{F}_{\alpha_n n}\epsilon^{\alpha_1\ldots\alpha_n} \\
(B_1)^a &= T^{\alpha_1 a}A^{\alpha_2\alpha_3}\ldots A^{\alpha_{n-1}\alpha_n}\epsilon_{\alpha_1\ldots\alpha_n} \\
(B_3)_a &= \epsilon_{abcd}T^{\alpha_1 b}T^{\alpha_2 c}T^{\alpha_3 d}A^{\alpha_4\alpha_5}\ldots A^{\alpha_{n-1}\alpha_n}\epsilon_{\alpha_1\ldots\alpha_n} \\
M_I^a &= T^{\alpha a}\bar{F}_{\alpha I},
\end{aligned} \tag{5.31}$$

plus the $SU(n)$ singlets a and $\bar{Q}_i$.

The superpotential is the sum of the tree-level terms from Eq. (5.30) and the confining superpotential [70].

$$\begin{aligned}
W \;=\; & X_{12} + \ldots + X_{n-2,n-1} + a\bar{Q}_2\bar{Q}_3 + \ldots + a\bar{Q}_{n-1}\bar{Q}_1 + \\
& M_1\bar{Q}_1 + \ldots + M_n\bar{Q}_n + \frac{1}{\Lambda_n^{2n-1}}\Big(B_{3a}M_{I_1}^a X_{I_2 I_3}\ldots X_{I_{n-1}I_n}\epsilon^{I_1\ldots I_n} \\
& + B_1^a M_{I_1}^b M_{I_2}^c M_{I_3}^d X_{I_4 I_5}\ldots X_{I_{n-1}I_n}\epsilon^{I_1\ldots I_n}\epsilon_{abcd} + \bar{B}B_1^a B_{3a}\Big),
\end{aligned} \tag{5.32}$$

where small Latin letters denote $SU(4)$ indices.

Note that in the confined theory, some of the Yukawa couplings have become mass terms. To deduce the infrared theory, we integrate out all massive fields. It is technically difficult to integrate out the fields using the full superpotential from Eq. 5.32. For simplicity we set the couplings of all $a\bar{Q}\bar{Q}$ terms to zero. We will argue based on symmetries that the models with the additional baryon operators included still break supersymmetry. It should be noted that the flat directions now present classically are lifted in the quantum theory [84], which is presumably a valid supersymmetry breaking model as well.

Because we have integrated out n massive flavors, the $SU(4)$ theory at low energy has an antisymmetric tensor and only one flavor. This theory dynamically generates a superpotential. The low-energy superpotential is therefore

$$W_{\text{eff}} = X_{12} + \ldots + X_{n-2,n-1} + \frac{1}{\Lambda_n^{2n-1}}\bar{B}m + \left[\frac{\tilde{\Lambda}_4^5}{\text{Pf}a\, m}\right]^{\frac{1}{2}}, \tag{5.33}$$

where $\text{Pf}a = a^{ab}a^{cd}\epsilon_{abcd}$, $m = B_1^a B_{3a}$, and $\tilde{\Lambda}_4$ is the dynamical scale of the effective one flavor $SU(4)$ theory. The equations of motion have set most terms to zero in the Λ_n dependent term. The $\bar{B}$ equation of motion would set $m = 0$. However, this is inconsistent with the

$\left[\frac{\tilde{\Lambda}_4^5}{\mathrm{Pf}a\, m}\right]^{\frac{1}{2}}$ term in the superpotential, which drives m from the origin in a theory with no flat directions. Therefore, we conclude that the equations of motion are contradictory, and supersymmetry is dynamically broken.

We have argued that supersymmetry is broken in the theory with $\gamma^{ij} = 0$, where γ^{ij} is the coefficient of the $a\bar{Q}\bar{Q}$ operators in the tree-level superpotential. It is clear that even with nonzero γ^{ij}, supersymmetry is still broken. From symmetries, it can be shown that the neglected terms can correct the superpotential by a power series in

$$\mathcal{A} = \Lambda_n^{-2n+1}(\mathrm{Pf}a)^{\frac{1}{2}}(X_{IJ})^{\frac{n-2}{2}} m^{\frac{1}{2}}(\gamma^{ij})(m^{iI})^{-2}, \tag{5.34}$$

where m^{iI} is the coefficient of the $T\bar{F}_I\bar{Q}_i$ operators. For small γ, these terms could only give a sufficiently large contribution to cancel a nonzero F-term at field values larger than Λ_n. In this case, the theory should have been analyzed in the Higgs phase, which is clearly inconsistent with supersymmetry since there were no flat directions.

As an aside, we note that in the version of the theory without the $a\bar{Q}\bar{Q}$ terms in the superpotential (and hence without the corrections of Eq. 5.34), there is an additional source of supersymmetry breaking. The terms $X_{12} + \ldots + X_{n-2,n-1}$ in the superpotential lead to supersymmetry breaking due to confinement, as described in Ref. [61]. Here we emphasize the first argument for supersymmetry breaking, which generalizes beyond confining models, as we describe below.

5.4.2 n-5-1

Next, we consider theories based on the gauge group $SU(n)\times SU(5)\times U(1)$ (n even) obtained by reducing the gauge group of the $SU(n+5)$ theory with an antisymmetric tensor and $n+1$ antifundamentals. The mechanism of supersymmetry breaking will turn out to be very similar to the previous models, despite the very different gauge dynamics.

The field content is

$$\begin{array}{rcl} \begin{array}{|c|}\hline \\ \hline \end{array} & \rightarrow & A(\begin{array}{|c|}\hline \\ \hline \end{array}, 1)_{10} + a(1, \begin{array}{|c|}\hline \\ \hline \end{array})_{-2n} + T(\Box,\Box)_{5-n} \\ (n+1)\cdot\bar{\Box} & \rightarrow & \bar{F}_I(\bar{\Box}, 1)_{-5} + \bar{Q}_i(1,\bar{\Box})_n, \end{array} \tag{5.35}$$

where $i, I = 1, \ldots, n+1$. The tree-level superpotential is

$$\begin{aligned} W_{tree} \;=\; & A\bar{F}_1\bar{F}_2 + \ldots + A\bar{F}_{n-1}\bar{F}_n + a\bar{Q}_2\bar{Q}_3 + \ldots + a\bar{Q}_n\bar{Q}_1 + \\ & T\bar{F}_1\bar{Q}_1 + \ldots + T\bar{F}_{n+1}\bar{Q}_{n+1}. \end{aligned} \tag{5.36}$$

Again a detailed analysis verifies the absence of flat directions.

The $SU(5)$ gauge group has an antisymmetric tensor and n flavors while the $SU(n)$ has an antisymmetric tensor and five flavors. The $SU(5)$ group is in the conformal regime while the $SU(n)$ group is in the free magnetic phase. Although it seems more obvious to dualize the $SU(n)$ which is in the free magnetic phase it is simpler to dualize the gauge group $SU(5)$, as it has an odd number of colors. This duality will increase the number of $SU(n)$ flavors by $n-3$ which takes the theory out of the free magnetic phase.

The dual description of $SU(5)$ with an antisymmetric tensor and n flavors is an $SU(n-3)\times Sp(2n-8)$ gauge theory[70] with the field content given in Table 5.1.

The $SU(n-3)\times Sp(2n-8)$ gauge group in Table 5.1 is the dual of the $SU(5)$ gauge group, while the $SU(n)\times U(1)$ is the remaining original gauge group unchanged by the duality

	$SU(n-3)$	$Sp(2n-8)$	$SU(n)$	$U(1)$	$SU(n+1)_{\bar{Q}}$	$SU(n+1)_{\bar{F}}$
A	1	1	$\begin{array}{|c\|}\hline\ \\ \hline\ \\ \hline\end{array}$	10	1	1
$\bar{F}$	1	1	$\overline{\square}$	-5	1	$\square$
x	$\square$	$\square$	1	0	1	1
p	$\square$	1	1	$5n$	1	1
$\bar{a}$	$\begin{array}{|c\|}\hline\ \\ \hline\ \\ \hline\end{array}$	1	1	0	1	1
$\bar{q}$	$\overline{\square}$	1	$\overline{\square}$	-5	1	1
l	1	$\square$	1	0	$\overline{\square}$	1
M	1	1	$\square$	5	$\square$	1
H	1	1	1	0	$\begin{array}{|c\|}\hline\ \\ \hline\ \\ \hline\end{array}$	1
B_1	1	1	$\square$	$5(1-n)$	1	1

(5.37)

Table 5.1: The field content of the $SU(n) \times SU(5) \times U(1)$ theory after dualizing the $SU(5)$ gauge group.

transformation. The $SU(n+1)_{\bar{Q}} \times SU(n+1)_{\bar{F}}$ global symmetries are the non-abelian global symmetries of the original $SU(n) \times SU(5) \times U(1)$ theory.

The superpotential consists of the terms corresponding to the tree-level superpotential of Eq. 5.36 and the terms arising from the duality transformation. It is given by

$$\begin{aligned} W &= A\bar{F}_1\bar{F}_2 + \ldots + A\bar{F}_{n-1}\bar{F}_n + H_{23} + \ldots + H_{n1} + M_1\bar{F}_1 + \ldots + \\ &\quad M_{n+1}\bar{F}_{n+1} + M\bar{q}lx + Hl^2 + B_1p\bar{q} + \bar{a}x^2. \end{aligned} \tag{5.38}$$

As in the $SU(n) \times SU(4) \times U(1)$ models, some of the tree-level Yukawa terms are mapped into mass terms in the dual description. To simplify the theory we again set the coefficients of the $A\bar{F}\bar{F}$ operators to zero, though in this case it is not difficult to leave them in. With this simplification, one can easily integrate out the massive flavors of $SU(n)$ since the $\bar{F}_I$ equations of motion set all M's to zero. There is just one $SU(n)$ flavor remaining and thus there is a dynamically generated term in the superpotential from the $SU(n)$ dynamics. The effective low-energy superpotential is

$$W = H_{23} + H_{45} + \ldots + H_{n1} + Hl^2 + \bar{a}x^2 + \tilde{M}p + \frac{\tilde{\Lambda}_n^{n+1}}{(\tilde{M}\tilde{X}^{(n-4)/2}\mathrm{Pf}\,A)^{1/2}}, \tag{5.39}$$

where $\tilde{M} = B_1\bar{q}$, $\tilde{X} = A\bar{q}\bar{q}$ and $\mathrm{Pf}\,A = A^{n/2}$, while $\tilde{\Lambda}_n$ is the effective $SU(n)$ scale. This superpotential looks very much like the one in Eq. 5.33, with $\tilde{M}$ playing the role of m and p the role of $\bar{B}$. The equations of motion are again contradictory. We again conclude that supersymmetry is broken.

The above analysis neglected the $Sp(2n-8)$ group that appears from dualizing the $SU(5)$ group. This group is however Higgsed by the VEV's of the l fields as a result of the H equations of motion and the terms linear in H in the superpotential. Although instanton terms can be generated in the broken $Sp(2n-8)$ group, these will not involve the fields $\tilde{M}, \tilde{X}, \mathrm{Pf}A$ or p and therefore do not affect the proof of dynamical supersymmetry breaking given above. The $Sp(2n-8)$ dynamics seems to be irrelevant to the analysis of the model.

The dynamics of the general $SU(n) \times SU(m) \times U(1)$ models $(n, m \geq 5)$ obtained in the same way is very similar to that of the $SU(n) \times SU(5) \times U(1)$ model, if one dualizes the $SU(n)$

corresponding to odd n. We expect that a similarly constructed tree-level superpotential lifts all flat directions. One can then show that the resulting low-energy superpotential is in one-to-one correspondence to the superpotential of Eq. 5.39, with the remaining gauge group being $SU(m-3) \times Sp(2m-8) \times SU(m) \times U(1)$ (m is even), which is obtained by dualizing the original $SU(n)$ group. Since the superpotential is exactly of the same form as the one in Eq. 5.39 we conclude that the general $SU(n) \times SU(m) \times U(1)$ models break supersymmetry as well.

The similarities between the $SU(n) \times SU(4) \times U(1)$ and $SU(n) \times SU(5) \times U(1)$ models is intriguing. In both models, the dynamics of the $SU(n)$ group leads to additional flavors of the second gauge group, in one case due to confinement, and in the other case, due to the dual description. In both cases, some of the tree level terms are mapped into mass terms due to dynamical effects in the $SU(n)$ gauge group. After integrating out these massive flavors the other gauge group has only a single flavor remaining besides the antisymmetric tensor and produces a dynamically generated superpotential. This dynamical superpotential together with a piece of the superpotential from the strong dynamics of the first group breaks supersymmetry. Thus supersymmetry breaking in these theories involves a subtle interplay between the gauge dynamics of both groups and the tree-level superpotential.

That these theories (and presumably the general $SU(n) \times SU(m) \times U(1)$ models as well) break supersymmetry suggests the existence of still more models of dynamical supersymmetry breaking. The flavor content of these models can be much larger than one would naively have anticipated by the requirement of a dynamical superpotential, because Yukawa couplings or other interactions in the presence of strong dynamics can change the phase of the theory in the infrared. The low-energy description might then have sufficiently few flavors to break supersymmetry dynamically.

Chapter 6

Summary

We have described several topics in non-Standard Model physics, in which analysis is based on non-perturbative techniques. Hopefully, more non-perturbative methods will be found in the future, which will allow to study possible extensions of the Standard Model in greater detail. In Chapter 2, we explored the implication of electroweak measurements for the Strongly-Coupled Standard Model. From our analysis of the SCSM exploiting recent electroweak data, we concluded that the currently allowed parameter space is so small as to strongly argue against the model. There is no reason to expect vector dominance to hold at a level of 3%. Nor can we understand how the W' could mix with the photon only 1/40 as much as the W mixes; yet we have found that this would have to be the case even if the coupling of the W' to the left-handed fermions is allowed to be as small as 1/4 the W coupling (itself already small for a strongly-coupled theory).

We investigated the phenomenology of realistic technicolor models that incorporate the GIM mechanism in Chapter 3. The PGBs of the TC-GIM models are not formed by the technifermions, unlike in old technicolor theories or more realistic walking technicolor scenarios. Anomaly-free models require additional fermions at low-energy scales, below the scale of ETC interactions. These extra fermions form PGBs, which are the lightest new states in the TC-GIM models. We have described and studied several possible realizations of the light-fermions sectors. The spectrum of the PGBs is very rich. In all cases, among the PGBs there are leptoquarks, color octet particles and color and charge neutral states. Despite the fact that couplings to fermions are relatively small, all PGBs are short-lived particles, with lifetimes small enough not to escape detection.

Hadron colliders are most suitable for studies of leptoquarks. Color octet particles are much more difficult to observe due to too large QCD background, even though they are produced more copiously than leptoquarks. By studying the processes $pp \to \theta\theta$ and $pp \to TT$, the LHC experiments can discover octet particles lighter than 375 GeV and leptoquarks lighter than 1160 GeV. Currently, the best limits are placed by experiments at Tevatron, which exclude leptoquarks lighter than 130 GeV.

Electron colliders are capable of studying both leptoquarks and P^0 production. However, electron colliders do not have large enough energy to contribute significantly to leptoquark searches. In TC-GIM, cross sections for single production of leptoquarks are too small to yield observable rates. This limits the discovery reach of e^+e^- colliders to half of the CM energy. P^0 is the only neutral particle that can be produced with large enough rates, which result from the anomalous couplings of P^0. The rate for the process $e^+e^- \to P^0\gamma$ depends on the strength of the anomalous coupling, so the rate is sensitive to f_{S-1}. At present, LEP

excludes f_{S-1} smaller than 38 GeV, but after analyzing all the data collected so far it can probe this scale up to 80 GeV. Significant improvement can be achieved at NLC, which can test f_{S-1} up to 390 GeV.

We have shown in Chapter 4 that it is possible to identify all theories which belong to a certain class of confining theories. A salient feature of these s-confining theories is that the massless degrees of freedom are given by the independent gauge invariant chiral operators. They describe the theory everywhere on the moduli space including the origin. Another important characteristic is that there is a non-vanishing superpotential for the confined degrees of freedom. We have given two necessary conditions for a theory to be s-confining.

Using these conditions and the requirement of 't Hooft anomaly matching we determined all s-confining theories with a single gauge group. We listed several new examples of s-confining theories with $SU(N)$ gauge groups. The $SU(N)$ theory with $\square\!\!\square + \overline{\square\!\!\square} + 3(\square + \overline{\square})$ is s-confining for any N, while other new examples s-confine only for particular N. There are no new examples of s-confinement with $Sp(N)$ gauge group. S-confinement in $SO(N)$ groups requires the presence of at least one spinorial representation, which restricts $N \leq 14$. It turns out that most of the $SO(N)$ theories which satisfy our index condition are s-confining.

In Chapter 5, we have explored a new class of theories based on a product group, in which neither gauge group generates a dynamical superpotential in the absence of perturbations. Nonetheless by exploring the exact superpotential, we could explicitly demonstrate that supersymmetry is broken in the $SU(4) \times SU(3) \times U(1)$ model. We also found interesting phenomena in the exact superpotential, which were discussed in Section 5.2.2. For the $SU(n) \times SU(3) \times U(1)$ models, we have found that the exact superpotential is quite complicated. However, in theories with $\beta^{ij} = 0$, we could demonstrate supersymmetry breaking with the addition of an extra flavor of $SU(n)$. In this theory, we also found a large number of classically flat directions which are lifted in the quantum mechanical theory. This is due to the fact that when $SU(n)$ confines, some of the Yukawa couplings in the tree-level superpotential turn into mass terms. This drives the $SU(3)$ group into the confining region and also lifts some of the classical flat directions. We showed how the same mechanism leads to supersymmetry breaking in the $SU(n) \times SU(4) \times U(1)$ and $SU(n) \times SU(5) \times U(1)$ models. These models had to be analyzed using the duality transformations.

Bibliography

[1] E. Sather and W. Skiba, *Phys. Rev.* **D53**, 527 (1996).

[2] L. F. Abbott and E. Farhi, *Phys. Lett.* **101B**, 69 (1981); *Nucl. Phys.* **B189**, 547 (1981).

[3] C. Korpa and Z. Ryzak, *Phys. Rev.* **D34**, 2139 (1986).

[4] P. Q. Hung and J. J. Sakurai, *Nucl. Phys.* **B143**, 81 (1978).

[5] M. Claudson, E. Farhi, and R. L. Jaffe, *Phys. Rev.* **D34**, 873 (1986).

[6] T. Banks and E. Rabinovici, *Nucl. Phys.* **B160**, 349 (1979); E. Fradkin and S. Schenker, *Phys. Rev.* **D19**, 3682 (1979); G. 't Hooft, in *Recent Developments in Gauge Theory,* edited by G. 't Hooft et al. (Plenum, New York, 1980); S. Dimopoulos, S. Raby and L. Susskind, *Nucl. Phys.* **B173**, 208 (1980).

[7] M. E. Peskin and T. Takeuchi, *Phys. Rev.* **D46**, 381 (1992).

[8] M. Golden and L. Randall, *Nucl. Phys.* **B361**, 3 (1991).

[9] M. Demarteau et al., *Combining W Mass Measurements,* CDF/PHYS/CDF/PUBLIC/2552 and D0 NOTE 2115, May 1994.

[10] UA2 Collaboration, J. Alitti et al., *Phys. Lett.* **276B**, 354 (1992).

[11] Internal note of the Subgroup of the LEP Electroweak Working Group on Z^0 Lineshape and Lepton Forward-Backward Asymmetries, P. Clarke et al., *Updated Parameters of the Z^0 Lineshape and Lepton Forward-Backward Asymmetries from Combined Preliminary Data of the LEP Experiments,* LEPLINE 94-01, ALEPH 94-120 PHYSIC 94-104, DELPHI 94-99 PHYS 416, L3 Note 1629, OPAL Technical Note TN244, July 1994.

[12] Internal note of the LEP Electroweak Working Group, A. Blondel et al., *Constraints on Standard Model Parameters from Combined Preliminary Data of the LEP Experiments,* LEPEWWG/94-02, ALEPH 94-121 PHYSIC 94-105, DELPHI 94-23 Phys 357, L3 note 1577, OPAL Technical Note TN245, July 1994.

[13] SLD Collaboration, K. Abe et al., *Phys. Rev. Lett.* **73**, 25 (1994).

[14] CDF Collaboration, F. Abe et al., *Phys. Rev. Lett.* **73**, 225 (1994).

[15] CDF Collaboration, F. Abe et al., *Phys. Rev. Lett.* **67**, 2609 (1991).

[16] W. Skiba, *Nucl. Phys.* **B470**, 84 (1996); hep-ph/9612481.

[17] S. Weinberg, *Phys. Rev.* **D19**, 1277 (1979); L. Susskind, *Phys. Rev.* **D20**, 2619 (1979).

[18] S. Dimopoulos and L. Susskind, *Nucl. Phys.* **B155**, 237 (1979);
E. Eichten and K. Lane, *Phys. Lett.* **90B**, 125 (1980).

[19] S. Dimopoulos and J. Ellis, *Nucl. Phys.* **B182**, 505 (1981).

[20] S.L. Glashow, J. Iliopoulous and L. Maiani, *Phys. Rev.* **D2**, 1285 (1970).

[21] R. S. Chivukula and H. Georgi, *Phys. Lett.* **188B**, 99 (1987);
R. S. Chivukula, H. Georgi and L. Randall, *Nucl. Phys.* **B292**, 93 (1987).

[22] L. Randall, *Nucl. Phys.* **B403**, 122 (1993);

[23] H. Georgi, *Nucl. Phys.* **B416**, 699 (1994).

[24] P. Sikivie, L. Susskind, M. Voloshin and V. Zakharov, *Nucl. Phys.* **B173**, 189 (1980).

[25] H. Georgi, *Nucl. Phys.* **B266**, 274 (1986).

[26] E. Farhi and L. Susskind, *Phys. Rep.* **74**, 277 (1981).

[27] T. Das, *et al.*, *Phys. Rev. Lett.* **18**, 759 (1967).

[28] K. Lane and M. V. Ramana, *Phys. Rev.* **D44**, 2678 (1991);
V. Lubicz and P. Santorelli, *Nucl. Phys.* **B460**, 3 (1996).

[29] R. S. Chivukula, R. Rosenfeld, E. H. Simmons and J. Terning, hep-ph/9503202.

[30] M. Leurer *Phys. Rev.* **D49**, 333 (1994).

[31] B. Balaji, *Phys. Rev.* **D53**, 1699 (1996).

[32] S. Dimopoulos, *Nucl. Phys.* **B168**, 69 (1980);
S. Dimopoulos, S. Raby and G. L. Kane, *Nucl. Phys.* **B182**, 77 (1981).

[33] P. Abreu, *et al.* (DELPHI Collaboration), *Phys. Lett.* **316B**, 620 (1993);
Phys. Lett. **275B**, 222 (1992).

[34] A. Manohar and L. Randall, *Phys. Lett.* **246B**, 537 (1990);
L. Randall and E. H. Simmons, *Nucl. Phys.* **B380**, 3 (1992).

[35] D. Decamp *et al.* (ALEPH Collaboration), *Phys. Rep.* **216**, 253 (1992).

[36] *ECFA Workshop on LEP 200*, edited by A. Böhm and W. Hoogland, **CERN 97-08.**

[37] *Proceedings of the Workshop on Physics and Experiments with Linear Colliders*, edited by R. Settles, **ECFA 93-154.**

[38] *Workshop on e^+e^- collisions at 500 GeV: The Physics Potential*, edited by P. M. Zerwas, **DESY 92-123A,B,C.**

[39] E. Eichten, I. Hinchliffe, K. Lane and C. Quigg, *Rev. Mod. Phys.* **56**, 579 (1984), *Erratum: Rev. Mod. Phys.* **58**, 1065 (1986).

[40] D. W Duke and J. F. Owens *Phys. Rev.* **D30**, 49 (1984).

[41] J. L. Hewett, S. Pakvasa, *Phys. Rev.* **D37**, 3165 (1988).

[42] J. C. Pati and A. Salam, *Phys. Rev.* **D10**, 275 (1974);
H. Georgi and S. Glashow, *Phys. Rev. Lett.* **32**, 438 (1974);
E. Eichten, K. Lane and M. Peskin, *Phys. Rev. Lett.* **50**, 811 (1983).

[43] S. Hagopian for the D0 Collaboration, hep-ex/9410003;
S. Abachi, *et al.* (D0 Collaboration), *Phys. Rev. Lett.* **72**, 965 (1994).

[44] F. Abe, *et al.* (CDF Collaboration), *Phys. Rev. Lett.* **75**, 1012 (1995).

[45] G. Jackson, talk presented at the Workshop on Electroweak Symmetry Breaking and TeV-Scale Physics, UC Santa Barbara, Feb. 1994.

[46] *Design Study of The Large Hadron Collider*, **CERN 91-03.**

[47] S. Parke and T. Taylor, *Phys. Rev. Lett.* **56**, 2459 (1986);
Z. Kunszt and W. J. Stirling, *Phys. Rev.* **D37**, 2439 (1988).

[48] R. S. Chivukula, M. Golden and E. H. Simmons, *Nucl. Phys.* **B363**, 83 (1991).

[49] E. Eichten, I. Hinchliffe, K. Lane and C. Quigg, *Phys. Rev.* **D34**, 1547 (1986).

[50] F. Abe, *et al.* (CDF Collaboration), *Phys. Rev. Lett.* **74**, 2626 (1995).

[51] C. Csáki, M. Schmaltz, and W. Skiba, *Phys. Rev. Lett.* **78**, 799 (1997).

[52] C. Csáki, M. Schmaltz, and W. Skiba, hep-th/9612207.

[53] N. Seiberg, *Phys. Rev.* **D49**, 6857 (1994), *Nucl. Phys.* **B435**, 129 (1995).

[54] S. Coleman and J. Mandula, *Phys. Rev.* **159**, 125 (1967).

[55] R. Haag, J. Łopuszański and M. Sohnius, *Nucl. Phys.* **B88**, 257 (1975).

[56] M. Luty and W. Taylor, *Phys. Rev.* **D53**, 3399 (1996).

[57] I. Affleck, M. Dine, N. Seiberg, *Nucl. Phys.* **B241**, 493 (1984).

[58] D. Amati, K. Konishi, Y. Meurice, G. Rossi and G. Veneziano, *Phys. Rep.* **162**, 169 (1988) and references therein.

[59] I. Affleck, M. Dine, and N. Seiberg, *Nucl. Phys.* **B256**, 557 (1985).

[60] K. Intriligator, R. Leigh, and N. Seiberg, *Phys. Rev.* **D50**, 1092 (1994).

[61] K. Intriligator, N. Seiberg and S. Shenker, *Phys. Lett.* **342B**, 152 (1995).

[62] K. Intriligator and N. Seiberg, *Nucl. Phys.* **B431**, 551 (1994).

[63] E. Poppitz and S. Trivedi, *Phys. Lett.* **365B**, 125 (1996).

[64] P. Pouliot, *Phys. Lett.* **367B**, 151 (1996).

[65] H. Murayama, *Phys. Lett.* **355B**, 187 (1995);

[66] K. Intriligator and N. Seiberg, *Nucl. Phys.* **B444**, 125 (1995).

[67] K. Intriligator and P. Pouliot, *Phys. Lett.* **353B**, 471 (1995).

[68] K. Intriligator, R. Leigh, and M. Strassler, *Nucl. Phys.* **B456**, 567 (1995); D. Kutasov, *Phys. Lett.* **351B**, 230 (1995); D. Kutasov and A. Schwimmer, *Phys. Lett.* **354B**, 315 (1995); D. Kutasov, A. Schwimmer, and N. Seiberg, *Nucl. Phys.* **B459**, 455 (1996); M. Berkooz, *Nucl. Phys.* **B452**, 513 (1995); M. Luty, M. Schmaltz and J. Terning, *Phys. Rev.* **D54**, 7815 (1996); N. Evans and M. Schmaltz, *Phys. Rev.* **D55**, 3776 (1997); K. Intriligator, *Nucl. Phys.* **B448**, 187 (1995); R. Leigh and M. Strassler, *Nucl. Phys.* **B447**, 95 (1995); *Phys. Lett.* **356B**, 492 (1995); hep-th/9611020; J. Brodie and M. Strassler, hep-th/9611197; O. Aharony, J. Sonnenschein and S. Yankielowicz, *Nucl. Phys.* **B449**, 509 (1995); O. Aharony, *Phys. Lett.* **351B**, 220 (1995); C. Csáki, M. Schmaltz, W. Skiba and J. Terning, hep-th/9701191.

[69] I. Pesando, *Mod. Phys. Lett.* **A10**, 1871 (1995);
S. Giddings and J. Pierre *Phys. Rev.* **D52**, 6065 (1995).

[70] P. Pouliot, *Phys. Lett.* **359B**, 108 (1995); P. Pouliot and M. Strassler, *Phys. Lett.* **370B**, 76 (1996); *Phys. Lett.* **375B**, 175 (1996).

[71] P. Cho and P. Kraus, *Phys. Rev.* **D54**, 7640 (1996).

[72] C. Csáki, W. Skiba and M. Schmaltz, *Nucl. Phys.* **B487**, 128 (1997).

[73] R. Slansky, *Phys. Rep.* **79**, 1 (1981).

[74] H. Georgi, "Lie Algebras in Particle Physics. From Isospin to Unified Theories" (Frontiers In Physics series, Benjamin/Cummings, 1982).

[75] J. Banks and H. Georgi, *Phys. Rev.* **D14**, 1159 (1976).

[76] I. Affleck, M. Dine, and N. Seiberg, *Phys. Rev. Lett.* **52**, 1677 (1984).

[77] C. Csáki, L. Randall and W. Skiba, *Nucl. Phys.* **B479**, 65 (1996).

[78] C. Csáki, L. Randall, W. Skiba and R. Leigh, *Phys. Lett.* **387B**, 791 (1996).

[79] W. Skiba, hep-th/9703159.

[80] E. Witten, *Nucl. Phys.* **B188**, 513 (1981).

[81] E. Witten, *Nucl. Phys.* **B202**, 253 (1982).

[82] I. Affleck, M. Dine, and N. Seiberg, *Phys. Lett.* **140B**, 59 (1984), *Phys. Lett.* **137B**, 187 (1984).

[83] M. Dine, A. Nelson, Y. Nir and Y. Shirman, *Phys. Rev.* **D53**, 2658 (1996).

[84] K. Intriligator and S. Thomas, *Nucl. Phys.* **B473**, 121 (1996).

[85] K. Izawa and T. Yanagida, *Prog. Theor. Phys.* **95**, 829 (1996).

[86] L. O'Raifeartaigh, *Nucl. Phys.* **B96**, 331 (1975).

[87] E. Poppitz and L. Randall, *Phys. Lett.* **336B**, 402 (1994).

[88] E. Poppitz, Y. Shadmi and S.P. Trivedi, *Nucl. Phys.* **B480**, 125 (1996).

[89] V. Kaplunovsky and J. Louis, *Nucl. Phys.* **B422**, 57 (1994).